UNIVERSITY OF CENTRAL FLORIDA

Milestone 6: Design Implementation

RDE Senior Design Team 2024-2025
Department of Mechanical and Aerospace Engineering
College of Engineering and Computer Science

Prepared By
Paul DeHart, Joshua Kopp, Nathaniel Michnoff, Arturo Negrette, Hunter Quinlan,
Egan Rigney, Subhan Wade, Edward Woodruff

Faculty Advisor
Taha Rezzag-Lebza

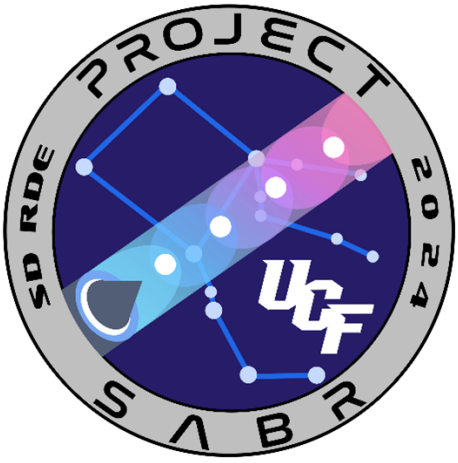

April 14, 2025

EAS 4710C / EML 4502C

Executive Summary

Project SABR or Small-Scale Air-Breathing Rotating Detonation Engine, is aimed at the demonstration of a small-scale RDE that uses GH2 and air as the fuel and oxidizer respectively. There are few RDEs in this configuration in the United States and therefore there is considerable effort in order to raise its TRL before it is commercially viable. The first steppingstone in the evolution of Project SABR is to design, build, and test the SABR RDE and its supporting systems, as well as future systems. The successful demonstration of the SABR RDE will open doors for continued research and development. To date, the SABR test stand, fluids system, data acquisition, and control systems have all been shown to reliably operate. The SABR RDE has successfully fired and given insight into future design improvements.

The SABR RDE features a three-inch annulus diameter that is comprised of JIC injectors, a 0.2-inch annular gap, an expansion-optimized cowl, aerospike, and an in-line ignition method. The fluids system interfaces with the Propulsion & Energy Research Laboratory (PERL) air tank farm and Hydrogen gas cylinders and effectively controls the flow up to MEOP. The test stand features a steel optical table mount for the modular aluminum extrusion structure that houses the fluids, the DAQ and control, and RDE systems into one compact yet accessible assembly. The DAQ and control systems include a custom control script, two DAQ cards, PTs, TCs, load cells, spark plug, and remotely controlled valves.

Prior to full-scale testing, component and subsystem testing was performed on the control script, DAQ electronics, plumbing seals, fluids instrumentation, load cells, spark plug, and torch igniter. Once the functionality and performance of these components were confirmed, full-scale testing was conducted. The torch igniter did not successfully light the engine, so a pre-detonator was swapped in. This ignition method switch successfully lit the engine multiple times under varying combustion modes. Further hot fire tests will be run with backend imaging to confirm detonation.

It is suspected that the torch igniter did not light the engine due to poor mixing and low residence time of the reactants. To mitigate this issue, a new injector has been machined and is ready to be included in full-scale testing. If this does not solve the issue of combustion, an area reduction at the throat of the aero-spike will be included to improve the chances of detonation. Additionally, the process of load cell calibration past the peak expected thrust should be further streamlined, potentially with hydraulic methods. Another improvement would be to make a larger DAQ box with a single c-DAQ unit to centralize and simplify the DAQ system and wiring.

Table of Contents

List of Figures

List of Tables

Glossary

CEA – Chemical Equilibrium with Applications
CFD – Computational Fluid Dynamics
CTE – Coefficient of Thermal Expansion
CV – Flow Coefficient
DAQ – Data Acquisition
DDT – Deflagration to Detonation
DFM – Design for Manufacturing
FEA – Finite Element Analysis
FMECA – Failure Modes and Effects Criticality Analysis (also FMEA)
FOD – Foreign Object and Debris
GH2 – Gaseous Hydrogen
GN2 – Gaseous Nitrogen
GOx – Gaseous Oxygen
GUI – Graphical User Interface
ID – Inner Diameter
IO – Input/Output
JAXA – Japanese Aerospace Exploration Agency
JIC – Jet-in-Crossflow
MEOP – Maximum Expected Operating Pressure
NASA – National Aeronautical and Space Administration
NI – National Instruments
NPT – National Pipe Thread
OD – Outer Diameter
ORB – O-Ring Boss
OS – Operating System
PERL – Propulsion and Energy Research Lab
PGC – Pressure Gain Combustion
PPE – Personal Protective Equipment
PRV – Pressure Relief Valve
PT – Pressure Transducer
R&D – Research and Development
RDE – Rotating Detonation Engine
RTD – Resistance Temperature Detector
RTV – Room-Temperature Vulcanizing
SABR – Small-Scale Air-Breathing RDE
SS – Stainless Steel
TC – Thermocouple
TRL - Technology Readiness Level
U.S.A. – United States of America
UCF – University of Central Florida
USB – Universal Serial Bus
ZND – Zeldovich Von Neumann Döhring

1 Introduction

Rotating Detonation Engines (RDEs) have been investigated as a novel propulsion concept since the 1950s and 60s. However, early research was hindered by an incomplete understanding of supersonic combustion, limited high-speed diagnostic capabilities, and the inability of contemporary materials to withstand the extreme thermochemical environments produced by detonation waves. With advancements in computational modeling, experimental diagnostics, and high-temperature materials in the 21st century, organizations like JAXA have successfully demonstrated full-scale flight-capable RDE prototypes [1], underscoring the technology's potential for space applications. Despite this progress, a significant gap remains in the development of air-breathing RDEs for atmospheric propulsion. These systems offer a compact, lightweight, and highly efficient alternative to conventional engines, capable of operating across a broad flight envelope, from takeoff to hypersonic speeds, making them a compelling candidate for next-generation aerospace vehicles.

Project SABR (Small-Scale Air-Breathing Rotating Detonation Engine) centers on the design, fabrication, and testing of an air-breathing RDE powered by gaseous hydrogen and atmospheric air. This includes the development of a compact igniter, a robust test stand, an optimized fluid feed system, and an integrated data acquisition suite. A key challenge in this configuration is the presence of nitrogen in the air, which acts as a thermal sink and dampens detonation propagation. To address this, targeted experiments have been conducted to isolate the role of nitrogen and its influence on small-scale detonation stability.

This report transitions the project from conceptual design to full-system validation, detailing efforts in risk assessment, performance modeling, and prototype testing. SABR serves as a foundation for future student-led innovation in sustainable propulsion, advancing RDE technology toward real-world implementation with hydrogen-based aviation, supporting a cleaner, more efficient future for air travel.

2 Project Objectives and Scope

2.1 Scope Statement

SABR Senior Design 2025-2026 has mainly focused on the physical construction, integration, and functional testing of the RDE and its supporting infrastructure. All components were designed for short-duration ground testing using gaseous hydrogen and air. While design philosophy considered future applications to flight vehicles, this design is by no means flight ready. All tests are limited purely to short duration (less than 1 second) static tests; including cold flows and controlled hot fire testing. Flight integration, long-duration, and varying equivalence ratios are out of scope for this project's objectives. Computational modeling was used purely to inform design parameters, not validate full system behavior. Emphasis was placed on producing a reusable and robust system that can generate reliable data for future groups.

2.2 Long Term Goals

- Advance an air-breathing hydrogen-fueled RDE toward a technology readiness level capable of passenger flight.
- Develop a compact, flight-capable ignition system suitable for flight applications.

2.3 Planned Semester Objectives

- Establish a modular test platform for experimental testing of RDEs for future senior design teams to use.
- Develop and validate a reliable data acquisition system for future senior design teams.
- Manufacture and assemble an operational RDE prototype for testing.
- Conduct final testing to obtain thrust measurements.
- Demonstrate performance and reliability of test stand and data-acquisition system under real operating conditions.

- Determine optimal timing and pressure setpoints for stable igniter operation.

- Determine required chamber pressures and mass flow rates for sustained detonation in the RDE.

3 Assessment of Relevant Existing Technologies and Standards

3.1 RDE Combustors

RDEs are a developing form of propulsion and power generation that utilize the radial propagation of detonation waves within an annulus to combust propellants. These combustors have been proven to work with a combination of solid, liquid, and gas fuels with liquid or gas oxidizers[6, 5]. They can run in either air-breathing or rocket modes. Additionally, small-scale rocket RDE combustors have been demonstrated as feasible; however, much work remains to characterize their operation with different sizes, propellant combinations, and operating conditions due to the remaining work that needs to be conducted on detonation physics and how it changes in RDEs with high curvature[8, 9].

Detonation is one of two forms of combustion (deflagration and detonation) that uses reacting, propagating shock-waves to induce combustion of reactants through autoignition. The detonation thermodynamic cycle, the Zel'dovich-von Neumann-Döring (ZND) cycle, shows a pressure gain during the heat addition process, which provides a greater work output[23]. This principle is why RDEs are such an attractive technology. If a higher work output per propellant mass is achieved, it can decrease the cost and weight required for a system as well as its environmental impact.

The ZND detonation model is characterized by a compression wave followed by a reaction zone, then an expansion wave. When the compression wave interacts with reactants, there exists a spike in pressure, density, and temperature of the chemical species. This in turn induces high pressure combustion and volume expansion, which causes the compression wave to propagate. The wave then propagates at a theoretical velocity, called the Chapman-Jouguet (CJ) velocity. This velocity can be determined by applying the definition of the Mach number (Ma) to the upper CJ point, which is the intersection of the Rankine and Hugoniot lines[6].

In practice, the velocity experienced in RDEs is about 60% of the CJ velocity. The explanation as to why this occurs is still heavily debated, but it is theorized that it is attributed to parasitic deflagration, where reactants combust due to deflagration. Due to the detonation combustion not being present in all the propellant injected, there is not an ideal pressure rise. This causes a decrease in the pressure applied to the compression wave. Thus, it does not propagate at

the ideal theoretical speed[7].

In aircraft engines, the performance parameters are typically the thrust generated, the specific impulse, the work output, and the thermodynamic efficiency. For a combustor, the means of optimizing these are through achieving full combustion by optimizing parameters such as equivalence ratio, mass flow rate, and the dimensions of the combustor. However, there are some additional unique parameters that affect RDEs.

It has been shown that detonation cell size is correlated to the overall performance of RDEs. This is because if the detonation cell size is large compared to the annular gap, there will not be enough detonation cells to induce new cell formation and thus wave propagation. This cell size is highly dependent on the propellant mixture and the pressure of the mixture prior to wave interaction[11, 12].

Various propellants have been tested in RDEs, especially small-scale RDEs. For the case of Project SABR, we will be using air as an oxidizer. Thus, the fuel chosen must optimize the key performance parameters of RDEs. The limiting parameter for our operation is the detonation cell size. The two fuels that have cell sizes small enough for a small-scale RDE are Hydrogen and Methane. From experimental data, it is shown that the cell size of Hydrogen is an order of magnitude smaller than Methane at our desired operating pressure, and thus will maximize our ability to achieve an ideal operation. Additionally, Hydrogen requires less energy input than Methane to induce detonation, and thus is a desirable choice[10].

Small-scale RDEs have been tested with a variety of designs and propellants. There are a series of theses from the Air Force Institute of Technology that have built on designs and reported challenges faced during operation. Additionally, they provide a template for small-scale RDE design for combustion, stabilization, injection, and material choice[8, 9].

Additionally, a three-inch RDE using air and Hydrogen was tested for operating condition limits in a collaboration between researchers in Beijing, China and Warsaw, Poland. It found stable detonation, quasi-stable detonation, unstable detonation, and fast-deflagration combustion for a variety of mass flow rates and pressure ratios. They also studied the detonation wave dynamics during their operation. Their findings for optimal operation will serve as guardrails in our desired flow properties[11].

Overall, detonation combustion is a very useful and efficient process of providing work to a system. The combination of physical, chemical, and thermodynamic models will lead to the definition of key performance parameters. This analysis can be complicated, but by using and customizing proven methods, it can be done relatively easily. Applying the known detonation properties of fuels to key performance parameter definitions and related equations, the resultant values should be compared to inform the decision on which fuel to use. Additionally, the phase at which the propellants are injected into the combustor may have an impact on performance, and thus should be taken into consideration during the analysis and/or decision-making process. Using proven methods of analysis, reviewing past successes and failures, and the effect of performance parameters on other design choices will assist in improving the quality of the system and the engineering process.

3.2 Injector Design Considerations

The overarching purpose of an injector is to introduce the propellants into the combustor and mix them as homogeneously as possible. There is not much variation between injectors for RDEs and conventional engines from a fundamental standpoint, as all compressible gas dynamics relations still apply when it comes to orifice sizing and performance. However, certain nuances apply that allow for easier initiation and maintenance of the detonation wave. Similar to conventional deflagration-based engines, the most basic type of injector geometry is impinging. Impinging injectors feature two streams of propellant colliding into a singular spray cloud, allowing for atomization of liquid propellants, as well as mixing for both gaseous and liquids. The mixing is determined by the angles and relative mass flows of each element. Mixing efficiency is directly connected to relative velocities between the propellants, as the overall goal is to introduce shear between the two with the intent of generating turbulence.

Jet-in-Crossflow (JIC) injection consists of one of the propellants being injected axially, while the other one is injected radially so the jets meet at 90 degrees from one another. This induces a large amount of mixing for a relatively simple geometry and allows for the propellant chosen to go through the center body possibly being used for regenerative cooling. JIC also allows for partial pre-mixing, where the jets are allowed to meet in a small cavity before transitioning to the annulus. However, a potential limitation for JIC comes from the difference in the

propellant streams. If the propellant put in crossflow cannot penetrate the other stream, the mixing capabilities are not fully harnessed, and mixing only occurs on the outer layers of the stream where they meet.

Mixing efficiency has been experimentally proven to correlate with detonation aspects such as wave speed, wave propagation, as well as conventional parameters such as thrust and specific impulse. Bigler et al. demonstrate the effects tied to these parameters, with one of the highlights being that improper mixing leads to counter-rotating waves, which are unfavorable due to their association with lower operating frequencies and wave speeds. These effects are also heavily dependent on local equivalence ratios. A combustor environment with poorly mixed propellants has experimentally been shown to have much more of an impact on wave propagation than the overall equivalence ratio[3].

Another alternative injection method is a pre-mixed jet. This method involves mixing the two propellants in a pre-injection chamber or plenum. By mixing upstream of injection, the gases are in contact with each other for a longer period, also known as residence time. The mixing chamber also allows the two gases to reach near stagnation properties while occupying the same space, which results in higher gas-gas diffusion rates and allows for a near uniform mixture before the propellants even enter the chamber. The drawback of this is creating a potentially explosive mixture in the plenum with a high risk of explosion due to the partial backflow characteristic of RDEs.

Key Items to Consider:

1. Well mixed propellants yield the best benefits in terms of thrust and specific impulse, similar to conventional (constant pressure) engines.

2. Smaller orifices with higher diodicity contribute to better injector replenishment rates, and reduced backflow in the environment directly downstream of the detonation wave.

3. Choked injectors tend to isolate the detonation waves from the feed system and help increase detonation stability.

4. Efficient injectors yield fewer but stronger detonation waves.

5. Injector design remains critical to achieve long-term detonation stability and needs to be carefully chosen to

meet the overarching goals for the RDE. Additionally, a proactive approach towards design for manufacturing and refurbishment capabilities is beneficial to maximize the testing time and the ability to recover from damage and erosion to internal engine components.

3.3 Data Acquisition and Control

Data acquisition is the backbone of any experimental setup. The accuracy and reliability of the collected data determine the extent to which conclusions can be drawn from the experiments conducted. Strategic placement of thermocouples, pressure transducers, flow controllers, load cells, and other instruments is required to evaluate and document critical test parameters and outcomes. These sensors are read and translated using DAQ devices, each of which has a maximum sampling rate and a maximum number of channels that sensors can occupy. These parameters determine how the DAQ is configured and what sensors can be utilized in this system.

Several factors play a critical role in this project, and although all the topics presented in the technology study memo are important, one of the most vital is the sampling rate. This is because the rest of the parameters heavily rely on high-quality, top-of-the-shelf sensors—which is not a luxury we can afford. Sampling rate, on the other hand, can be easily configured and is set by the DAQ itself. The specific DAQ model we purchased (NI USB-6210) has the capability to sample up to 250 kS/s. However, this is not 250 kS/s per channel; it is the total combined sampling rate across all channels. Due to the quick operation time and short duration of our tests, a high sampling frequency is recommended to observe the full scope of phenomena occurring within the system. In reality, sampling at a rate of 10 kS/s per channel would be more than sufficient for our sensors.

Another consideration when designing the data acquisition schematic is the number of DAQ channels. This is also a highly important topic, as it determines how many total sensors we can utilize in our system. With the selected hardware—NI USB-6210, NI USB-6001, and the Arduino—we have a combined total of 30 analog voltage inputs (±10V), 2 analog voltage outputs, 4 digital inputs, 4 digital outputs, and 25 digital I/O. The analog input channels are where the sensors will reside and thus are the most important here. The analog channels can be configured in either single-ended or differential mode. Single-ended only utilizes one channel per sensor, using the common ground as

the reference. While this allows the use of all 30 channels, it introduces a significant amount of noise in the resultant data. Differential, on the other hand, uses the common from the sensor as the reference voltage, thus producing a much cleaner signal but occupies 2 channels per sensor. After assessing the needs of each sub-system, we have decided to proceed with the differential configuration for all sensors. The total number of sensors we need at this stage is minimal and can be reduced to fit within the 15-channel maximum.

With these DAQ restrictions in mind, sensor selection may begin. However, given the budget constraints, there will likely only be a few options. Nevertheless, the following sensor parameters still greatly affect how the data acquisition is implemented and understood: accuracy, resolution, range, sampling rate, and response time all play a critical role in sensor selection. For additional information on sensor selection, please refer to Milestone 3, Section 3.4.

Data acquisition is the most important factor when it comes to experimental testing. Without clear, concise, and reliable data, the results of an experiment are left unsupported. To procure reliable data, the optimal selection of sensors must be completed by quantifying expected outputs and selecting sensors that adhere to the accuracy, resolution, range, sampling rate, and response time requirements of the system. These sensor selection parameters can be applied to the small-scale RDE system to evaluate critical measurements such as fuel flow rate, oxidizer flow rate, specific impulse, fuel injection parameters, and wave propagation speed.

3.4 Test Stand Configuration

The purpose of this technology assessment is to provide background information on the design requirements for a test stand tailored to small-scale air-breathing rotating detonation engines (RDEs) and their impact on the project as a whole. This section outlines the essential principles of test stand design and assembly, describes relevant technologies for thrust measurement, and explores their implications for the successful testing of RDEs. The following information has guided the process of further defining our project requirements, informed system architecture development, and enabled further investigations into the testing and evaluation of test stand technology.

Throughout the project, the focus has been on designing a test stand capable of meeting the structural, measurement,

and operational demands that are unique to RDEs. Unlike conventional rocket engines, RDEs generate thrust through supersonic detonation waves, which introduces many challenges to the design and development process. These factors require a specialized approach to test stand design, enabling reliable structural stability and high-accuracy thrust data collection. The two primary goals of test stand development are: providing stability to minimize external forces on engine performance and enabling precise thrust measurement. Addressing these ensures the test stand serves as a reliable platform for evaluating RDE performance.

One of the most important features of the test stand is the ability to combine robustness with adaptability under extreme operating conditions. Through research, two frequently used structural support techniques emerged: mounting the engine on linear rails to constrain motion along one axis, or mounting it to a floating plate connected only by load cells. Linear rails direct thrust forces more accurately into load cells, minimizing distortion from lateral forces. Floating plates offer similar benefits while being simpler and cheaper to fabricate.

Calibration of load cells is another crucial feature for ensuring accurate thrust data. Two common calibration methods emerged: using a hydraulic ram and static structure to apply a known force, or using a mass and pulley system where known weights apply a force. Both approaches have trade-offs, and selection depends on project limitations. Regardless of the method, calibration is essential to validate thrust readings.

The test stand must also accommodate all actuators, electronics, and support systems required for safe and reliable engine operation. The DAQ and control system will be closely integrated with the test stand, with all electrical connections routed through the structure to their respective sensors and controllers.

While the test stand does not directly affect the RDE's internal combustion process, its design decisions have significant implications on budget, manufacturability, and timeline. Each design trade-off involves balancing data accuracy, cost, and complexity. Simpler designs may be favored when project constraints are tight, as long as they fulfill the primary requirements. Moreover, some configurations offer better adaptability for future RDE iterations, though they may be more costly and complex.

In conclusion, the test stand is a vital component of RDE system development. Its design supports safe, accurate, and reliable testing, enabling detailed evaluation of RDE operational characteristics. Drawing from proven designs

will ensure the test stand meets the rigorous demands of RDE experimentation and contributes significantly to the overall success of the project.

3.5 Fluid Systems

Introduction

There are many considerations when it comes to the design of the test stand feed system for a small-scale air-breathing rotating detonation engine (RDE). The goals of project SABR are to design, build, and test the RDE and determine the ranges of total mass flow rate and equivalence ratios over which the RDE can operate and produce stable detonation. This section introduces the propellant feed systems in the context of the project as well as the fundamental principles of fluidic hardware, fluid flow, and the safety and handling of high-pressure systems.

Small-scale RDEs reduce the requirements for fuel and oxidizer flow rates, which makes the RDE more portable and easier to iterate upon [7]. This is due to the small channel geometries of these engines, which result in lower mass flow rates, smaller detonation cell sizes, and higher frequencies of operation [9, 8, 10]. One of the biggest challenges is refreshing propellants quickly enough to ensure proper mixing. Although this is mainly the injector's responsibility, a steady, repeatable feed into the injector plenums is crucial to reduce transience. Flow rates are calculated from detonation cell size, chamber radii, channel widths, combustor lengths, and frequencies. Equivalence ratios, calculated based on equilibrium conditions [5], help maximize reaction efficiency.

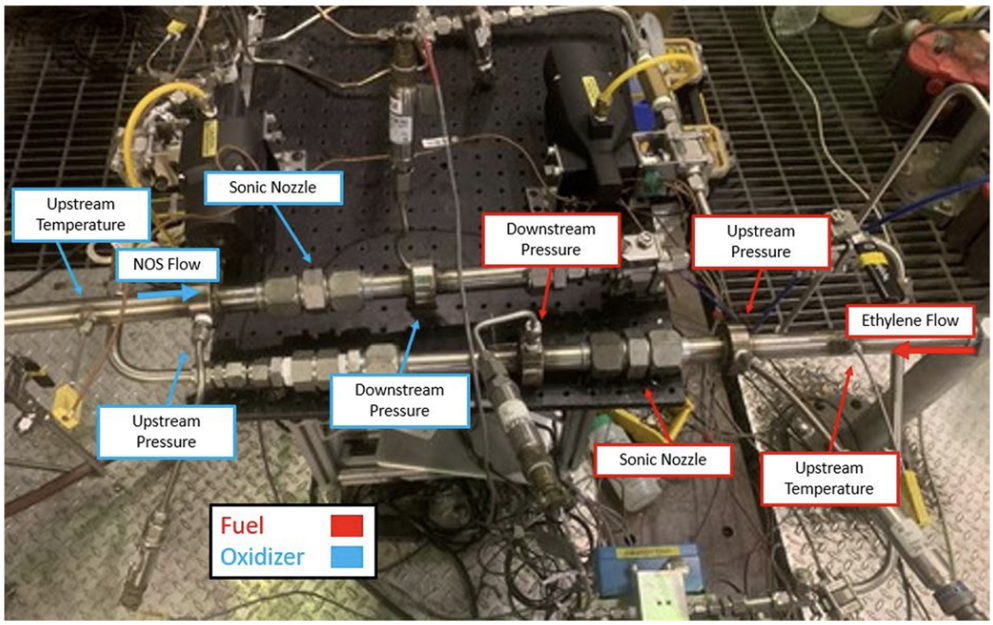

Figure 43. Position of Pressure Transducers and Thermocouples in relation to Sonic Nozzles

Figure 1: Example of RDE feed system [from Wyatt]

Feed System Considerations

Reactants must be replenished in the detonation channel before each wave [9, 8, 10]. Detonation waves can temporarily block flow through injector inlets due to extreme downstream pressures [9]. Required propellant flow rates depend on parameters such as cell size and fill height [9, 10, 11, 12]. These flow rates, along with equivalence ratio, will be derived from isentropic and compressible flow equations [14, 15].

Mass flow meters can be inaccurate due to oscillations, but sonic orifices offer a robust alternative. With known upstream conditions and geometric constraints, flow rates can be calculated and averaged for accuracy.

To simulate air-breathing conditions, separate lines for air and hydrogen will be used. These lines will use sonic orifices for metering and control. Plenums upstream of injectors help distribute flow evenly. Plenum-to-chamber pressure ratios should maintain choked conditions at injectors, enhancing detonation characteristics [5, 7].

Choking is vital for preventing backflow. Without it, detonation waves can increase line pressure and destabilize the system [9].

Fluidic Components and Hardware

Precise flow control will be implemented using solenoid valves driven by the DAQ system. Key performance metrics like pressure, flow, temperature, and thrust will be measured.

Flow losses will be characterized by CdA or Cv, which account for resistance in bends, valves, and orifices [20, 21, 22]. These losses require careful modeling and validation to ensure correct operation.

Fitting types may include Swagelok, NPT, ORB, JIC, and cone-thread. Swagelok and NPT are favored for sealing under high pressure. Tubing material will primarily be stainless steel, selected for pressure compatibility and minimal losses.

Safety Protocols

Testing involves high-pressure gases such as hydrogen and compressed air. Handling requires adherence to rigorous protocols using PPE and constant monitoring [17, 18, 19]. Cleaning—especially for oxygen compatibility—is essential to prevent contamination or combustion.

System integrity will be protected by PRVs and burst discs, designed to activate when safe pressure thresholds are exceeded. Components will also fail in safe states in the event of power loss.

Design Summary

Small-scale RDE feed system design demands careful control of mass flow, equivalence ratio, and reactant quality. These factors are harder to manage in compact systems. The feed system must mitigate backflow, friction losses, and contamination while maintaining stable performance.

Ignition Strategy

Ignition of fuel-oxidizer mixtures occurs via either deflagration or detonation. Detonations propagate at supersonic speeds, forming shock waves that pre-compress unburned reactants. This leads to rapid and powerful combustion [23].

Deflagration-to-detonation transition (DDT) depends on mixing quality and channel length. In a confined tube, subsonic deflagration accelerates via shock reflection and focusing, forming a detonation front if allowed sufficient distance [24].

Pre-detonation igniters exploit this transition by filling a long tube with propellants and triggering via spark. The resulting detonation travels into the main combustor. While powerful, the process can stress engine components if misfired.

Alternatively, torch igniters offer a controlled heat source for initiating combustion directly within the annulus. Though less likely to damage components, they introduce thermal concerns and require more complex control. This project uses a torch igniter that can be retrofitted for detonation tubes if needed. Success with the torch method simplifies integration into flight systems-an essential goal for SABR.

4 Professional and Societal Considerations

4.1 Broader Impacts of RDE Integration

Rotating Detonation Engines (RDEs) have the potential to address several critical challenges within the aerospace community, extending far beyond propulsion performance alone. Owing to their inherently higher thermodynamic efficiency, RDEs can deliver significantly greater range for a given thrust and propellant mass. This not only reduces emissions and fuel consumption, but also allows for more compact propulsion systems, offering compelling economic, environmental, and safety benefits.

4.2 Economic Effects

Fuel costs represent a substantial portion of airline operating expenses, with up to 30% of the ticket price attributed to fuel, according to the International Air Transport Association [2]. By reducing fuel usage per flight, RDEs could meaningfully lower airfare costs, alleviating financial pressure on consumers.

Furthermore, transitioning from conventional deflagration-based turbofans to RDE-powered engines is expected to stimulate job growth within the domestic aerospace sector. The need for new engine manufacturing, testing infrastructure, and retrofitting of legacy aircraft would open numerous opportunities for engineers, technicians, and supply chain professionals, especially in regions supporting advanced manufacturing.

4.3 Environmental Effects

The SABR system is a hydrogen-air RDE, a configuration that promises drastic reductions in greenhouse gas emissions. For emissions analysis, a hydrocarbon-fueled RDE is assumed due to current hydrogen storage limitations in aviation. Detonations occur over millimeter-scale reaction zones, resulting in minimal residence time for incomplete combustion products. This short-scale, high-efficiency reaction minimizes carbon monoxide and unburnt hydrocarbon emissions. However, the elevated temperatures inherent to detonation combustion present challenges in limiting NO_x emissions. Current mitigation strategies, such as ammonia doping of the exhaust stream, are under investigation and could drive further research and employment in green propulsion.

4.4 Health and Safety

RDEs may also contribute to improved public health and flight safety. Environmentally, reduced engine emissions correspond to cleaner air and improved respiratory outcomes for communities near airports. From a safety perspective, the compact design of RDEs allows for multiple engines to be integrated onto a single aircraft, increasing redundancy in the event of an engine-out condition. Additionally, their efficiency reduces the required onboard fuel volume, lowering the risk associated with carrying large amounts of combustible material.

5 System Requirements and Design Constraints

The requirements for the SABR system are broken down into overall project requirements, as well as individual system requirements, broken down as follows: RDE, Test Stand, Fluid System, and Data Acquisition and Control Systems. All requirements can be found in Appendix A: Customer Requirements. The overall project requirements can be found in Appendix A's section titled "SABR Requirements", while the system requirements can be found in their respective sections of Appendix A. Each requirement has a specified requirement type and a verification method. The verification and validation methodology and results are presented in Section 9.

Nearly all system requirements were derived from the SABR Requirements. These included producing measurable thrust, attempting to demonstrate detonation, using atmospheric air as the oxidizer, having a small-scale combustor, being reusable, interfacing properly with the PERL facilities, being able to operate at various equivalence ratios, and not exceeding the cost budgeted through the allocated funds from the department, sponsorships, and team members.

6 System Concept Development

6.1 Igniter

There are ultimately several methods for ignition in rotating detonation combustors. Traditionally, literature has used two major methods with moderate success. These include direct spark ignition and pre-detonation tube ignition.

6.1.1 Direct Spark Ignition

In the case of direct spark ignition, the spark plug is allowed to directly engage with the propellants in the annulus, which when ignited after proper mixing, initiate the detonation wave. The major drawback to this method is that the longevity of the system is greatly reduced since the spark plug is exposed to shockwaves repeatedly, degrading it to an extremely early failure.

6.1.2 Pre-Detonation Tube Ignition

Predetonator (predet) tubes have been used extensively with major success. In this configuration, a length of tubing is filled with an explosive gas mixture and lit with a spark plug. The deflagration-to-detonation transition (DDT) is allowed to occur in a controlled manner along said length of tube. This yields a very repeatable starting energy input which allows researchers to isolate variables when performing operational testing of RDEs. The drawback to a predet tube becomes packaging, especially considering SABR's final goal of integration with a flight vehicle.

6.1.3 Torch Igniter Selection

The initial chosen approach was an unconventional one—a torch igniter. This method effectively incorporated the strengths of both the predet and direct spark ignition methods under the hypothesis that the DDT could occur in the annulus given an energetic enough flame. It moved the spark plug to an isolated chamber with very controlled propellant inputs like the predet but allowed for more compact integration with the RDE much like the direct spark ignition method.

As a backup, the system was designed so any sort of ignition system could be retrofitted if the torch igniter did not

perform correctly. A predet backup solution was kept on standby to ensure the system could be tested with a known working ignition system.

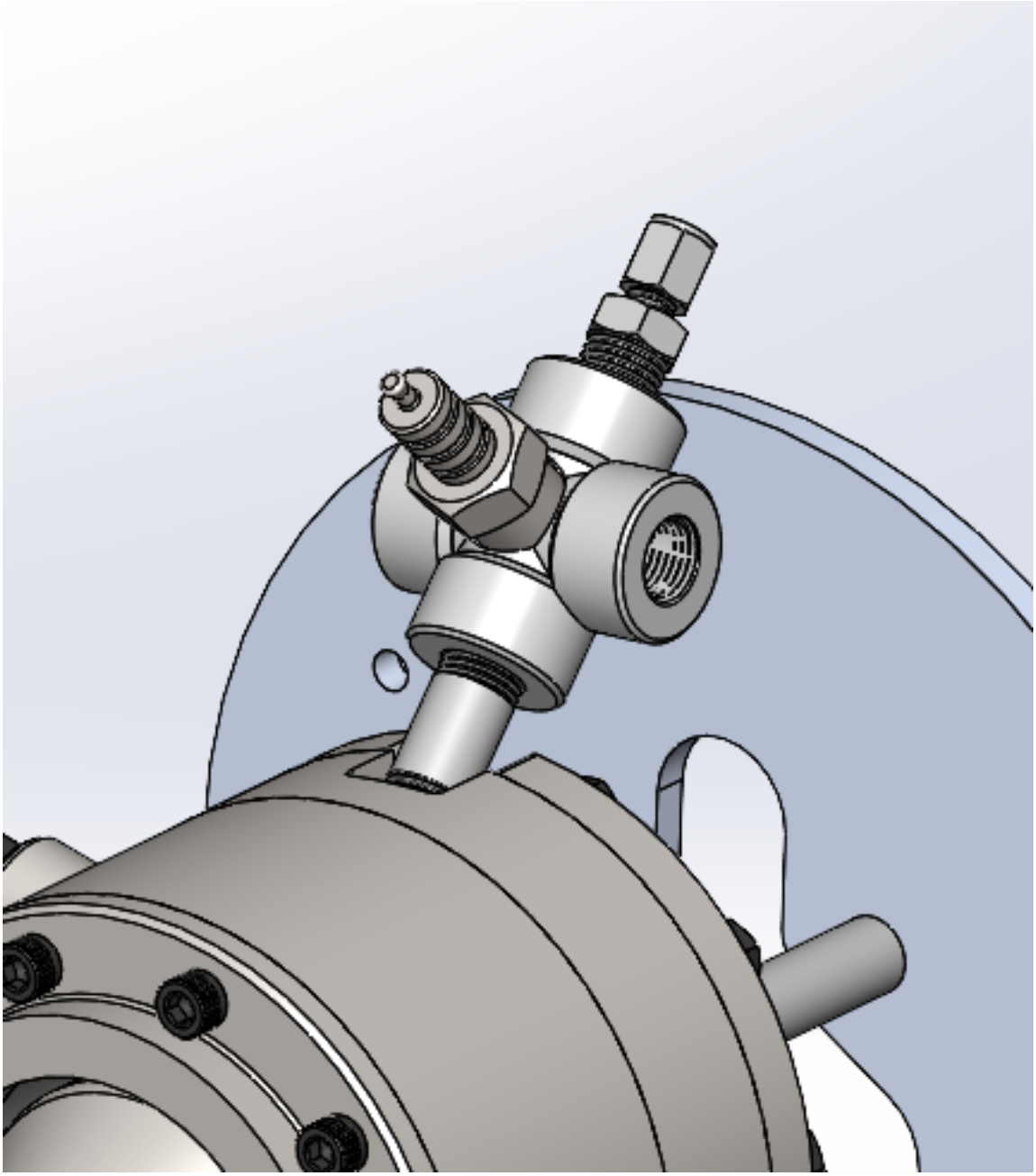

Figure 2: Final integration of the torch igniter on the RDE

6.2 Injector Design

6.2.1 Overview

The key challenge when designing injectors in the context of Rotating Detonation Engines (RDEs) is designing the elements to compensate for rapidly changing chamber pressures. For one cycle of the detonation wave, the injector will either be experiencing backflow into the plenum or exhausting into the chamber.

Therefore, it is common practice in gas/gas RDEs to design the injectors to be choked, where the outlet flow is sonic ($M = 1$). This allows for rapid flow recovery and short refill times, which are desirable for sustaining the detonation wave.

6.2.2 Choked Orifice Sizing

Using the classical equation for compressible choked orifices, the desired total cross-sectional injector area can be solved using:

$$\dot{m} = C_d A \sqrt{\gamma \rho_1 p_1 \left(\frac{2}{\gamma + 1}\right)^{\frac{\gamma+1}{\gamma-1}}}$$

Figure 3: Classical Mass Flow Choked Equation

where C_d is the discharge coefficient, A_t is the throat area, P_0 and T_0 are the total pressure and temperature of the upstream flow, respectively, and γ is the specific heat ratio.

6.2.3 Transient Chamber Pressure Effects

However, this model does not consider injector flow as a function of time, as the chamber pressure decays from peak detonation pressure back down to the initial plenum pressure. In our case, the initial static pressure of reactants is around 100 psi, and the peak detonation pressure (for an H_2/air mixture at $\phi = 1$, $T_0 = 293$ K) is around 2000 psi. This means the injectors are only flowing into the combustion chamber for approximately 10% of the cycle period. Chamber pressure as a function of time, as well as refill time and cycle period, is visualized in Figure 4.

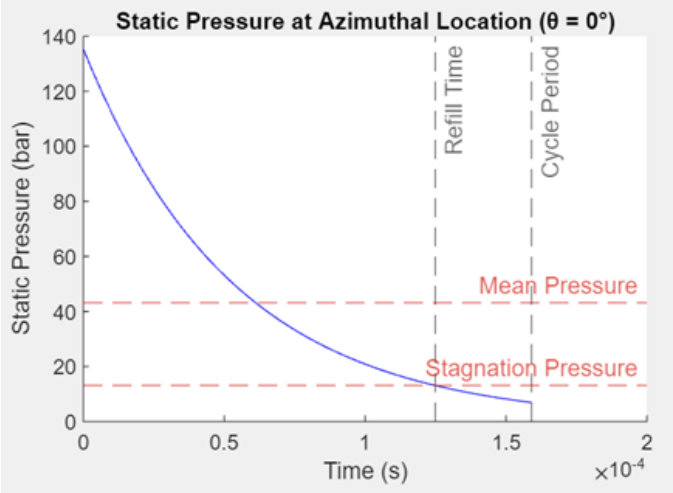

Figure 4: Static Pressure at azimuthal location

6.2.4 MATLAB-Based Injector Sizing Model

Plugging these values into the MATLAB-based Detonation Combustor Analysis (DCA) model, the diameter per injector element is obtained by accounting for transient pressure effects. This is shown in Figure 5.

The following time-dependent formulation is used to evaluate the instantaneous mass flow from the injectors during the refill cycle:

$$\dot{m}(t) = C_d A \sqrt{2\rho_1 p_1 \left(\frac{\gamma}{\gamma-1}\right)\left[\left(\frac{p(t)}{p_1}\right)^{\frac{2}{\gamma}} - \left(\frac{p(t)}{p_1}\right)^{\frac{\gamma+1}{\gamma}}\right]}$$

Figure 5: Choked Area Formula Solution

The MATLAB program uses the integral average of this formula to iteratively solve for the actual injector area needed, using the choked flow equation result as the initial guess.

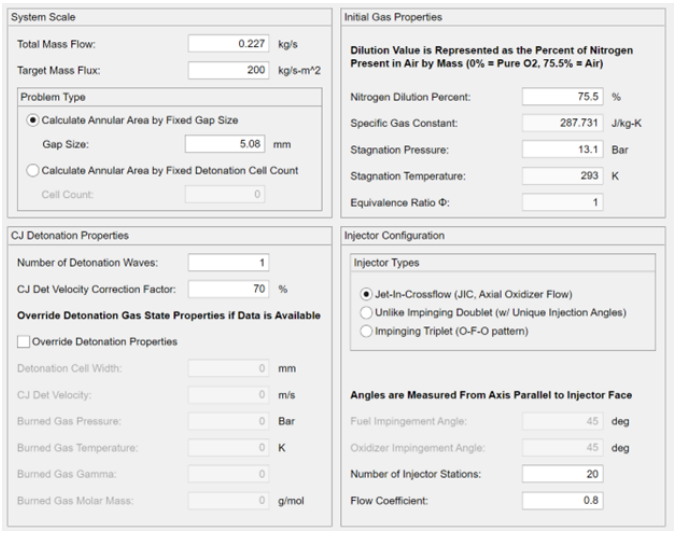

Figure 6: Inputs to the MATLAB program, 20 injector elements were used for the first version of the injector with an estimated Cd of 0.8

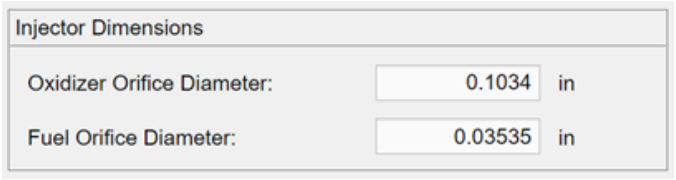

Figure 7: Injector diameter as displayed by the MATLAB program

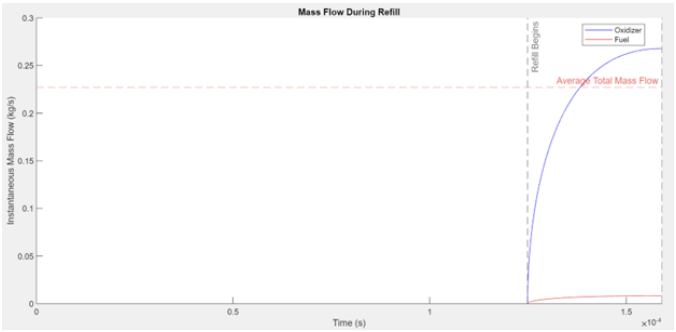

Figure 8: Resulting transient mass flow plot. Notice how the mass flow tapers off as the flow reaches the sonic condition and is choked

6.2.5 Model Parameters and Results

For the SABR engine, 20 injector elements were used in the first version, with an estimated C_d of 0.8. The injector diameter result is displayed in Figure 6, and the corresponding transient mass flow curve is shown in Figure 8.

Note the tapering of the mass flow rate as the chamber pressure rises and the injector approaches sonic choking

conditions.

6.3 Data Acquisition and Control

6.3.1 Software Selection

Data acquisition and control systems can be built in a variety of ways, particularly regarding software implementation. Early in the process, two software options—Synnax and LabVIEW—were evaluated. LabVIEW was selected as the primary system due to its robust documentation, wide industry use, and familiarity to the SABR team.

6.3.2 State Machine Implementation

A standard while-loop-based DAQ system was deemed infeasible due to the number of unique control sequences required. Thus, a state machine system was implemented using LabVIEW.

The state machine was constructed by placing a ‘case‘ structure wired to an ‘ENUM‘ constant inside a ‘while‘ loop. Each time the loop iterates, a state is chosen based on user input, and logic for that state is executed. Operations that should be executed regardless of the state—such as data reading, scaling, and saving—are placed outside the case structure.

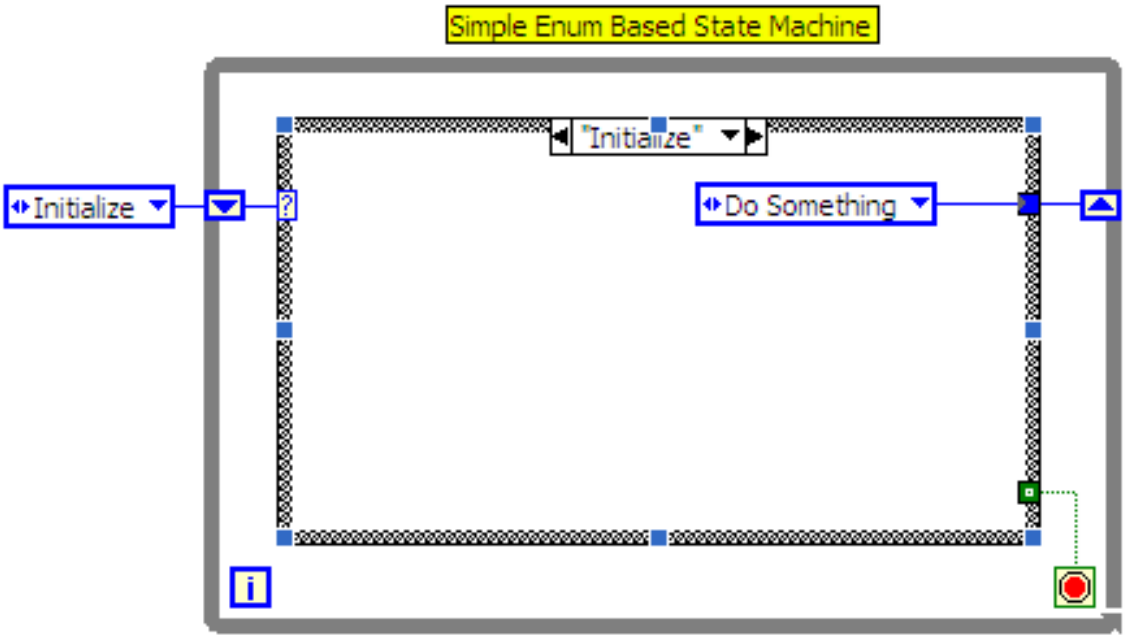

Figure 9: Example LabVIEW state machine for SABR DAQ system

6.4 Test Stand Configuration

6.4.1 Structural Design Considerations

The development of the experimental test stand involved exploring multiple structural configurations to address challenges in thrust measurement and operational stability. Key considerations included stability, load path management, ease of maintenance, modularity, and cost-effectiveness.

The use of 8020 aluminum extrusion allowed the test stand to remain modular while providing sufficient structural support. The design focused on integrating with load cells for thrust measurements and minimizing parasitic forces.

6.4.2 Engine Integration Methods

Two engine integration methods were considered:

- **Static/Floating Thrust Plate Configuration**: Engine mounted to a floating plate connected only via load cells.
- **Sliding Platform on Rails**: Engine mounted on a rail-guided platform that pushes into load cells.

Due to increased cost and complexity, the static/floating plate was selected.

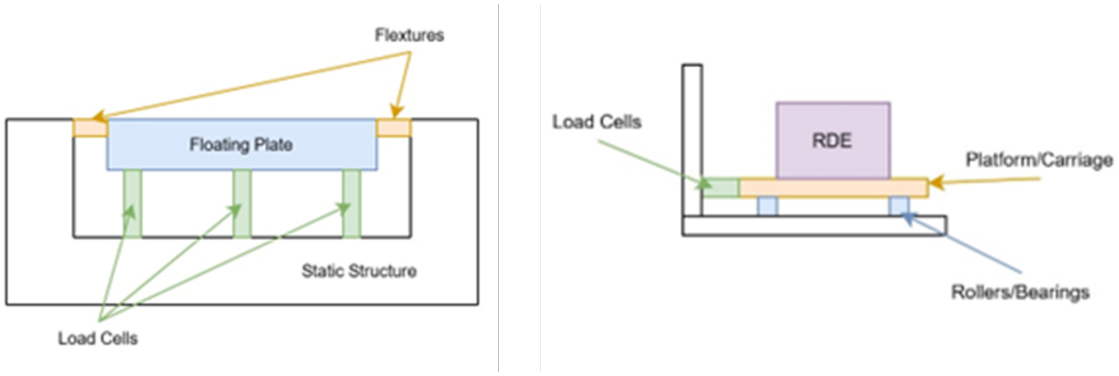

Figure 10: Comparison of static/floating thrust plate vs. sliding rail platform

6.4.3 Load Cell Calibration Approaches

Two calibration methods were researched:

- **Hydraulic Calibration**: Uses a hydraulic structure to apply known force.
- **Mass-Pulley Calibration**: Uses known weights on a pulley system.

The final design used the mass-pulley system due to its simplicity and low cost.

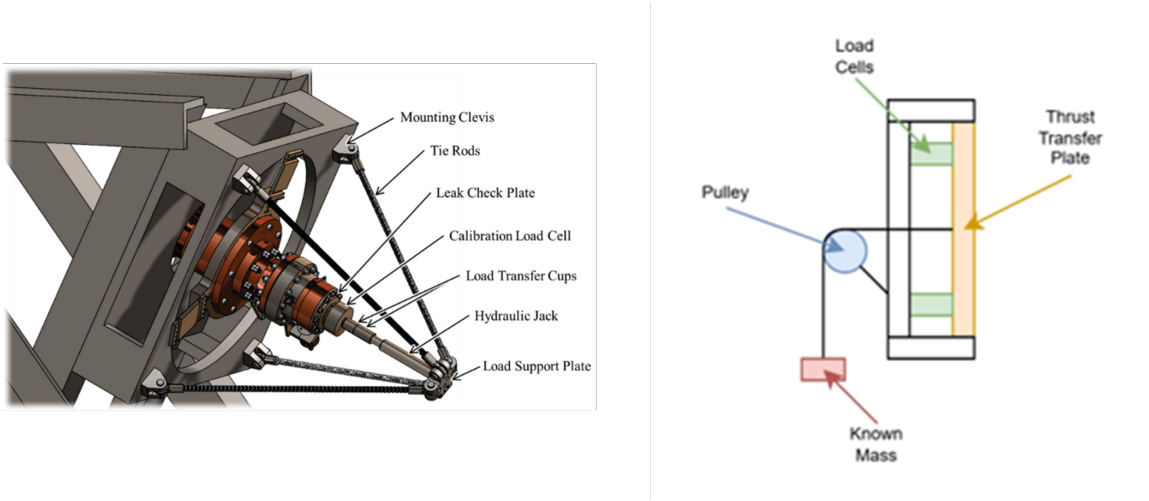

Figure 11: Hydraulic (left) vs. mass-pulley (right) load cell calibration systems

6.4.4 Final Stand Configuration

The final test stand was a five-foot 8020 aluminum frame mounted on a steel optical table. The modular design allowed flexible integration of plumbing and data systems. The engine integrated via a half-inch aluminum floating plate.

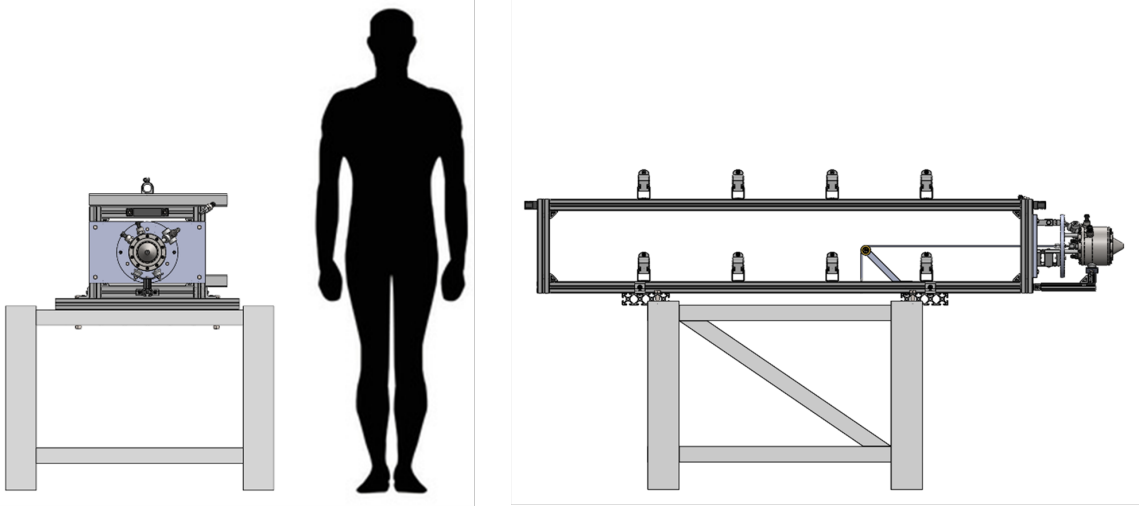

Figure 12: Final test stand design with integrated systems

6.5 SABR Fluid System Design

The SABR Fluid System was developed to deliver gaseous hydrogen and compressed air to the inlet plenums of the RDE body. The design prioritized robustness, safety, and simplicity, with a layout that allows for straightforward setup, testing, and teardown within the constraints of the test stand and available infrastructure. Two separate flow paths were constructed for the air and hydrogen lines, with each line designed around the expected flow rates, pressure requirements, and integration needs of the RDE.

6.5.1 Hydrogen Flow Path

The hydrogen line originates at a compressed gas cylinder and is routed through a primary regulator to reduce the supply pressure to nominal operating pressures. Following pressure regulation, the line is instrumented with a pressure transducer and a thermocouple to record upstream flow conditions. An O'Keefe orifice fitting is placed downstream to induce sonic flow, decoupling the upstream flow from any dynamic pressure oscillations that may originate from the detonation chamber [53].

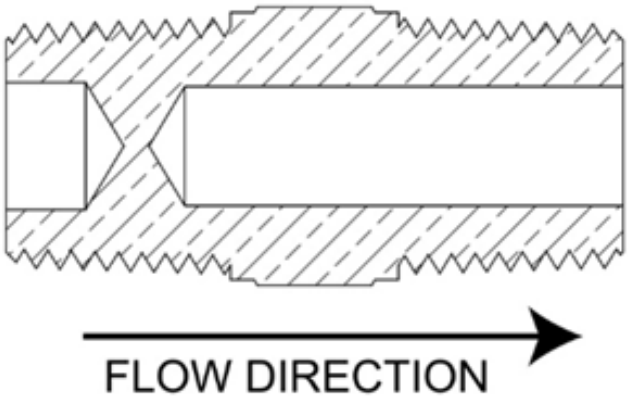

Figure 13: O'Keefe orifice fitting used to induce choked flow

The restriction is followed by a pneumatically actuated run valve, which controls the start and stop of hydrogen flow into the engine. A check valve is included downstream to prevent backflow, and the line terminates in a flexible stainless-steel braided hose that connects to the hydrogen inlet plenum.

6.5.2 Air Flow Path

The air line was designed with a similar flow path and instrumentation scheme. The SABR air line does not have a pressure regulator, as it relies on upstream pressure regulation via a dome-loaded regulator at the PERL facility. A restriction orifice union (ROU) is used instead of an O'Keefe fitting due to the higher flow demands [54].

Figure 14: Mac-Weld Restriction Orifice Union (ROU) for air line

The line features the same sensors and valve layout as the hydrogen line and is also terminated with a flexible hose to minimize rigid coupling between subsystems.

6.5.3 Choked Flow Strategy

As referenced in Section 3, establishing choked flow at the orifices was a central design strategy. This isolates upstream pressure conditions and enables control of the oxidizer-to-fuel (O/F) ratio by modifying inlet pressure and orifice diameter.

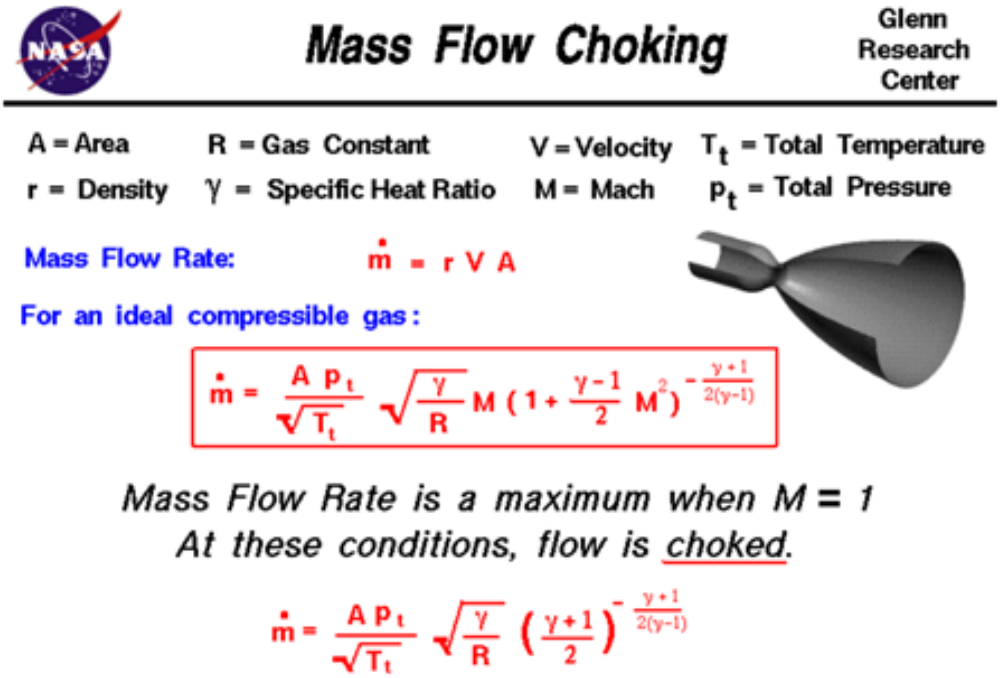

Figure 15: NASA Mass Flow Choking Equation

6.5.4 Flow Control Tradeoffs

Alternatives like mass flow controllers and sonic nozzles were considered. Sonic nozzles [55] are ideal for choked conditions, but cost-prohibitive. Orifice plates were chosen for simplicity and availability. Pneumatic run valves were favored for rapid control and were available at no cost. Solenoid valves were used in the ignition circuit due to their fast response and low flow requirements.

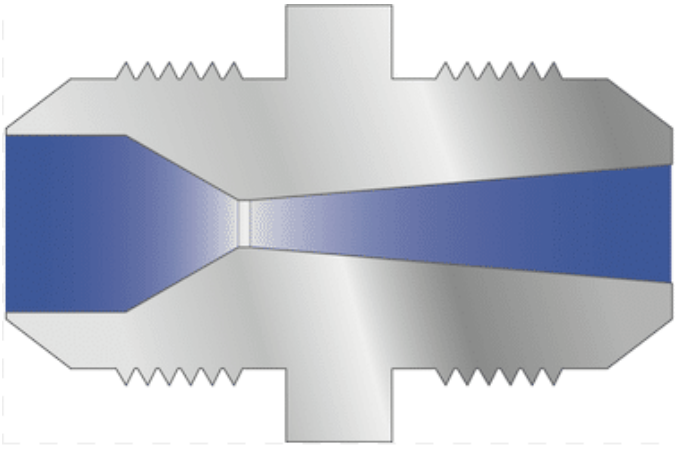

Figure 16: Sonic Nozzle Example

6.5.5 System Safety and Modularity

The system incorporates pressure relief valves (PRVs) and vent ports on all lines to prevent overpressurization and ensure safe depressurization in failure scenarios. Multiple isolation valves and vent lines enable modularity, ease of maintenance, and safe teardown.

Overall, the system emphasizes reliability and adaptability for supporting the unique requirements of rotating detonation engine experimentation.

2

7 Design Analysis

7.1 RDE Modeling and Analysis

The Rotating Detonation Engine (RDE) has undergone a rigorous series of system validations to ensure a well-defined and operable design. Every design decision has been based on the most up-to-date scientific principles, experimental data, and industry consultation. The system has been designed for seamless integration with adjacent subsystems, ensuring compatibility and alignment with previously established performance objectives.

Figure 17: Full RDE Assembly

To facilitate a successful design and pre-manufacturing validation, geometric models have been created for each individual component as well as the full system. Interfaces have been carefully designed to support easy integration. Each design decision and material selection was made with considerations for manufacturability, assembly, and overall functionality. Engineering drawings have also been drafted and reviewed by technicians to verify dimensional accuracy and fabrication feasibility.

Fundamental engineering principles applied to this system include:

- Compressible gas dynamics
- Combustion and detonation theory

- Plumbing
- Data Acquisition (DAQ) Integration
- Structural Analysis
- Material Compatibility
- Design for Manufacturing (DFM)

Analysis has been conducted using a variety of techniques, ranging from general zero-dimensional analysis to full-system Computational Fluid Dynamics (CFD) and Finite Element Analysis (FEA).

7.2 Static Structural FEA

The finite element methods performed to analyze the structural capabilities of the RDE cover an extensive variety of cases. In order to accurately break down and assess the sub-system and system capabilities of the prototype, separate models must be analyzed to prove positive margins on all system components.

Finite element methods are a sufficient method for validating design choices and boundary conditions. These iterative methods are very valuable in validating general analytical data while providing deeper insight into stress concentration locations that would be hard to calculate or unforeseen in the design selection and analytical solutions.

7.2.1 Bolt Pre-Tensioning

To follow the convention of bolt pre-tensioning, an analysis was performed using the 1.5 safety factor method for pre-tension. As calculated, the black oxide and stainless-steel bolts would be pre-tensioned to 600 lbf of preload, while the bolts holding the aluminum standoffs would be pre-tensioned to 300 lbf of preload, so as to avoid unnecessary stresses on the aluminum.

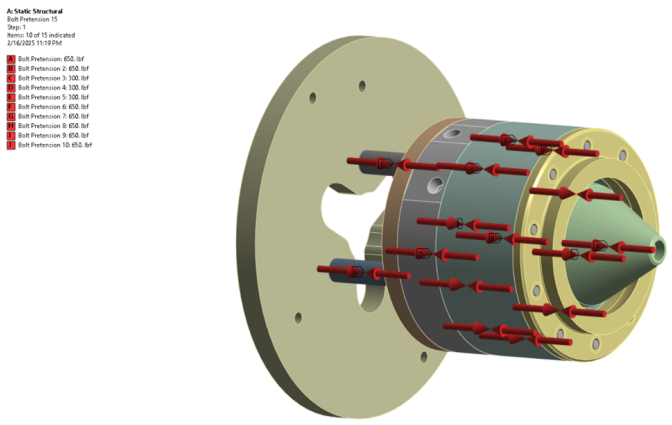

Figure 18: Bolt Pre-tension ANSYS Setup

7.2.2 Fixed Supports and External Accelerations

As the RDE will be mounted horizontally with load cells on the floating plate design (as evaluated during the M3 report), other factors must be considered. Required for all static structural simulations, a model must be constrained in all six degrees of freedom (DoF) to prevent infinite movement of the body. These faces of fixation were determined as the approximate cross-sectional areas of the interaction between the load cell and the floating plate. All load that is transferred from the RDE to the test stand will be through these points (and minimally through the plumbing system, whose stresses are neglected for these simulations due to unnecessary complexity and high flexure).

Additionally, gravity is accounted for in the simulation as acting in the direction of the specified orientation of the RDE when mounted to the test stand, to ensure that the body is able to maintain a stable position during static fire without altering the thrust vector.

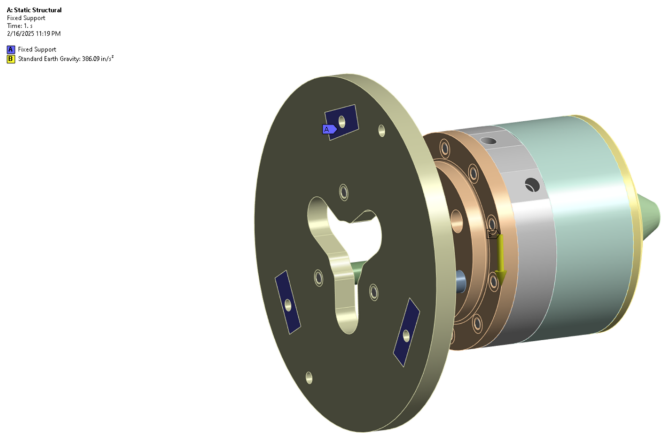

Figure 19: Load Cell Fixation Regions

7.2.3 Thrust and Pressures Applied

An extremely important facet of the simulation is an evaluation of the proper location and placement of the hydrostatic pressures and thrust transfer onto the body of the RDE. Some simplifications were necessary for model simplification and computational feasibility.

Fuel, oxidizer, and pre-combustion pressures were modeled to represent the plenum pressures of the fuel and oxidizer ports, as well as the post-injection static pressure. The post-injection pressure is not equivalent to chamber pressure, as there is a short distance before detonation occurs. A conservative flat post-combustion pressure of 1600 psi was used to bound worst-case scenarios.

Lastly, the expected thrust case of at most 200 lbf (with a likely lower value due to instability and unideal combustion) was distributed over the area of the aerospike to simulate the pressure thrust generated by the RDE.

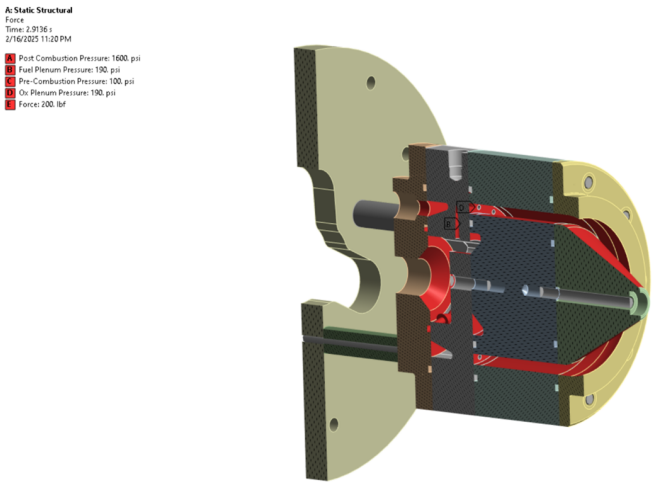

Figure 20: ANSYS Pressure Application Zones and Loads

7.2.4 Meshing and Element Quality Analysis

The quality of the finite element mesh is critical to the fidelity of the simulation. A balance must be maintained between mesh refinement and computational efficiency. Stress concentrations must be resolved adequately without causing excessive computation.

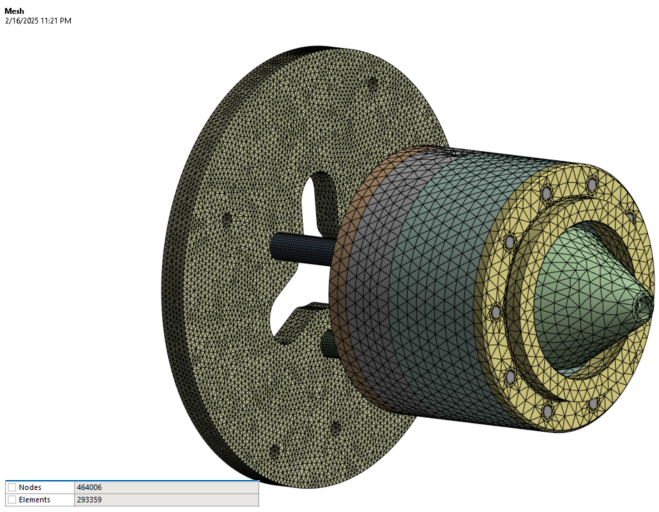

Figure 21: Mesh visualization showing node and element distribution.

The current model consists of approximately 293,000 elements and 464,000 nodes. Keeping the node count under one million allows for efficient computation while providing sufficient resolution.

Element quality is another critical metric, as elements with poor aspect ratios or distortion can significantly degrade solution accuracy. The mesh quality distribution shown in Fig. 21 indicates that over 90% of elements fall in the high-quality range (quality > 0.5).

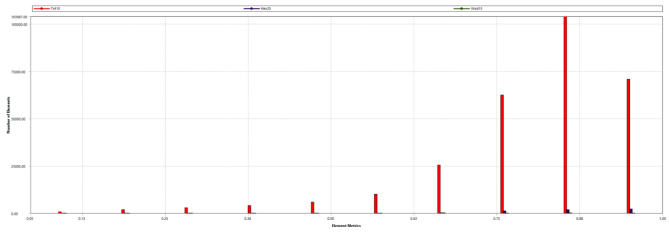

Figure 22: RDE Statistical Mesh Analysis Breakdown

7.2.5 Finite Element Results

The FEA results predict stress concentrations at expected locations. The RDE body itself does not experience high stress concentrations from internal pressures or generated thrust, even in worst-case scenarios. The highest stress occurs at the fixation interface of the floating plate, due to large bending stresses and sharp geometry around the load cell.

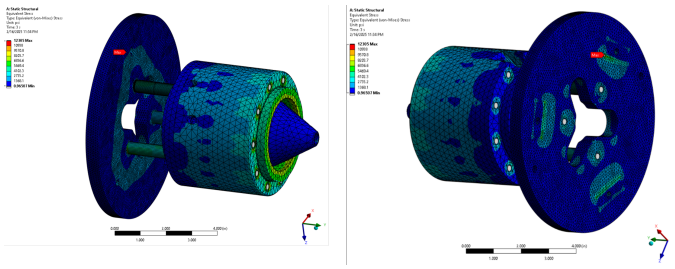

Figure 23: FEA stress distribution showing peak stress near plate fixation.

Despite localized high stress, the design maintains positive margins of safety throughout all critical components.

Table 1: Material Yield Properties

Material	Compressive Yield (ksi)	Tensile Yield (ksi)
SS-304	39.0	31.2
6061-T6	62.5	40.0

Table 2: Stress Evaluation and Margins of Safety

Location	Material	Max Stress (ksi)	Type of Stress	Margin of Safety
Aerospike	SS-304	2.38	Compressive	9.92
Cowl	SS-304	12.10	Compressive	1.15
Outer Body	SS-304	7.63	Compressive	2.41
Injector Plate	SS-304	6.15	Compressive	3.23
Port Plate	SS-304	6.76	Compressive	2.83
Inner Body	SS-304	5.76	Tensile	2.61
Standoff 1	6061-T6	10.36	Compressive	3.02
Standoff 2	6061-T6	10.62	Compressive	2.92
Standoff 3	6061-T6	11.12	Compressive	2.75
Floating Plate	SS-304	12.305	Compressive	1.11

As shown above, each component was evaluated with respect to their tensile or compressive yield stress. The values were extracted from the finite element simulation and subject to a Margin of Safety Calculation. All margins are above 0 (which represented as equal to 1.5 factor of safety). These values indicate that the RDE could take 2.11 times more loading capacity than what is expected and still maintain a 1.5 factor of safety.

7.2.6 RDE Modal Analysis

Modal analysis is extremely important to consider when analyzing cyclic systems. Vibrations play a large role in stress amplification and can fundamentally change the behavior and dynamics of how a system responds to loads

being applied to it.

To compensate for these probabilities, iterative methods must be used to find operating frequencies that can cause severe disruption or stress amplification. When performed in *ANSYS*, a limitation of the mode ranges varied from 9.9 kHz to 10.1 kHz to encompass the operational zone of the RDE, occurring at 10 kHz. As a result of the simulation, no modes were found in the performed range.

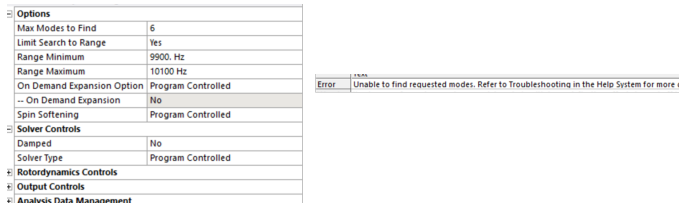

Options	
Max Modes to Find	6
Limit Search to Range	Yes
Range Minimum	9900. Hz
Range Maximum	10100 Hz
On Demand Expansion Option	Program Controlled
-- On Demand Expansion	No
Spin Softening	Program Controlled
Solver Controls	
Damped	No
Solver Type	Program Controlled
Rotordynamics Controls	
Output Controls	
Analysis Data Management	

Error	Unable to find requested modes. Refer to Troubleshooting in the Help System for more

Figure 24: RDE Modal Analysis

Another consideration, expanding on the previous idea, is the vehicle integrability of the system. A modal analysis is performed to prove no modal stress amplification in the event the prototype is to be integrated into a larger vehicle platform. A modal analysis is typically performed between 0 and 100 Hz to prove capability as per NASA specifications (source not disclosed).

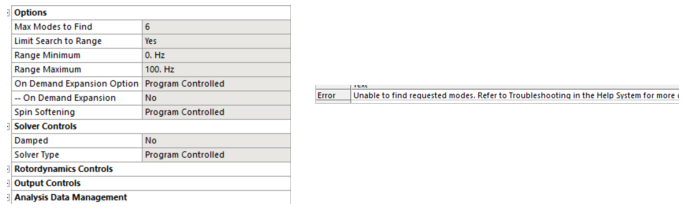

Options	
Max Modes to Find	6
Limit Search to Range	Yes
Range Minimum	0. Hz
Range Maximum	100. Hz
On Demand Expansion Option	Program Controlled
-- On Demand Expansion	No
Spin Softening	Program Controlled
Solver Controls	
Damped	No
Solver Type	Program Controlled
Rotordynamics Controls	
Output Controls	
Analysis Data Management	

Error	Unable to find requested modes. Refer to Troubleshooting in the Help System for more

Figure 25: NASA Vehicle Specification Modal Analysis

7.2.7 RDE Eigenvalue Buckling Analysis

Buckling analysis is also important to assess large beam deflection in the event of stress amplification. Because large beams are present in this model (the aluminum standoffs), there is a non-zero probability of stress amplification causing a buckling mode, as elaborated by Euler's beam buckling modes.

In the event of finite element methods, a buckling analysis is able to be performed using eigenvalues and stiffness matrices (mathematical formulation not elaborated in this report).

After performing the simulation, the first two buckling modes were found to be at 110.13 and 110.5 times the load

factor. What this means is that the current stress state of the RDE must be increased by a factor of 110 to achieve these buckling modes. Functionally, this is equivalent to a safety factor of 110 on the loads required to reach buckling. Both modes were found to be related to the standoffs (as predicted).

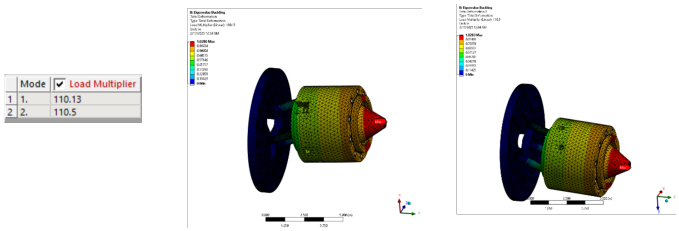

Figure 26: Eigenvalue buckling and load factors

7.2.8 Evaluations Not Covered in Finite Element Analysis

Thermal considerations were not evaluated in this simulation. Thermal convection and thermal expansion of the bodies due to the combustion gases pose a very complex analysis that requires the support of cluster computational models and fluid dynamic simulations.

At this point in time, little consideration has been given to performing these simulations, but basic analysis and "flight heritage" of the design and selection of materials/components for this RDE provide confidence in its resilience, even if such characteristics are unable to be quantified in this report.

7.3 Non-Reacting CFD

The CFD cases analyzed were mainly focused on the goal of analyzing the extent to which the propellants mixed upon injection in order to verify the design is capable of sustaining at least one rotating detonation wave. Computational Fluid Dynamics uses finite volume methods to iteratively compute fluid flow through a system and is made up of many codependent parameters to ensure an accurate result is outputted by the simulation. The topics regarding this CFD simulation are as follows: Solver Settings, Initial and Boundary Conditions, Mesh, and Results.

7.3.1 Solver Settings

This simulation was run in *STAR-CCM+*, using the 3-dimensional, steady, inviscid, and multi-component gas models. Inviscid was selected for this case as the computational cost required to run turbulence models is exponentially higher than that of inviscid. Additionally, since different turbulence models can have a drastic, positive or negative, effect on the diffusive mixing of gases, the decision to run inviscid takes the worry out of selecting the correct model, and gives us a baseline for the mixing, as turbulence and diffusion can only enhance the mixing efficiency in real life.

Steady was chosen over unsteady as small-scale high-frequency turbulence did not require analysis. This is also a non-reacting case so the unsteady effects of a detonation wave would not need to be captured. The multi-component gas model was selected to allow the analysis of hydrogen and air mixing. As hydrogen is a gas that is very responsive to changes in temperature, the Soret Effect model under multi-species was enabled. Implicit integration utilized second-order discretization. Unsteady low-Mach preconditioner was turned off as this is meant for a Mach of less than 0.3. Flow Boundary Diffusion was enabled, and the AUSM+ FVS Coupled Inviscid Flux model was used. The CFL method was set to automatic for the duration of the simulation.

7.3.2 Initial and Boundary Conditions

The full area of interest was set to the initial condition of standard temperature and pressure, with an initial velocity of 50 m/s in the $+\hat{y}$ direction to allow the implicit solver to begin without reaching a singularity. The initial mass fraction was set to be pure air.

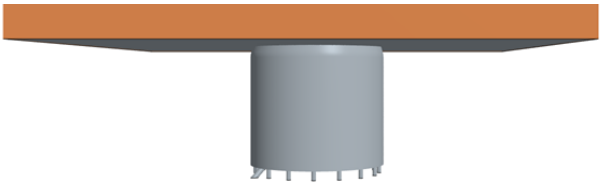

Figure 27: Simulation Fluid Volume

The area of interest analyzed begins at the hydrogen injectors and air injectors, given a freestream boundary with a

Mach number of 1, a static pressure of 100 psi, and a static temperature of 250 K to enforce choked conditions. The ignitor was set to a wall boundary, as this simulation is meant to model cold flow at operating conditions.

7.3.3 Mesh

Mesh generation is an incredibly important part of CFD. If a mesh is too fine, the solution may take an infeasible amount of time to converge to an accurate solution. If a mesh is too coarse, the results will not accurately capture local variations in the flowfield. Different locations within a simulation require different levels of refinement to achieve an accurate result, with fine cells at an inlet or outlet not letting the flow properly propagate, and a coarse mesh at the main area of interest causing a loss of accuracy.

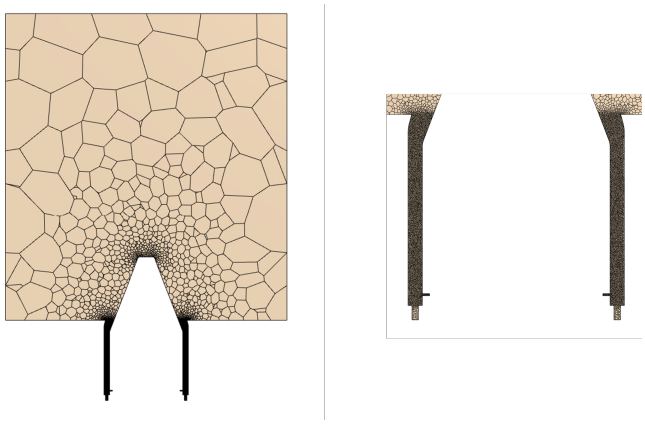

Figure 28: StarCCM+ Mesh

This mesh utilizes volumetric refinement with a slow growth rate to achieve a fine mesh in the annulus to capture mixing, while expanding to a large cell size at the outlet to ensure the flow within the annulus is not impacted by any extraneous conditions imposed by the program at the outlets. A polyhedral mesh is used with surface remesher enabled, a base size of 5 centimeters, with the area of refinement going down to 0.25 millimeters. Since this is inviscid, use of prism layers was not necessary.

7.3.4 Results

The results show an acceptable level of mixing. The figures below show the cross-section of the annulus halfway up the fill height, and the plane of an injector pair. While there are some local spots of higher concentrations, the flow

field shows a decent degree of mixing, with no absurdly high hydrogen hotspots, meaning the flow is effectively mixed with purely momentum diffusion interactions. In future experimental testing, with the added effects of real viscosity and viscous diffusion, the flow will be mixed enough to support the detonation.

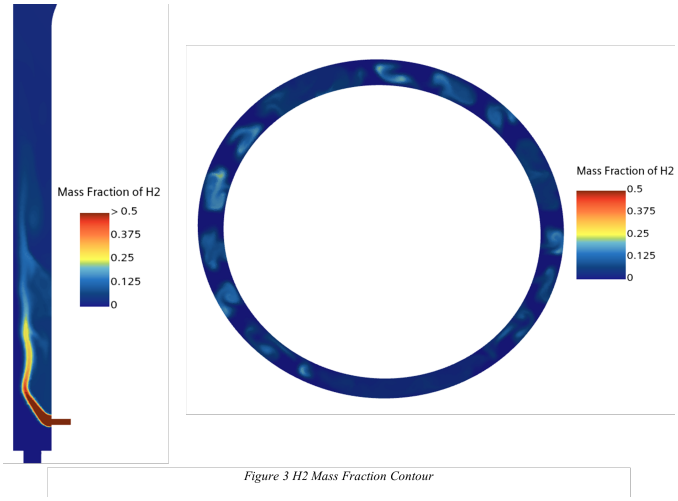

Figure 29: StarCCM+ Mass Fraction Results

7.4 RDE Simple Model - MatLab Analysis

Due to the nature of the scope of the project, a software tool was developed to provide combustor sizing and performance for any given air-breathing propellant mixture and mass flow. The program takes into consideration total system mass flow, stagnation pressure, chemical composition of air at various conditions, number of injector elements, empirical injector flow coefficient, and expected number of detonation waves. This provides the program with enough information to determine the state of the gas at pre-injection, post-injection, post-detonation, and post-expansion conditions. Using compressible isentropic relations, publicly available detonation kinetics data, and results from NASA's online CEA (Chemical Equilibrium Analysis) tool, the following variables are solved to provide the user with the following relevant information:

1. Mole fraction of reactants
2. Detonation wave propagation velocity
3. Pressure of detonation products

4. Temperature of detonation products

5. Specific heat ratio of detonation products

6. Detonation cell size

7. Injector size

8. Combustor size

9. Nozzle geometry

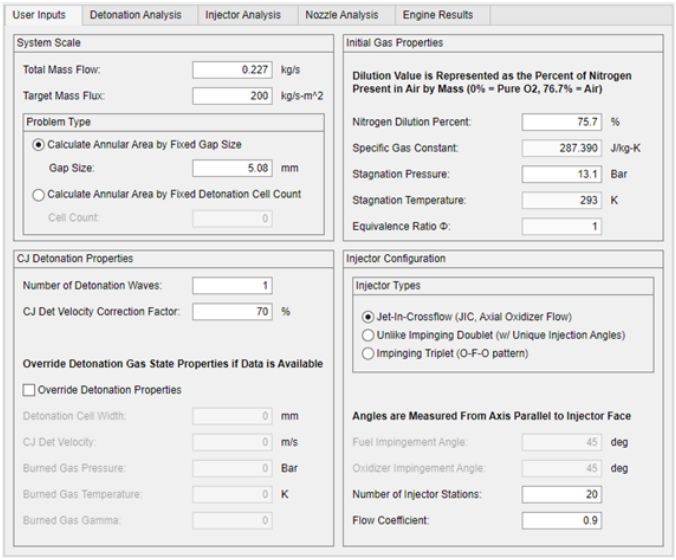

Figure 30: Required user inputs as seen in program GUI

7.4.1 Detonation Analysis

The performance model needs to solve for the state of the gas post-detonation (after constant volume heat addition). This is accomplished by using lookup tables of data obtained from NASA CEA for several given mixtures of hydrogen and air and varying initial conditions and mixtures. A pressure profile of the engine is generated by fitting the initial and detonation pressures to a logarithmic decay function for one period of the detonation wave. This pressure profile is then used to determine time-averaged properties of the gas inside the combustor.

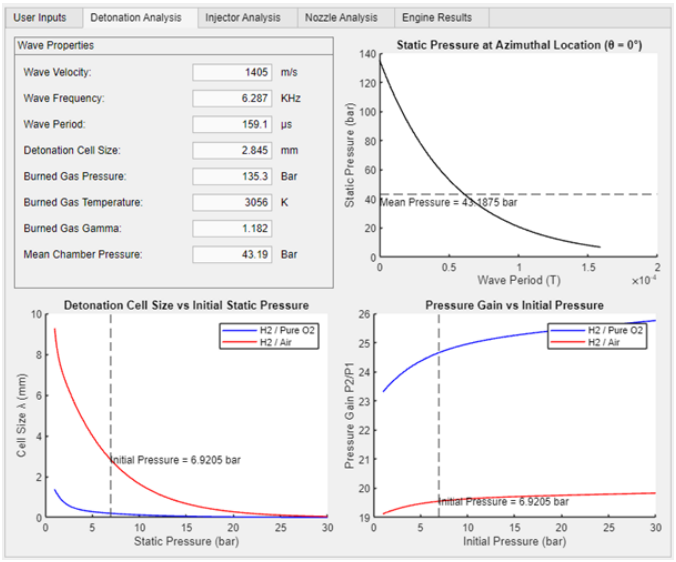

Figure 31: Detonation analysis outputs

7.4.2 Injector Analysis

The diameter and position of each injector station is solved for using the compressible orifice equation as defined in ISO 5167 and the number of user-defined injector stations. Because the combustor fill height depends on the vertical velocity of the resulting stream, the angle and velocity of the resulting propellant stream must be solved for. This is calculated assuming a two-dimensional inelastic collision between the propellants after exiting the injectors. Because the oxidizer is supplied to the RDE non-concentrically, a compressible viscous CFD simulation was run using ANSYS to ensure that flow distribution was even and did not cause any discontinuities between injector stations. The simulation was run using boundary conditions of 220 g/s mass flow of air and an inlet pressure of 200 psi.

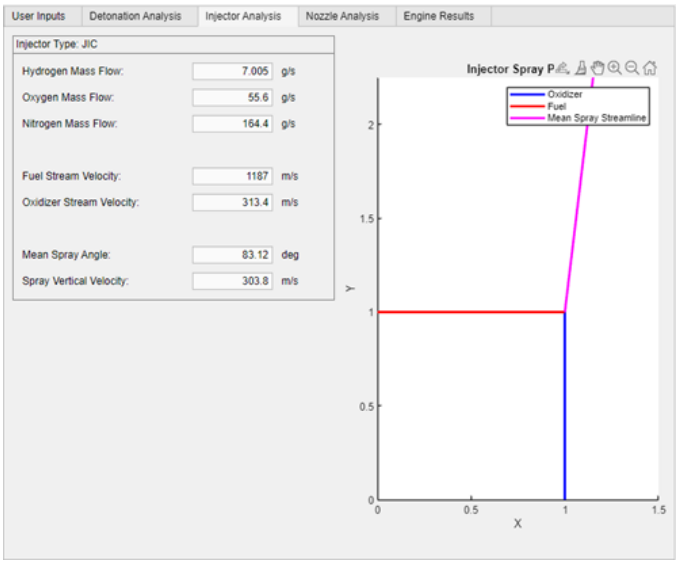

Figure 32: Injector spray plot as displayed by the program

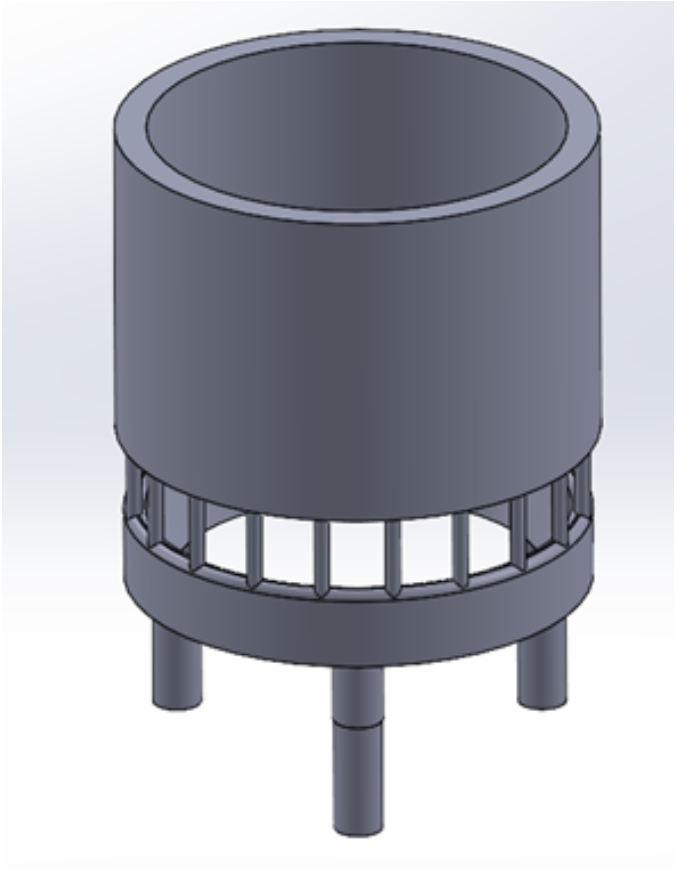

Figure 33: CAD model of air plenum flow path

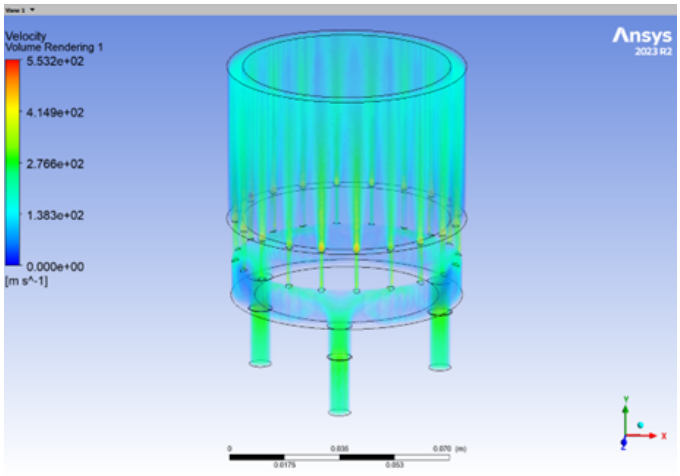

Figure 34: ANSYS results of air plenum flowfield

7.4.3 Nozzle Analysis

Now that the pressure of detonation is known, the program can calculate the geometry of a nozzle required to expand the flow to ambient conditions as well as the exit velocity. This is later used to determine the performance of the engine. The engine utilizes an internal-expansion (IE) aerospike nozzle to accelerate the flow from choked conditions to ambient conditions using two expansion fans. This allows for a compact and efficient design with topology that integrates well into the engine architecture.

The internal section is solved for using a method-of-characteristics solver that expands the flow to a user-defined Mach number that is less than the maximum exit Mach number. The external section geometry is solved for using Angelino's method for calculating aerospike contours. The sum of these two geometries is plotted in the figure as seen below.

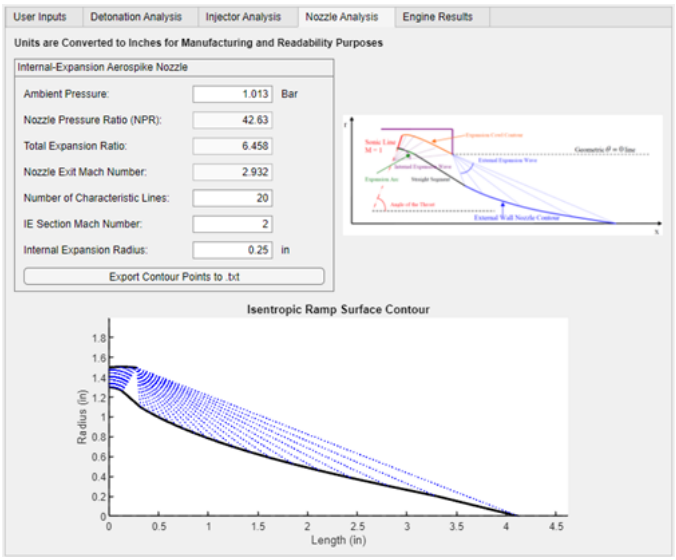

Figure 35: Nozzle analysis outputs

7.4.4 Engine Sizing and Stability

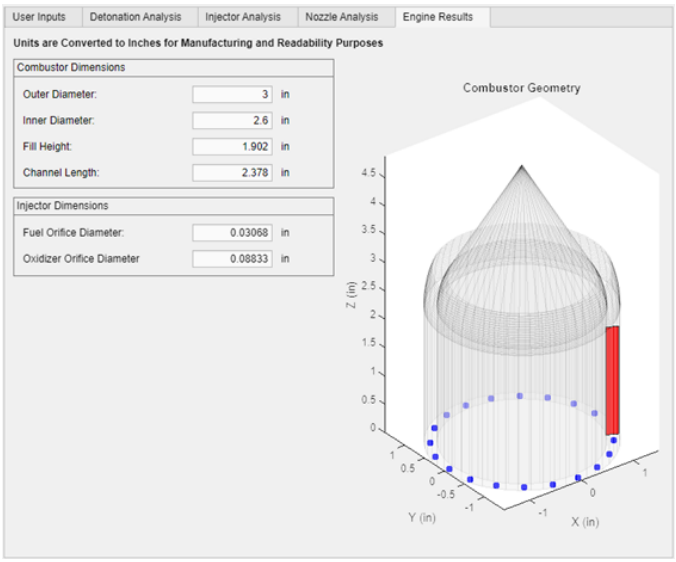

Figure 36: Performance model final outputs

The program provides the user with the relevant dimensions for the combustor and injector based upon isentropic and derived detonation relations. A 3D visual of the engine is also provided using a non-truncated conical nozzle for the sake of manufacturing, as machining a true isentropic curve would require significant effort and additional cost. The Bykovskii relations are a set of empirically determined equations used to define the dimensions of an RDE given how energetic the detonation is. These relations are known to be valid for gaseous propellant RDEs based upon the

numerous works from Bykovskii's team and efforts by the AFRL. By comparing our results from the performance model to these relationships we can determine if the engine will be stable or not during operation assuming one detonation wave in the combustor. Based upon all available information and empirical data, we can say that there will be at least one stable detonation wave within the combustor.

Parameter	Performance Model	Bykovskii Relations
Gap width	0.2 in	0.157 in – 0.380 in
Fill Height	1.902 in	0.783 in – 1.878 in
Channel Height	2.378 in	1.565 in – 3.8 in
Outer Diameter	3 in	2.135 in – 3.844 in

Table 3: Comparison of performance model and Bykovskii outputs

7.5 Test Stand

Throughout the design and development of this project, one of the most critical potential failure modes identified was the structural failure of the experimental test stand. While such a failure would have been catastrophic to the completion of the project, it was deemed easily avoidable through proper design and analysis. Due to the high material strength of many components used in constructing the test stand—combined with the relatively low expected thrust of the engine's first iteration—there was a high level of confidence that a robust and effective test stand could be developed using results from similarly sized test stands constructed in past projects. While structural simulations were conducted in areas of higher stress, the methodology behind the test stand design was largely supported by material choice, prototyping, and experimental validation.

One of the earliest design decisions was to construct the main frame from 8020 aluminum extrusion. This material was selected due to its extensive prior use in comparable test stands and the availability of extrusions provided by UCF's Propulsion and Energy Research Laboratory. Additional support for this decision came from existing literature, such as the University of Southampton's RDE development efforts (Fig. **??**) [35]. Furthermore, all fasteners and structural hardware were grade 5 or higher steel, ensuring sufficient strength to handle the maximum expected thrust of 200 lbf. Prototyping played a key role during development—multiple smaller-scale frames were assembled

to verify feasibility, assess integration with plumbing and engine interfaces, and evaluate component compatibility. This hands-on approach provided vital feedback on alignment tolerances and strength, which led to refined design iterations.

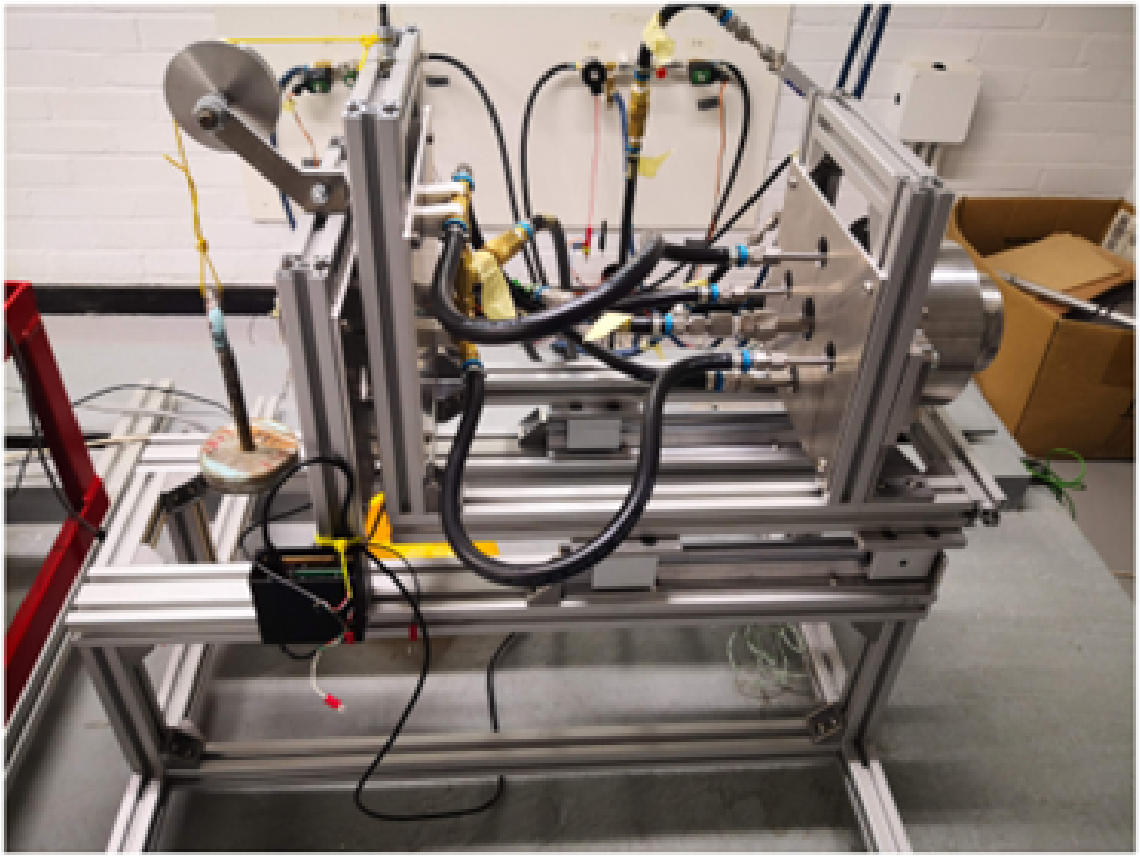

Figure 37: The test stand utilized by the University of Southampton [35]

Following the assembly of the full-scale test stand and subsequent engine testing, it was found that the design exceeded expectations in both structural stability and usability. Load testing showed minimal deflection and stress concentrations, even during simulations of abnormally high peak thrusts. These results confirmed that the stand could reliably withstand operational forces without compromising test integrity. Moreover, the frame's modularity allowed for flexible integration of plumbing and data acquisition systems. The five-foot extendable frame length provided ample space for additional features, and the adjustability of aluminum extrusion enabled rapid reconfiguration to support various test conditions.

A particularly critical subsystem was the load cell calibration setup, which ensured accurate and repeatable thrust measurements. Drawing from prior research on small-scale RDEs and existing test stand designs, including those at

the University of Southampton, a static/floating thrust plate configuration was adopted in conjunction with a mass and pulley calibration mechanism. This choice was influenced by its mechanical simplicity and proven effectiveness. To safely calibrate for thrusts up to 200 lbf, every component of the calibration rig-including steel cables, quick links, eye bolts, and pulleys-was constructed from stainless steel rated for loads of 600 lbf or more. This provided a safety factor of at least 3 against failure.

The effectiveness of the calibration system was confirmed during full-scale testing. Applying known loads to the pulley assembly prior to hot fire tests allowed for quick verification of load cell outputs. The measured thrust values during calibration closely matched those recorded during actual engine firings. The system also supported rapid attachment and detachment of weights, streamlining the test procedure without disrupting other test stand operations. Overall, the calibration subsystem validated its design intent and proved to be a reliable contributor to the success of the project's thrust measurement efforts.

7.6 DAQ System

To ensure the DAQ systems were fully operational before full-scale system testing, National Instruments Measurement & Automation Explorer (NI-MAX) was used to simulate DAQ hardware. NI-MAX can create virtual channels on specific NI devices, such as the NI-USB 6210 and NI-USB 6001, which produce dummy signals that can be read using LabVIEW.

Thus, all pressure transducers, thermocouples, and digital signals can be imported into LabVIEW, and the general script functionality can be evaluated. Because the simulated hardware is bound by the same operating characteristics as the physical hardware, errors can be identified and resolved before actual testing begins.

7.7 Fluids System - Methodology and Analysis

7.7.1 Piping and Instrumentation Diagrams (P&IDs)

Throughout the design process, Plumbing and Instrumentation Diagrams (P&IDs) were used as critical tools for visualizing the fluid system architecture and defining the layout and connectivity of components. This diagram,

shown in Fig. 38, outlined all major flow paths and interfaces, including those between the propellant tanks, run lines, vent lines, engine inlet, and various support subsystems. By mapping out both mechanical and operational relationships, the P&ID enabled the design team to identify logical groupings of components, anticipate integration issues, and maintain a clear understanding of system flow logic.

Regular iteration of the P&ID was essential for refining component selection and ensuring the system architecture remained aligned with evolving performance requirements. Each update to the diagram informed the development of a comprehensive and accurate Bill of Materials (BOM), as well as planning for system fabrication and assembly. The finalized P&ID includes detailed annotations such as flow coefficients (Cv), pressure ratings, valve actuation types (manual or solenoid), and line sizing, making it a valuable reference for both design verification and test procedure development.

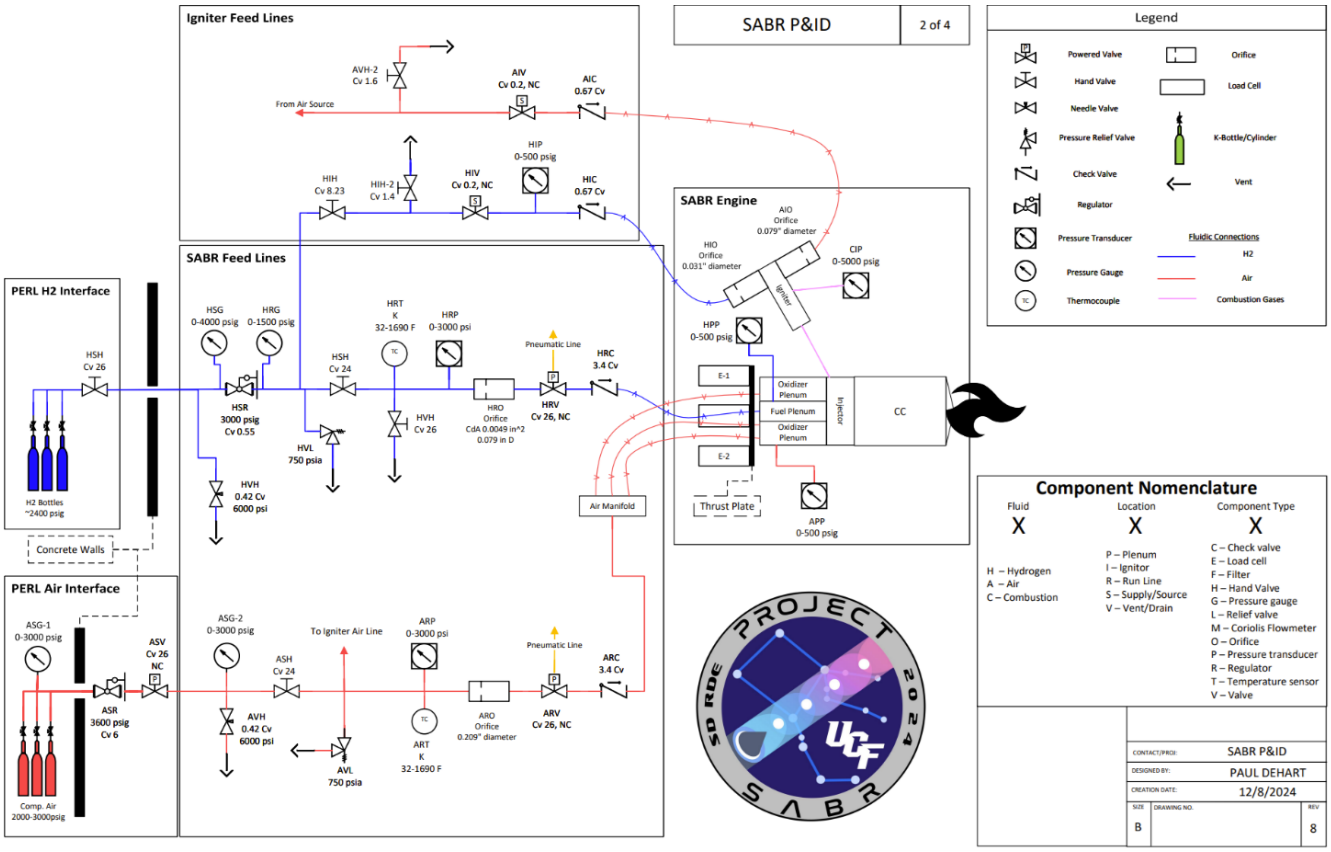

Figure 38: Final SABR P&ID diagram

7.7.2 MATLAB-Based Flow Calculator

To validate the SABR fluid system architecture and to inform component sizing, a MATLAB-based flow calculator was developed and used throughout the design phase. This tool applied compressible flow theory to predict the behavior of air and hydrogen as they flowed through the regulated system, through restriction orifices, and into the engine's inlet plenums. The calculator took user-defined inputs such as desired flowrates and plenum pressures to output pressure and velocity profiles at various points in the system and help inform required supply pressures, regulator setpoints, and orifice sizes.

The model assumed choked flow at the orifices and used isentropic flow relations for ideal gases to determine Mach number, temperature, and mass flux through the lines. It operated under several simplifying assumptions to support rapid iteration, including horizontal flow, adiabatic flow conditions, and the use of steady-state approximations for short-duration flow events. The gases were assumed to behave as calorically perfect gases, with constant specific heats and molecular weights. Although these assumptions limited the precision of predictions under extreme conditions, they were sufficient to guide orifice sizing, valve selection, and pressure regulation for initial testing.

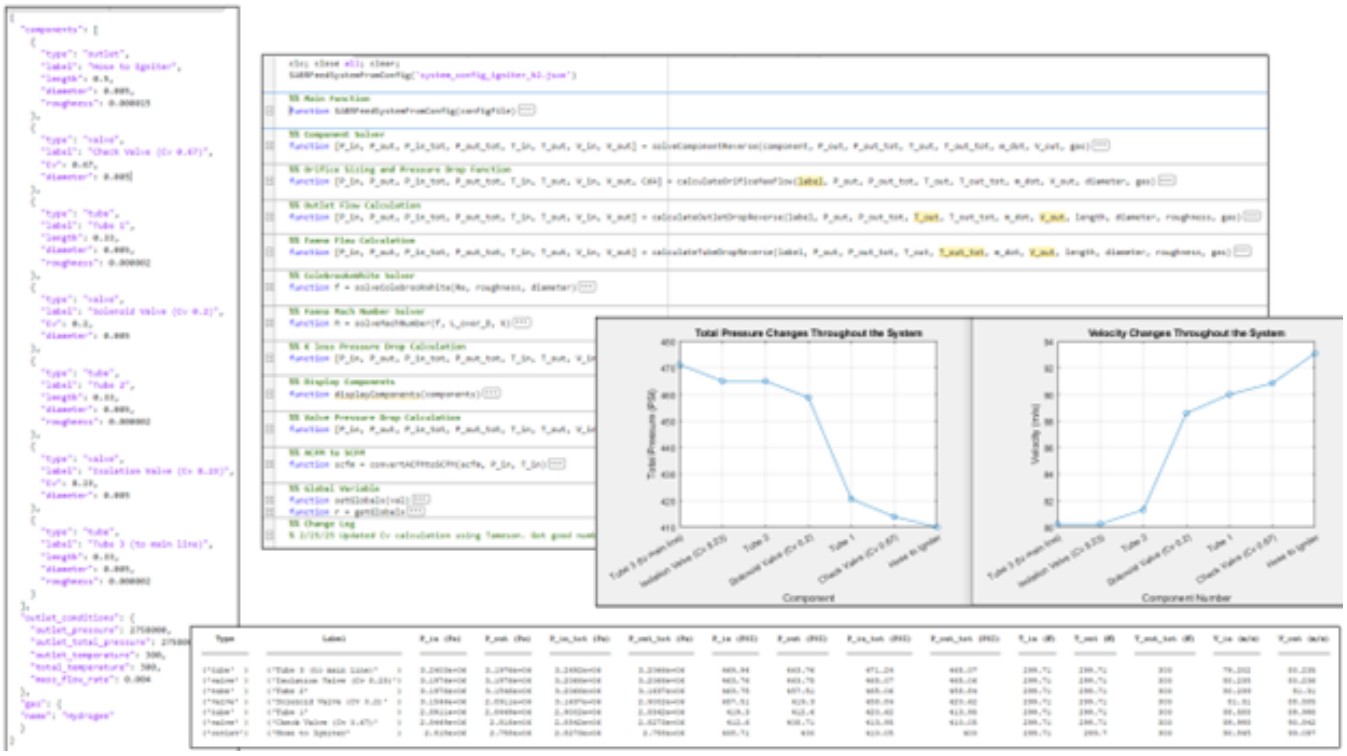

Figure 39: Screenshots from the Pressure Loss MATLAB Calculator

7.7.3 Spreadsheet Analysis and Integration Tools

The team also developed a set of spreadsheet tools to supplement the MATLAB calculator during integration and testing. These tools enabled quick recalculations of orifice flow behavior based on measured pressures and temperatures, allowing operators to adjust system parameters to hit target flow rates and equivalence ratios. These supplementary tools were used to make real-time decisions regarding regulator tuning and orifice sizing and were especially valuable during cold flow verification tests.

D	0.00571501	m
A	2.5652E-05	m2
gamma	1.4	
Rsp	287	J/kg-K
T	300	K

Possible Cd
0.8
0.85
0.9
0.95

mdots				Phis
223.7396008	g/s	0.22374	kg/s	0.5
223.0987278	g/s	0.223099	kg/s	0.6
222.4615156	g/s	0.222462	kg/s	0.7
221.8279331	g/s	0.221828	kg/s	0.8
221.1979493	g/s	0.221198	kg/s	0.9
220.5715337	g/s	0.220572	kg/s	1
219.9486559	g/s	0.219949	kg/s	1.1
219.3292861	g/s	0.219329	kg/s	1.2

Phi = 0.5	
Pressure (psi)	Cd
677.6037635	0.8
637.7447185	0.85
602.3144564	0.9
570.6136955	0.95

Phi = 0.6	
Pressure (psi)	Cd
675.6628554	0.8
635.9179816	0.85
600.5892048	0.9
568.9792467	0.95

Phi = 0.7	
Pressure (psi)	Cd
673.7330346	0.8
634.1016796	0.85
598.8738085	0.9
567.3541344	0.95

Phi = 0.8	
Pressure (psi)	Cd
671.8142062	0.8
632.2957235	0.85
597.1681833	0.9
565.7382789	0.95

dP btw Cases	
1.940908035	1.90811475
1.929820834	
1.918828365	
1.90792955	
1.897123329	
1.886408655	
1.875784499	

Figure 40: Mass flow rate spreadsheet for equivalence ratio and orifice calculations

8 Final Design and Engineering Specifications

8.1 RDE Combustor

The final iteration of the combustor design arrived at a plate stack approach, which involves each part being modular and simple, allowing short turnaround times and lower costs to replace or adjust dimensions of individual components. This plate stack consists of the port plate which handles gas connections to the fluids system, the injector plate featuring the plenums, the inner and outer bodies, and the nozzle and cowl. The modularity allows for the RDE to reliably function in several different configurations, including the ability to compare the effects of different injector designs and exit geometries without introducing much variation into the overall geometry of the combustor. Figure 41 highlights the level of modularity achieved.

The combustor was machined out of 304 grade stainless steel with the goal of taking advantage of the large heat capacity and conductivity of the material, letting the combustor perform for short bursts without any cooling. The ability for stainless to wick away the heat and take a large amount of energy to elevate its temperature, combined with its high melting point, makes it a great candidate for a heat sink design. In testing, this effect proved to be true, with zero erosion being detected after inspection, even with longer and more consecutive tests being performed.

Figure 41: Exploded view showing modularity of the RDE combustor plate stack.

The combustor also allows for plenum pressure data to be collected via taps into each of the plenums for the different

propellants injected, as seen in Figures 42 and 43. This clever design involves nothing more than simple holes being drilled on the side of the injector plate, allowing for no sealing necessary beyond the NPT threads on the transducers themselves.

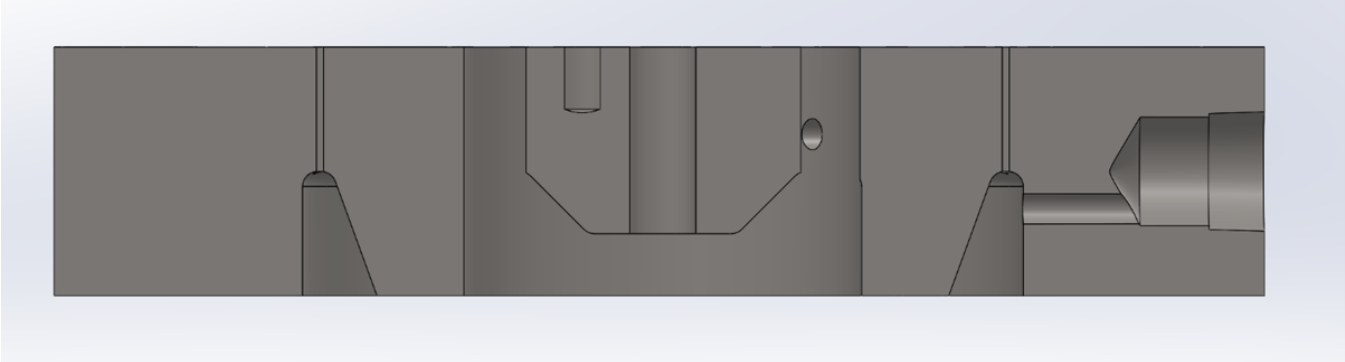

Figure 42: Plenum pressure tap location (view 1).

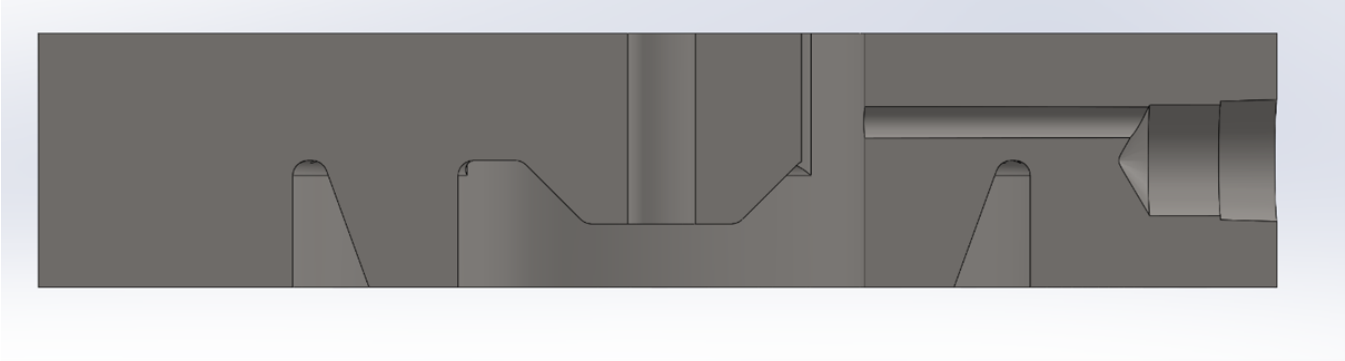

Figure 43: Plenum pressure tap location (view 2).

Additionally, the combustor features the igniter channel directly into the annulus from the injector plate, an innovative approach compared to other research combustors that suffer from erosion issues due to the igniter outlet being perpendicular to the outer body wall, effectively pointing a directed shock into their inner body, as well as including a discontinuity on the outer body wall. This discontinuity is avoided by this design, pictured in Figure 44. This approach proved beneficial during testing as it allowed swapping between torch and pre-detonator ignition options while avoiding disturbing the flow characteristics inside the chamber.

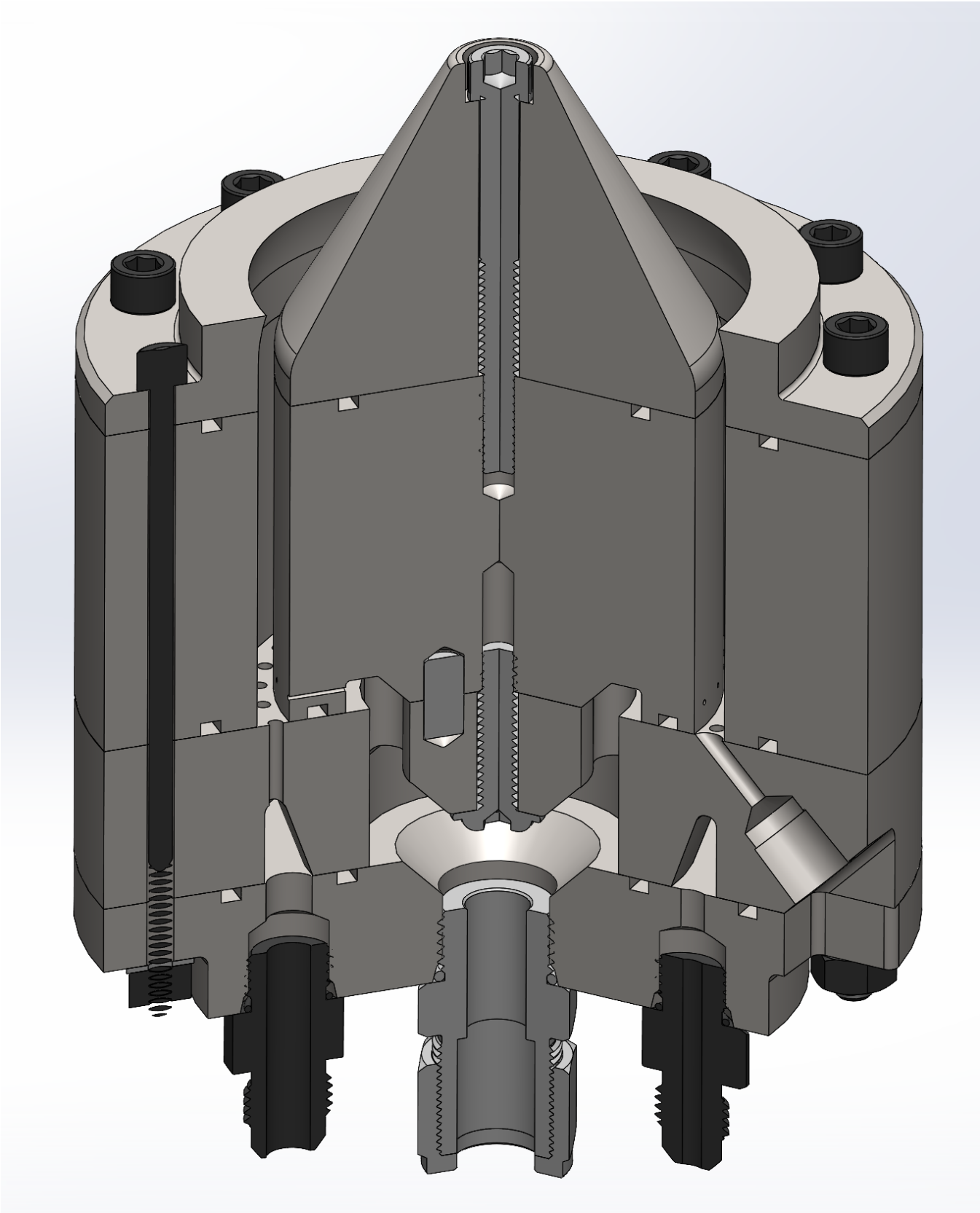

Figure 44: Innovative igniter channel geometry routed through the injector plate.

8.2 Igniter

The final approach to the torch igniter system consisted of a stainless steel ¼ NPT cross fitting drilled out to accept a standard spark plug thread. This cross allowed for a very robust and simple structure to feature Jet in Crossflow elements, swappable injector orifices, and allowed for a pressure transducer to be incorporated to monitor torch operation. The torch is then attached to the RDE itself via a thick wall stainless steel pipe nipple, funneling the combusting gases safely into the annulus, pictured in Figure 45.

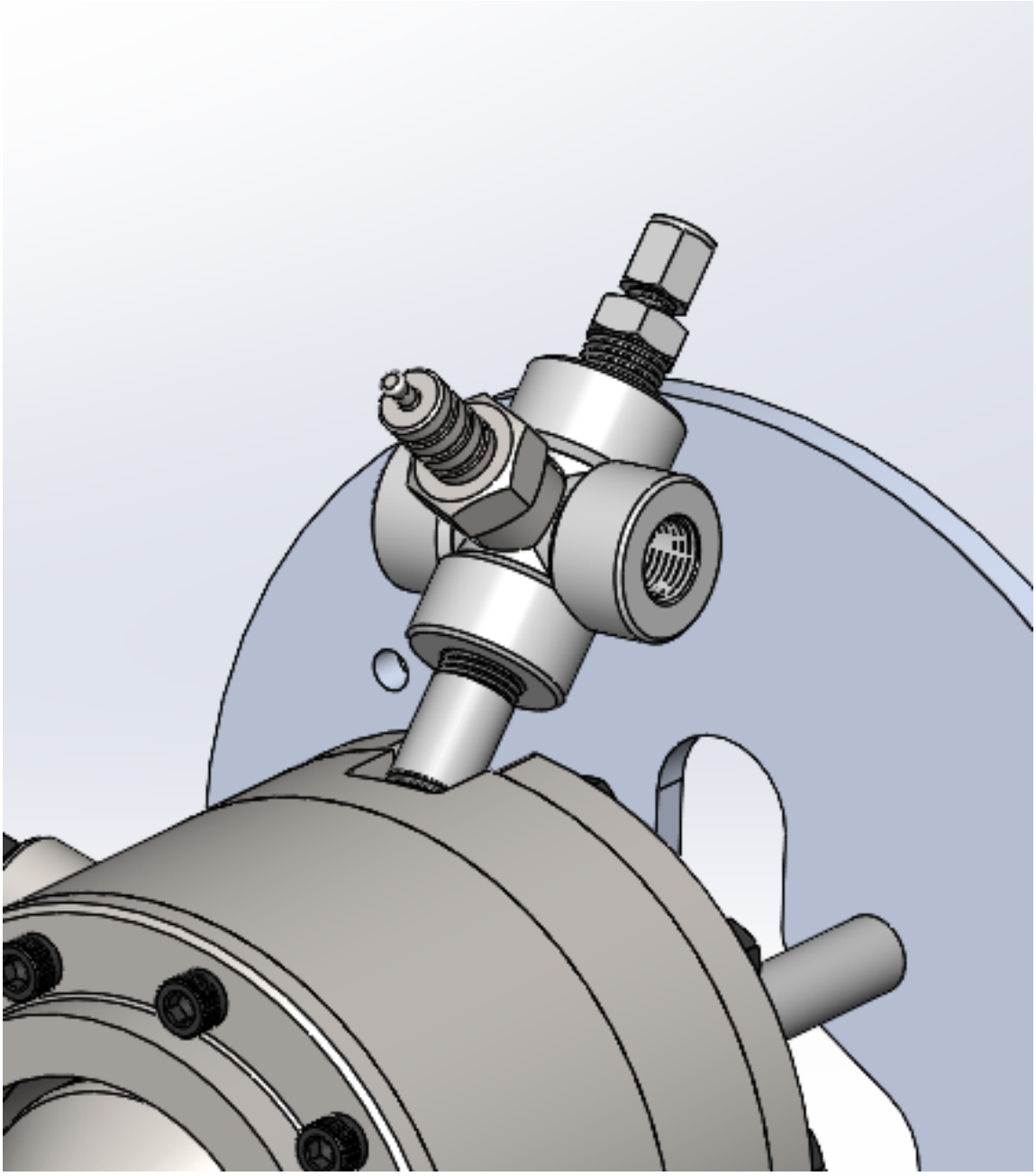

Figure 45: Final integration of the torch igniter on the RDE

A convenient side effect of having a transducer integrated is that once the torch is no longer running, due to its fluidic connection to the annulus conditions, an attenuated pressure could be measured. This allowed for the outer body to avoid any discontinuities in its inner surface and prevent erosion from the detonation wave.

In terms of driving the spark plug, a basic yet robust approach was chosen using an ignition coil driven by an oscillating relay. As the signal line circuit is closed, it allows for the relay to energize itself, which leads to it opening its own circuit and cutting off its own power, resetting the cycle. The specific timing of this cycle can be fine-tuned via the addition of a capacitor and resistor, taking advantage of the relay's behavior as an inductor. As the relay opens and closes, it charges the primary coil in the ignition coil shown in Figure 46.

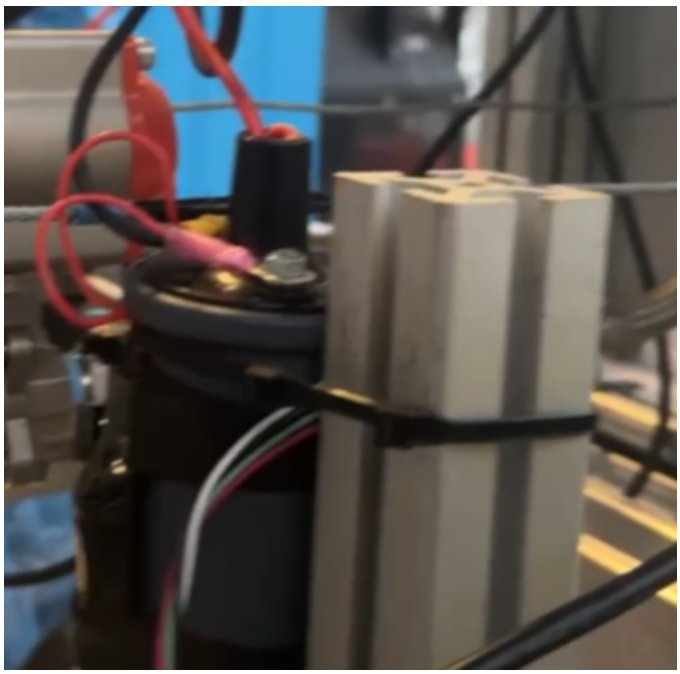

Figure 46: Automotive ignition coil used for spark generation.

Once the power is removed from the primary, the magnetic fields collapse in an inductive spike into the secondary coil, which multiplies the voltage up to more than 30kV. A capacitor bank is placed in parallel with the primary coil to ensure the voltage remains high for longer, allowing for a larger energy release in each spark pulse to aid ignition. To prevent unwanted damage to upstream circuitry, a ZVS (zero voltage switching) diode is incorporated as a flyback diode, providing a safe dissipation path for the energy spike. A simplified schematic of the full ignition circuit is shown in Figure 47, with the open circuit on the right representing the spark plug gap.

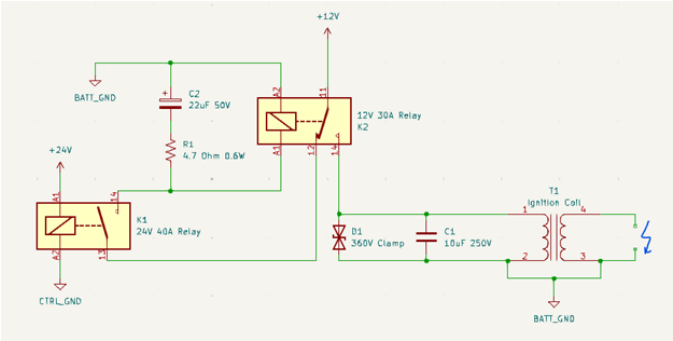

Figure 47: Simplified ignition circuit schematic.

8.3 Injector

During testing, an audible (and visible) detonation mode was observed. However, a fast Fourier transform of the audio captured from these runs revealed that the prominent frequency was only about 3 kHz, roughly half of the expected 6.2 kHz predicted during the design phase. Plugging these values back into the MATLAB DCA program, it was revealed that the combustor was only operating at about 40% of the maximum CJ detonation velocity (approximately 802 m/s). It was theorized that poor mixing, resulting from the large gap distance between the injector pairs, was responsible for this weaker detonation mode.

To improve this, the injector element count was later increased to 32 (up from 20), and a discharge coefficient (Cd) of 0.65 was used to account for the larger length-to-diameter (L/D) ratio of these new, smaller injector posts. The visual difference between these two injector configurations is shown in Figures 48 and 49. Thanks to the modularity of the RDE design, this new injector configuration was swapped out with relative ease.

A minor upgrade was also made to the hydrogen flow path, reducing the amount of dribble volume in order to maintain consistent gas velocity and uniform propellant distribution.

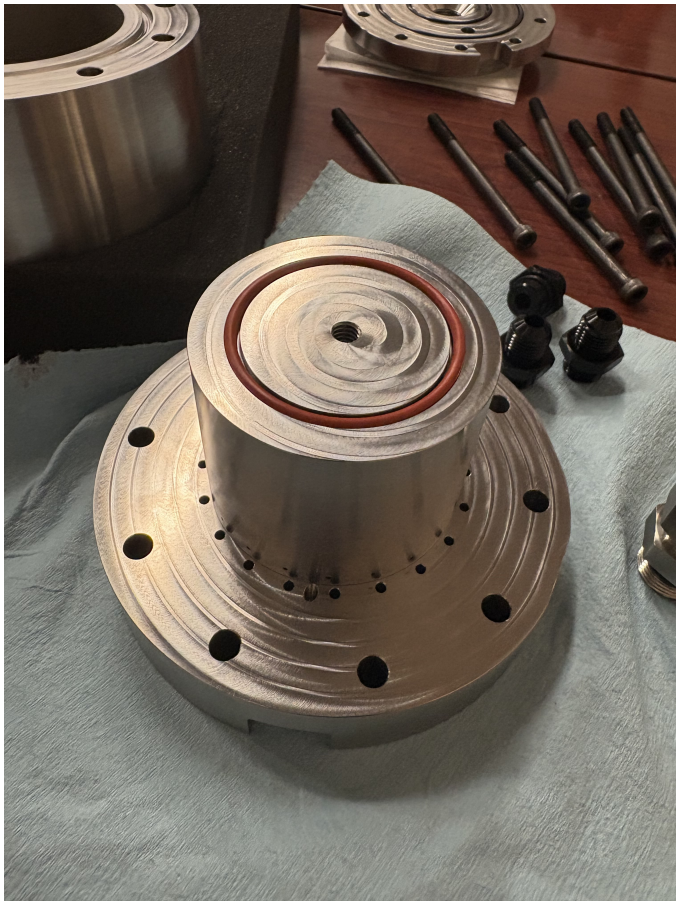

Figure 48: Old injector configuration with 20 jet-in-crossflow (JIC) pairs.

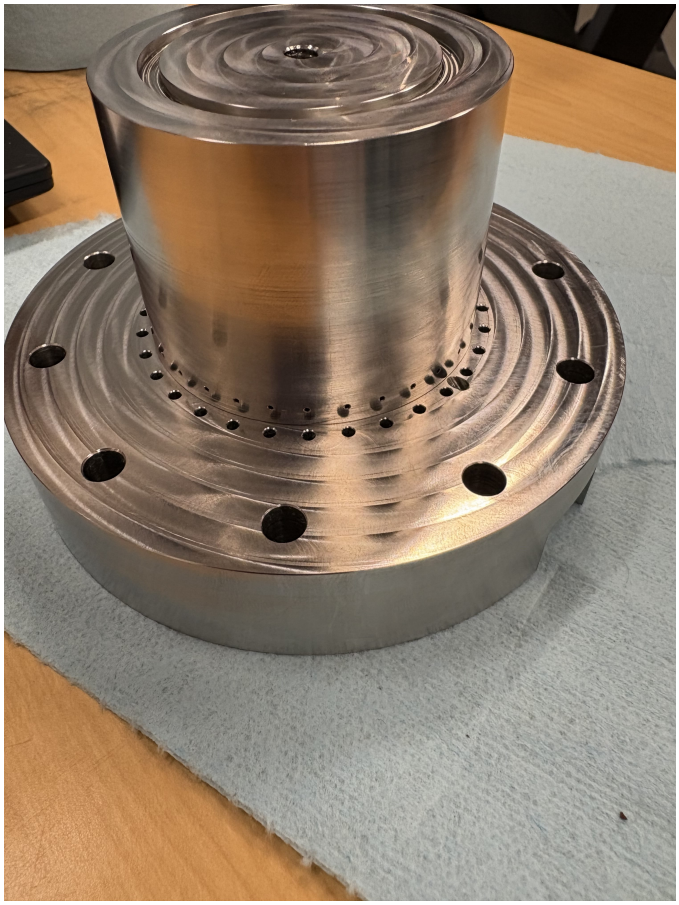

Figure 49: New injector configuration with 32 jet-in-crossflow (JIC) pairs.

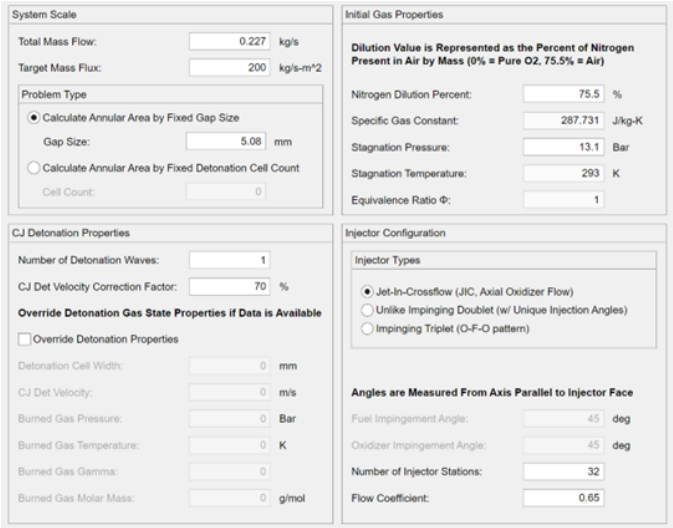

Figure 50: Outputs from the MATLAB DCA program for the 32-element injector configuration.

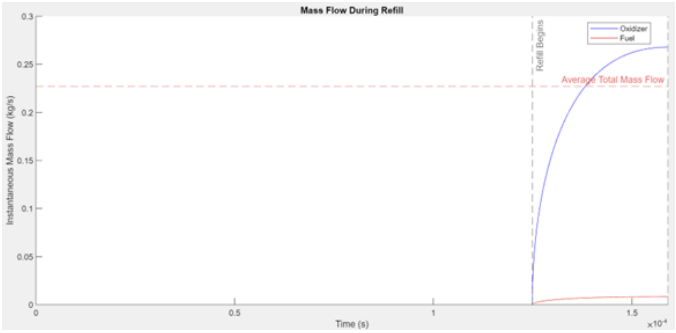

Figure 51: Outputs from the MATLAB DCA program for the 32-element injector configuration.

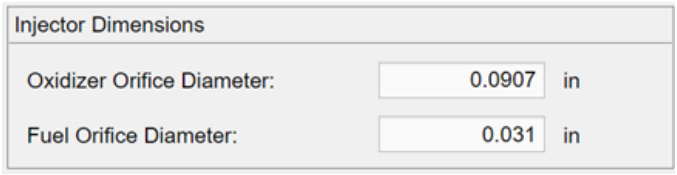

Figure 52: Outputs from the MATLAB DCA program for the 32-element injector configuration.

8.4 Data Acquisition and Control

The Data Acquisition and Control System consists of two major sub-components: the hardware (sensors, relays, etc.) and the control software. Most of the hardware was purchased from third-party vendors, except for the pressure transducers, which were borrowed from the Propulsion and Energy Research Laboratory (PERL). Due to time constraints, it was ultimately decided that a LabVIEW software system would provide the best control solution without the need to learn a completely new data acquisition scheme.

8.4.1 Final Electronics Hardware Configuration

The hardware configuration evolved significantly throughout the testing process as the team adapted to testing conditions, faulty sensors, and increased sensor noise levels. The updated electronics schematics are shown below and represent the final assembled hardware system.

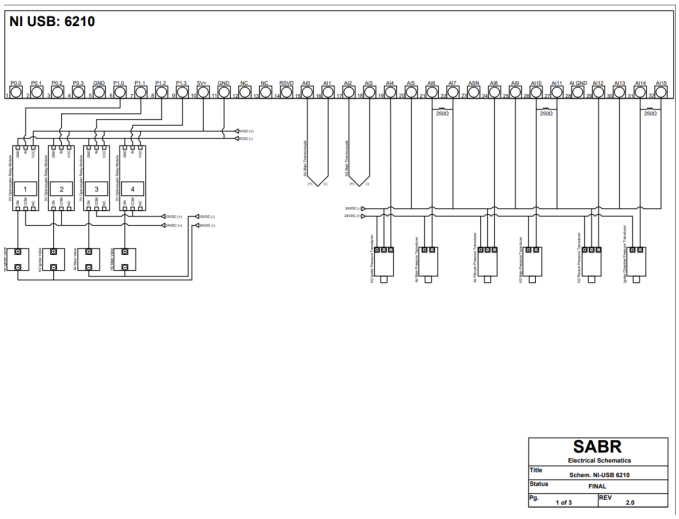

Figure 53: NI USB 6210

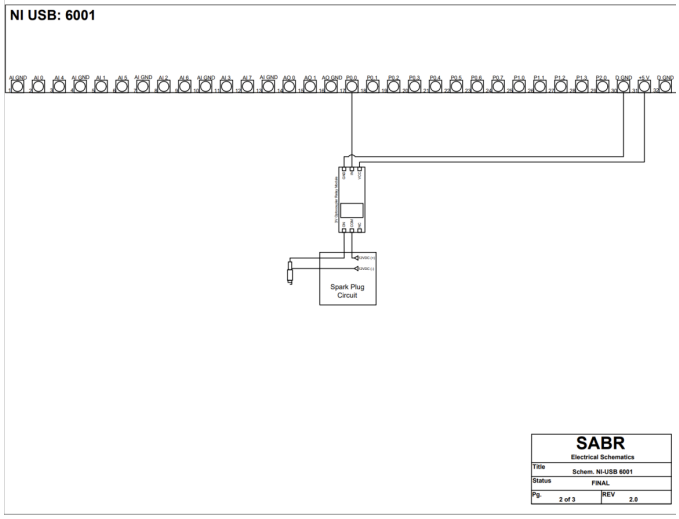

Figure 54: NI USB 6001

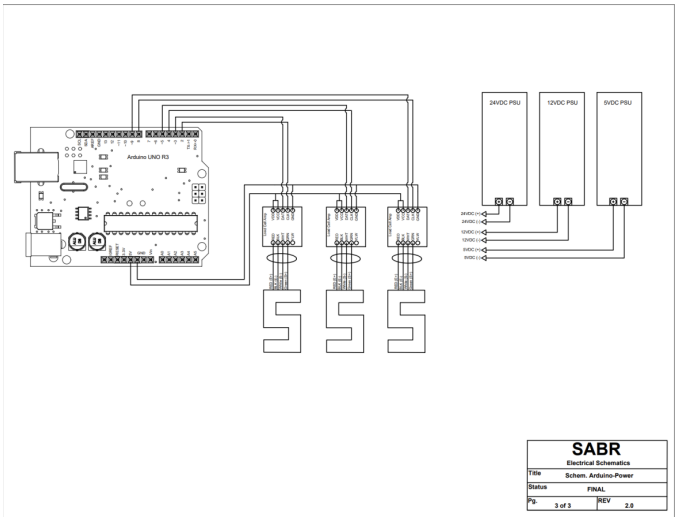

Figure 55: Arduino/Load Cell/PSU Configuration

Due to budget constraints, it was impractical to purchase a single DAQ device to meet all system needs. Instead, channels were distributed across three readily available devices: an NI-USB 6001, NI-USB 6210, and an Arduino UNO R3. The I/O list for each device is shown in Figure 56.

NI 6210

Channel	Channel Name	Description	Occupation	Location
1	P0.0	Digital Input 1		
2	P0.1	Digital Input 2		
3	P0.2	Digital Input 3		
4	P0.3	Digital Input 4		
5	GND	Ground		
6	P1.0	Digital Output 1	3V Optocoupler Relay	Air Igniter
7	P1.1	Digital output 2	3V Optocoupler Relay	H2 Igniter
8	P1.2	Digital Output 3	3V Optocoupler Relay	Air Main
9	P1.3	Digital Output 4	3V Optocoupler Relay	H2 Main
10	5V+	5V+	5VDC PSU (+)	
11	GND	Ground	5VDC PSU (-)	
12	NC	No Connection		
13				
14	RSVD	Reserved		
15	AI0+	Analog Input 1	Thermocouple	T_air
16	AI0-			
17	AI1+	Analog Input 2	Thermocouple	T_H2
18	AI1-			
19	AI2+	Analog Input 3	Transducer	Air Plenum
20	AI2-			
21	AI3+	Analog Input 4	Transducer	H2 Plenum
22	AI3-			
23	ASN	??		
24	AI4+	Analog Input 5	Transducer	H2 Igniter
25	AI4-			
26	AI5+	Analog Input 6	Transducer	Air Main
27	AI5-			
28	AI GND	Analog Input Ground		
29	AI6+	Analog Input 7	Transducer	H2 Main
30	AI6-			
31	AI7+	Analog Input 8	Transducer	Igniter Chamber
32	AI7-			

NI 6001

Channel	Channel Name	Description	Occupation	Location
0	AI GND	Ground		
1	AI0	Analog Input 1		
2	AI4			
3	AI GND	Ground		
4	AI1	Analog Input 2		
5	AI5			
6	AI GND	Ground		
7	AI2	Analog Input 3		
8	AI6			
9	AI GND	Ground		
10	AI3	Analog Input 4		
11	AI7			
12	AI GND	Ground		
13	AO 0	Analog Output 1		
14	AO 1	Analog Output 2		
15	AO GND	Ground		
16	P0.0	Port 0 Line 0	3V Optocoupler Relay	Spark Plug
17	P0.1	Port 0 Line 1		
18	P0.2	Port 0 Line 2		
19	P0.3	Port 0 Line 3		
20	P0.4	Port 0 Line 4		
21	P0.5	Port 0 Line 5		
22	P0.6	Port 0 Line 6		
23	P0.7	Port 0 Line 7		
24	P1.0	Port 1 Line 0		
25	P1.1 / PFI1	Port 1 Line 1		
26	P1.2	Port 1 Line 2		
27	P1.3	Port 1 Line 3		
28	P2.0 / PFI 0	Port 2 Line 0		
29	D GND	Ground		
30	5V	5V+	Relay (igniter)	
31	D GND	Ground	Relay (igniter)	

Arduino UNO R3

Channel	Channel Nam	Description	Occupation
0	NC	NC	
1	IOREF	IOREF	
2	RESET	Reset	
3	3V3	3V+ Out	
4	5V	5V+ Out	Load Cell Amp Boards
5	GND	Ground	Load Cell Amp Boards
6	GND	Ground	
7	VIN	5V+ Out	
8	A0	Analog Input 0	
9	A1	Analog Input 1	
10	A2	Analog Input 2	
11	A3	Analog Input 3	
12	A4	Analog Input 4	
13	A5	Analog Input 5	
14	RX0	RX Line 0	
15	TX0	TX Line 0	
16	DIO 2	Digital Input / Output Line 2	Load Cell 1 CLK
17	DIO 3~	Digital Input / Output Line 3 (PWM)	Load Cell 1 DTA
18	DIO 4	Digital Input / Output Line 4	Load Cell 2 CLK
19	DIO 5~	Digital Input / Output Line 5 (PWM)	Load Cell 2 DTA
20	DIO 6~	Digital Input / Output Line 6 (PWM)	
21	DIO 7	Digital Input / Output Line 7	
22	DIO 8	Digital Input / Output Line 8	Load Cell 3 CLK
23	DIO 9~	Digital Input / Output Line 9 (PWM)	Load Cell 3 DTA
24	DIO 10~	Digital Input / Output Line 10 (PWM)	
25	DIO 11~	Digital Input / Output Line 11 (PWM)	
26	DIO 12	Digital Input / Output Line 12	
27	DIO 13	Digital Input / Output Line 13	
28	GND	Ground	
29	AREF	Analog Reference	
30	I2C Data	I2C Data	
31	I2C Clock	I2C Clock	

Figure 56: DAQ I/O map across the NI-USB 6210, NI-USB 6001, and Arduino UNO R3.

The NI-USB 6210 is the primary DAQ system and is responsible for acquiring data from all pressure transducers and thermocouples, translating voltage signals into pressure and temperature readings. To reduce noise in thermocouple signals, 100kΩ bias resistors were used to tie the negative lead to AI Ground, as suggested in the National Instruments technical documentation [37].

Two types of OMEGA PX309 pressure transducers were used: 0–500 PSI (0–5V output) for low-pressure zones, and 0–3000 PSI (4–20mA output) for high-pressure zones. The 4–20mA signals were converted to 1–5V using 250Ω resistors to create voltage-divider circuits readable by the DAQs.

The NI-USB 6210 also sends digital signals to four 3V optocoupler relays for valve actuation. An external 5VDC power supply was linked to the 5V+ and DGND terminals to boost available current beyond the device's 50mA native limit.

The NI-USB 6001 was solely dedicated to spark plug control via a 3V optocoupler relay. Though this could eventually be offloaded to the Arduino, doing so would have required significant integration effort.

The Arduino UNO R3 was used due to its seamless compatibility with Sparkfun HX711 load cell amplifiers. These amplifiers convert millivolt-scale signals into digital data streams, which the Arduino can read and calibrate using vendor-provided code. Attempting to use the NI-DAQs for this task would have slowed down system-wide sampling and compromised performance.

8.4.2 Final Electronics Software Configuration

A custom LabVIEW state machine script was created to automate valve control, sensor monitoring, and display data on a user-friendly GUI. The software runs on a 30ms loop and includes the following states:

- **Initialize:** Sets default values, defines variables, and configures control channels.
- **Default:** Waits for user input to switch states, logs valve positions and timestamps.
- **Valve Test:** Sequentially tests each valve (DAQ-side only).
- **FIRE:** Executes full test sequence. Cold Flow option disables spark control.
- **Manual Actuation:** Allows individual valve control via GUI.
- **Shut Down:** Closes all valves and disables the spark plug.
- **E-STOP:** Rapidly vents air to clear residual fuel, then disables ignition and closes valves.

Sensor data is acquired continuously, regardless of system state. Both pressure and thermocouple data are sampled at 1000Hz. Calculations such as O/F ratio and total flow rate are updated once per loop. A “Full Resolution Pressure Data” option is available for high-speed data logging.

To prevent signal interference (ghosting), thermocouples must be sampled before pressure transducers. High-impedance transducers take longer to discharge, which can contaminate adjacent analog channels if sampled first.

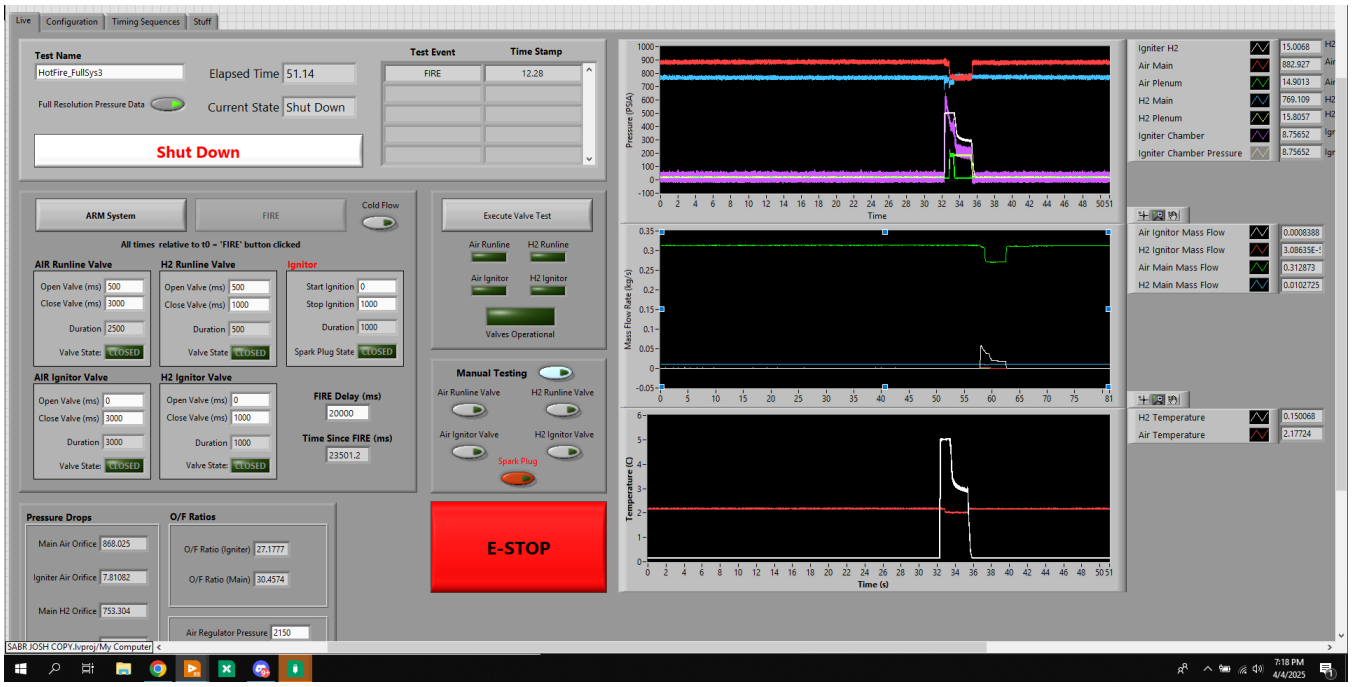

Figure 57: LabVIEW user interface for real-time DAQ control and monitoring.

This DAQ/control system is modular and scalable. The NI-USB 6001 can be repurposed or removed if future upgrades allow spark plug control via the Arduino. With a few LabVIEW optimizations, the loop time could be reduced to 1ms by switching to a per-sample acquisition mode, enabling real-time data matching the hardware sensor rate.

8.5 Test Stand Configuration

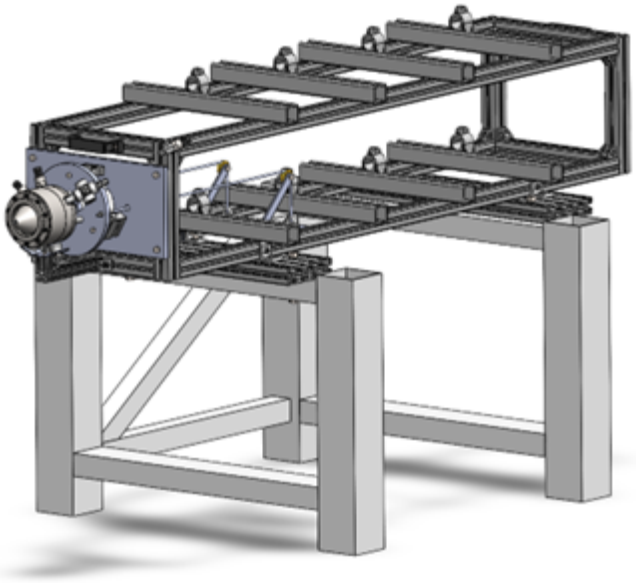

Figure 58: The full-scale test stand assembly with the integrated engine, sans plumbing and electronics.

The final full-scale design for the test stand consists of a rectangular frame constructed out of 8020 aluminum extrusion, bolted onto a steel optical table for extra structural support, as seen in Figure 59. The frame itself was specifically constructed out of 1515-sized extrusion into a rectangular "box" shape, approximately 1 ft $\times$ 1 ft $\times$ 5 ft in size. These extrusions were connected with open-gusset corner brackets and stainless-steel T-nuts, consisting of a single universal size that could be used across the entire top-level assembly. This frame was mounted to two 1560 extrusion sections, which themselves were attached to holes in the top of the optical table via four half-inch bolts. By removing the half-inch bolts, the relatively lightweight frame could be easily moved and worked on. The frame also featured handles for easy handling, as well as clamps for mounting the air and hydrogen plumbing lines.

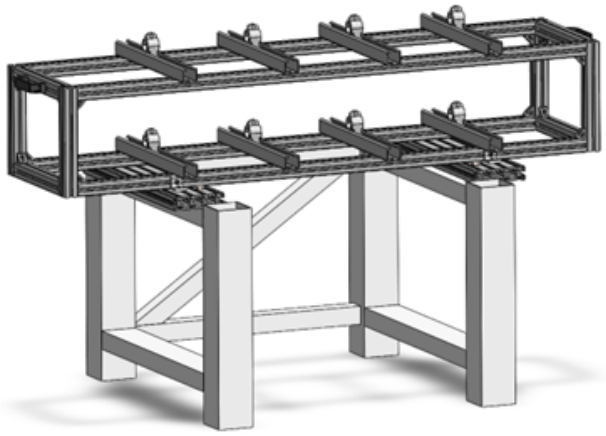

Figure 59: The rectangular frame of the test stand mounted on the optical table.

The assembly for integrating the engine to the stand was designed as the previously mentioned static/floating thrust plate system, as shown in Figure 60. This subassembly consists of two half-inch thick aluminum plates, sandwiching three load cells held via M6 bolts. The front plate is only attached to the rest of the stand via these load cells, hence the "floating" namesake. This allows the entirety of thrust force to be directed through the load cells before being dissipated throughout the rest of the frame structure. Connected to the floating plate via two eyebolts are $\sim$3 ft lengths of 1/16-inch diameter steel cable, which run partially down the length of the frame, over pulleys, and down to a 1/4-inch rectangular aluminum plate. From this rectangular plate, large weight plates were able to be suspended during the load cell calibration process. The pulleys themselves were mounted on custom 1/4-inch aluminum brackets which were attached to the same 1560 extrusion sections on top of the optical table.

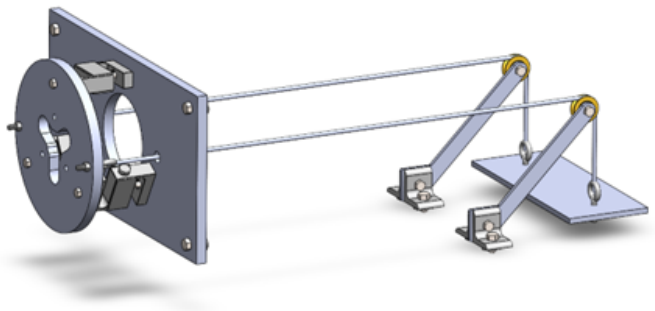

Figure 60: The static/floating plate subassembly, as well as the load cell configuration subassembly.

Paired with the static/floating plate subassembly, an additional subassembly was developed to help support the weight of the engine from the bottom, in order to minimize any parasitic forces from affecting the thrust measure-

ments. This structure utilized additional 1010 extrusion sections mounted to the front of the frame structure and holds two ball transfer studs with a custom 1/4-inch aluminum mount, as seen in Figure 61. If needed, additional shims could be placed between the vertical extrusion piece and the aluminum mount to help properly support the engine at any given height relative to the frame structure.

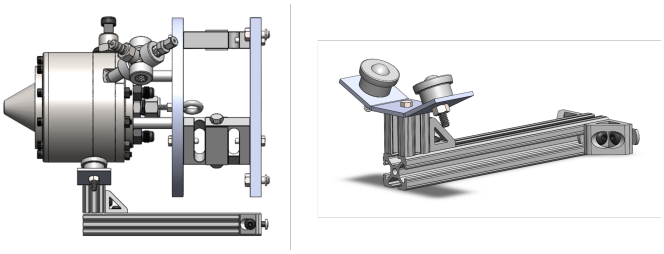

Figure 61: The ball transfer mount structure viewed as a standalone feature (right) and with the engine integrated (left).

From a cost standpoint, the test stand was relatively inexpensive, with most of the components being donated or bought utilizing corporate sponsorships. The development of the stand was also very simple from a manufacturing standpoint, with the only machined components being the custom laser cut aluminum plates. Further details about the cost of the test stand, along with other manufacturing info, can be found in Appendix E and Appendix H.

8.6 Fluid Systems

The final SABR fluid system design successfully incorporated all major subsystems required to deliver controlled flows of air and hydrogen to the engine inlet plenums. The system architecture emphasized symmetry between the two flow lines while allowing for tailored regulation and instrumentation to meet the specific demands of each gas. Key system features included the use of pressure and temperature sensors upstream of the chokes, pneumatically actuated run valves, downstream check valves, and high-pressure-rated tubing and fittings (Figure 62). The inclusion of flexible braided hoses in the final segments of both lines minimized mechanical stress on the engine mount to aid in thrust data collection and reduced the risk of leaks due to vibration during testing.

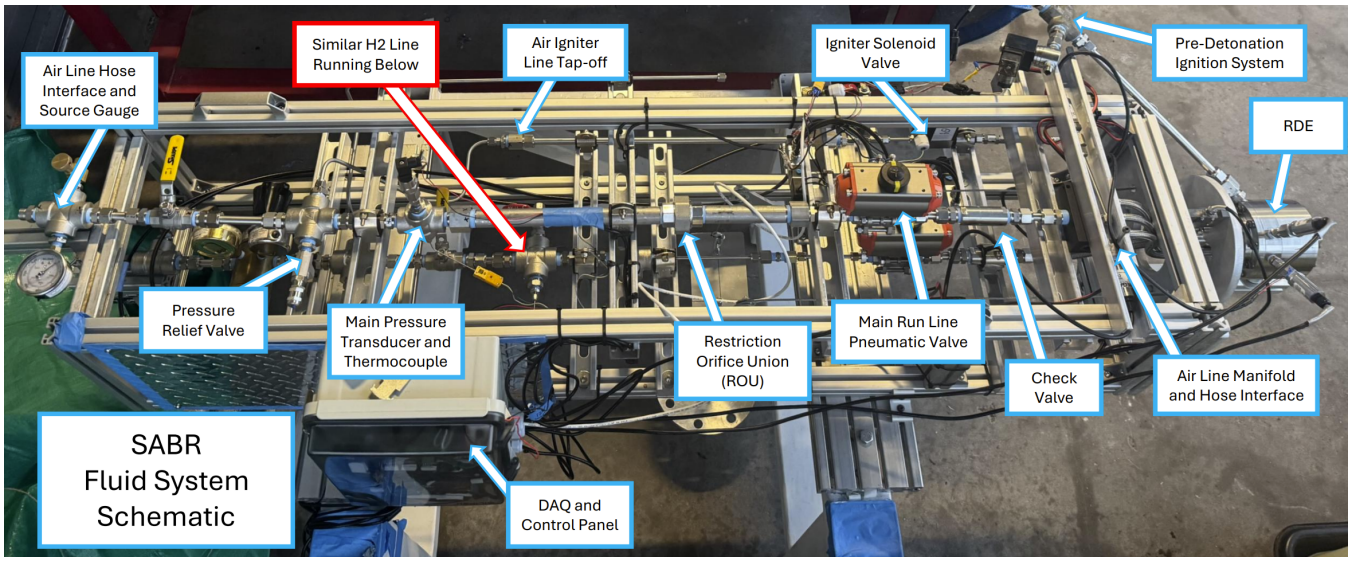

Figure 62: Schematic of the SABR Fluid System.

The design ensured that flow through the orifices was choked at all expected test conditions, thereby decoupling the upstream plumbing from the transient pressure environment in the combustion chamber. The check valves downstream of the run valves further reinforced this decoupling and provided an additional safety element by eliminating any potential for reverse flow during combustion events or engine shutdown.

Component selection was informed by modeling results, experience with fluid system design and build up, and practical testing constraints. Swagelok instrumentation fittings and tubing were used for all hard plumbing due to their reliability, availability, and compatibility with high-pressure gases. NPT fittings, while not as ideal for high-pressure sealing and precision applications, were used everywhere else because of their availability to the team and the cost effectiveness of off-the-shelf NPT components. Off-the-shelf pressure transducers and thermocouples were selected to interface with the data acquisition system and placed strategically within the system to provide reliable data for calculating mass flow rates. The air line ROU was custom bored based on the outputs of the MATLAB model, reducing cost and allowing for iterative refinement.

The CAD layout of the SABR fluid system played a critical role in finalizing the design. A complete 3D model of the fluid system was constructed using SolidWorks to ensure compatibility with the existing test stand and to facilitate rapid integration (Figure 63). The CAD model allowed the team to preemptively identify spatial constraints, prevent interference between system components, and determine optimal mounting strategies for regulators, valves, and

sensors. Mounting brackets were selected and placed based on the CAD models, which helped greatly during final assembly and effectively provided structural support to the fluid system lines. The visual layout also served as a communication tool between team members and with test stand operators, ensuring alignment on component locations, sensor access, and maintenance procedures.

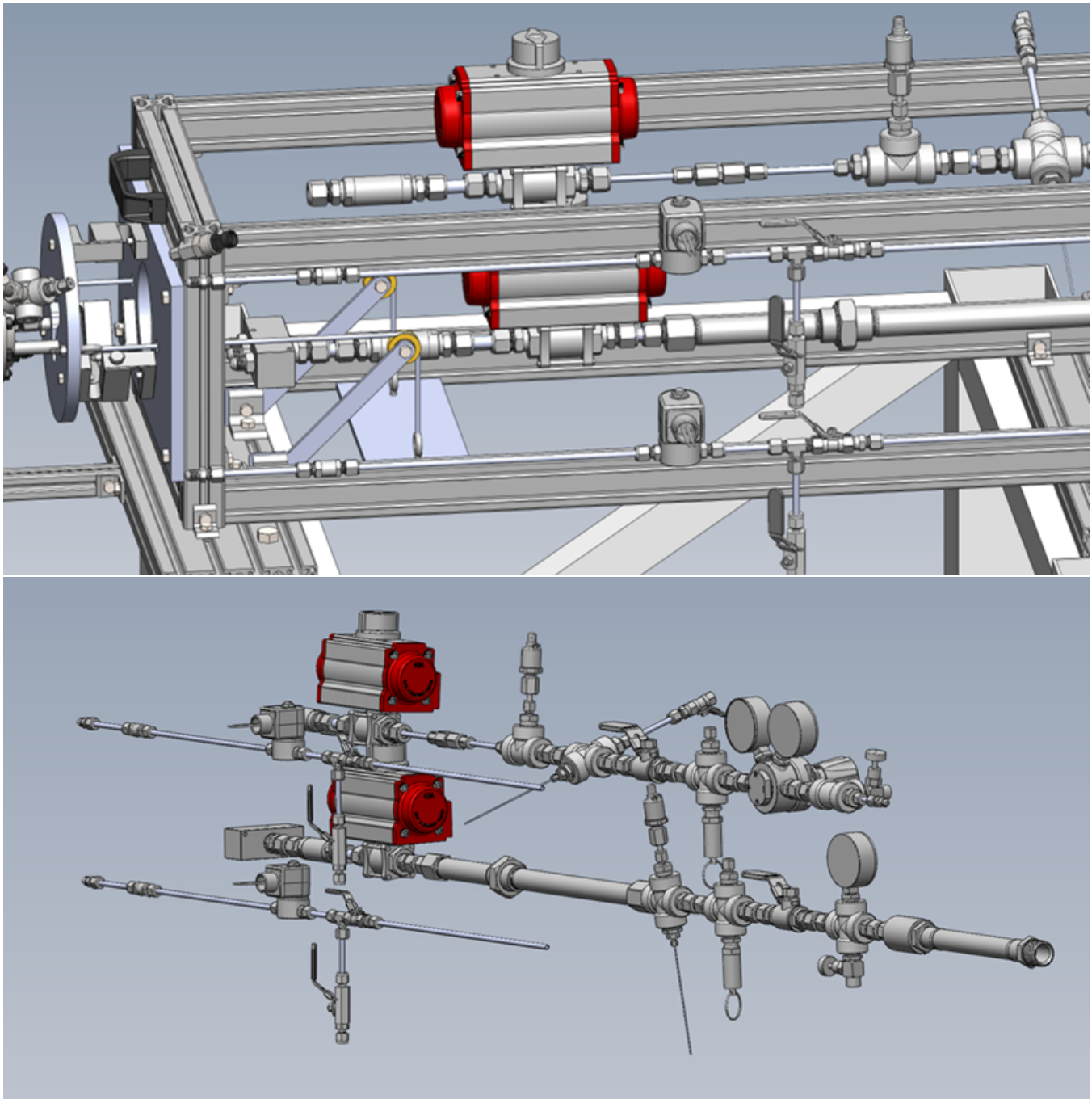

Figure 63: CAD images of the Fluid System and the fluid system integrated on the test stand.

9 System Evaluation

9.1 RDE Combustor

The primary goal with the RDE combustor was to demonstrate successful operation using an air-breathing rotating detonation engine (RDE) at a small annulus diameter. While most air-breathing RDEs operate at or above 6 inches in diameter, our design targeted a more compact configuration.

9.1.1 SABR-RDE-1 Ignition

This requirement focused on validating a custom ignition method specific to the SABR system. A torch igniter integrated into the injector face was selected based on industry feedback due to its reduced volume and gentler operating conditions compared to a pre-detonator. Although this method did not successfully ignite the engine, likely due to insufficient mixing, it was retrofitted with a pre-detonator from PERL, resulting in successful chamber ignition and meeting the requirement.

9.1.2 SABR-RDE-2 Injection

Injection performance was validated by comparing measured pressures upstream and downstream of the restriction orifices to the expected pressure drops calculated in the system pressure drop model. Using conservation of mass and orifice equations, it was confirmed that the injectors delivered the target mass flow rates.

9.1.3 SABR-RDE-3 Flow Stabilization

Flow stabilization was achieved within the plenums by choking the injector flow. While the orifices were used to limit mass flow, the analysis also showed that sonic conditions were reached, isolating upstream flow from disturbances in the chamber. Pressure data validated this condition.

9.1.4 SABR-RDE-4 Thrust Structure

The thrust-bearing structure of the RDE was verified through finite element analysis using ANSYS and post-test inspections. No visible damage was observed after multiple hot fires.

9.1.5 SABR-RDE-5 Startup Time

Startup time has not yet been experimentally verified. High-speed imaging will be used in future testing to validate model predictions and observe ignition transients.

9.1.6 SABR-RDE-6 Material Selection

304 Stainless Steel was selected based on a heat transfer analysis and survived hot fire tests with minimal discoloration near the igniter outlet. No structural erosion was observed.

9.1.7 SABR-RDE-7 Mass Flow

This requirement was validated through pressure-based analysis consistent with SABR-RDE-2 and SABR-RDE-3.

9.1.8 SABR-RDE-8 Thrust

Load cell measurements after calibration confirmed thrust values up to 100 N, consistent with expected performance for the test conditions.

9.1.9 SABR-RDE-9 Propellants

Hydrogen and air were delivered from standard PERL facilities-compressed hydrogen cylinders and an air farm-satisfying this requirement.

9.1.10 SABR-RDE-10 Operational Time

Hot fire tests were conducted successfully with durations up to 1 second, verified by video capture of the exhaust flame.

9.1.11 SABR-RDE-11 Propellant Interface

Cold flow tests confirmed propellant delivery through visible and tactile exhaust observations.

9.1.12 SABR-RDE-12 Structural Interface

Thrust-induced loading was successfully captured by load cells, verifying structural integration.

9.1.13 SABR-RDE-13 Data Acquisition Interface

Pressure transducers were threaded into the hydrogen and air plenums and the torch ignitor chamber, confirming interface integration.

9.1.14 SABR-RDE-14 Interface Verification

Dry-fitting of all RDE components confirmed internal and external interfaces prior to testing.

9.1.15 SABR-RDE-15 Functional Verification

Cold and hot flow tests verified the torch ignitor and injector functionality. Successful combustion was verified visually at off-stoichiometric conditions and via surface heating at stoichiometric conditions.

9.1.16 SABR-RDE-16 Performance Verification

Initial hot fire tests failed with the torch ignitor but succeeded using the pre-detonator. FFT analysis of audio data revealed detonation-relevant frequencies, suggesting proper wave formation.

9.1.17 SABR-RDE-17 Manufacturability Verification

A full-scale 3D print and machinist review confirmed that all RDE components could be fabricated using in-house equipment.

9.1.18 SABR-RDE-18 Operational Safety

Safety reviews were performed with senior personnel. Safe operating practices and system placement were employed, including avoiding premixed flows for added safety.

9.1.19 SABR-RDE-19 Manufacturability

All components were designed to be compatible with UCF machine shop tooling. The design avoided complex tolerances and surface finishes.

9.1.20 SABR-RDE-20 Sustainability

The modularity of the RDE combustor allows quick part replacement and integration of design updates without requiring a full system rebuild.

9.2 Data Acquisition and Control

The developed DAQ system satisfied all design requirements listed in Section 5. Temperature and pressure sensors were placed throughout the system, and calibrated load cells achieved better than 3% accuracy.

9.2.1 Sensor and DAQ Specifications

The final hardware performance was confirmed through testing and simulation. Specifications including sensor response time, DAQ sampling rate, and resolution are included in Table 4 and Table 5.

Table 4: Sensor Specifications

Device	Range	Total Error Band	Accuracy	Response Time
Omega PX-309 Pressure Transducer	0–500 PSI (0–5V), 0–3000 PSI (4–20mA)	±1.0%	±0.25% BSL, max	¡1ms
Evolution Sensors K-Type Thermocouple	0–920°C	Unlisted	Unlisted	Unlisted
Phidgets S-Type Load Cell	0–100kg	∼0.0437% FS	0.03% FS	Unlisted

Table 5: DAQ Analog Input Specifications

Device	Maximum Sampling Rate	ADC Resolution	Timing Accuracy	Timing Resolution
NI-USB 6210	250 kS/s	16 bit	50 ppm	50 ns
NI-USB 6001	20 kS/s	14 bit	100 ppm	12.5 ns
Arduino UNO R3	∼100 kS/s	10 bit	50 ppm	62.5 ns
Sparkfun HX711 ADC	80 S/s	24 bit	Unlisted	Unlisted

9.2.2 System Checkout Procedure

Before any pressurized test is conducted, the DAQ system undergoes a rigorous checkout procedure to ensure all components function nominally. The procedure is as follows:

1. Turn on all power supply units (PSUs) and validate their status via the onboard LEDs:
    - Green LED indicates 5V and 24V PSUs are operational
    - Blue LED indicates the 12V PSU is active
2. Connect all data acquisition devices and launch the LabVIEW control script.
3. Run the script and verify sensor readings:
    - Thermocouples should read approximately 30°C
    - 0–500 PSI transducers should read around 14 PSI (ambient)
    - 0–3000 PSI transducers should read close to 0 PSI
4. Perform a valve actuation test using the steps outlined in Appendix C under the table titled *Valve Actuation Test (Depressurized)*.
5. Confirm proper system function by analyzing the generated data files.

If any sensors or valves fail to respond during checkout, verify all wiring connections. Pay close attention to relay circuitry and ensure adequate switching current is provided via the external 5V PSU to the NI-USB 6210. The NI-DAQ's digital output pins cannot supply sufficient current to reliably trigger relays without this external boost. Faulty valve behavior can often be traced to insufficient current delivery or reversed polarity on the optocoupler inputs. Sensors should be cross-referenced with the wiring schematic found in LabVIEW script and validated against the I/O list in LabVIEW script to ensure correct LabVIEW channel mapping.

9.2.3 Safety Protocol and Emergency Handling

To prevent unintentional ignition or opening of fuel lines, a two-step verification is required prior to starting any pressurized test. Operators must manually confirm proper system status and initialize fuel systems only under test-ready conditions.

An emergency software stop (E-Stop) function is included in the LabVIEW control script. If triggered, the system immediately:

- Closes all fuel system valves
- Opens all air lines to purge the engine and plumbing with clean air
- Waits a fixed delay, then shuts down all valve actuators

This mechanism ensures quick and automatic safe-down procedures in the event of abnormal operation, power failure, or human error during testing.

9.3 Test Stand Configuration

The primary objective of the test stand was to provide a safe, robust, and adaptable platform for engine mounting, thrust measurement, and data acquisition. The design was driven by a set of clearly defined engineering specifications as defined in Section 5, primarily involving ease of integration and structural stability. A series of analyses, inspections, and demonstrations were performed to evaluate the system's ability to meet these requirements, as well as to characterize the reliability and identify potential failure modes.

In regard to the functional requirements set for the test stand, each one was met with relative ease. Most of these requirements were verified through demonstration, whether statically through fit checks and sub-scale testing, or dynamically through full hot-fire tests of the engine. The requirements surrounding the structural stability of the test stand were all demonstrated across multiple hot fires of the engine, in which the stand maintained structural integrity throughout the duration of the test, with no observable deformation, loosening, or extreme resonance behavior.

Additionally, the requirements surrounding the test stand's interfaces and overall performance were verified through

constant inspection and demonstration, specifically in regard to the stand's ability to effectively integrate with the other subsystems. Throughout the development process, the engine, plumbing, and data acquisition systems experienced minimal issues integrating with the test stand, even through multiple design iterations across the project as a whole. There were also multiple demonstrations throughout the entire project timeline in which the test stand was shown to be easily operable, free from unnecessary complexities, and maintained within the allocated lab space at UCF's Propulsion and Energy Research Laboratory.

To assess the overall safety of the test stand assembly, the structural frame and load cell calibration systems were subjected to repeated testing to assess long-term reliability and functionality. Multiple full-scale engine tests were completed, along with full component assembly and disassembly, and no hardware degradation or measurable performance losses were observed. All of the structural components were selected with minimum safety factors of 2, including the steel cables, fasteners, and frame materials. Operator safety was also maintained, primarily by enforcing standoff zones during testing, and reinforcing data cables and other high-priority components away from pressurized lines. As a result, no incidents or component failures occurred during the testing campaign.

The failure modes for the test stand were mostly comprised of events with a low probability of occurrence, but were also mostly undetectable and would result in very severe consequences. As a result, most of the failure modes were addressed through the proper design and component analysis, a method which turned out to work very well. Some of the rarer modes, such as structural yielding, buckling, and modal failure, which had the highest severity, did not occur across the entire testing campaign, leading to a robust test stand system that can continue to be used indefinitely. Slightly more common failures, such as failure to secure the engine, plumbing, or electronics, as well as the failure to remain electrically grounded or prevent stress concentration within the plumbing system, were also properly mitigated as well, as zero serious integration issues or data collection failures were observed throughout the testing campaign. Finally, the most common failure mode of inaccurate load cell data was also properly mitigated, as the force readings provided by the load cells both prior to and following calibration were consistent with expected loads.

As shown, the evaluation of the test stand confirms that it has successfully met all functional, performance, safety,

and interface requirements established at the outset of the project. Through a combination of thoughtful design, rigorous testing, and careful integration with supporting subsystems, the test stand demonstrated high reliability, operational safety, and structural robustness across a wide range of testing conditions. The absence of hardware degradation, data inconsistencies, or integration issues over multiple hot fire tests further validates the effectiveness of the design. These results not only establish this test stand as a dependable platform for RDE experimentation but also provide a solid foundation for future iterations within the same framework.

9.4 Fluid Systems Evaluation

During testing, full functional performance of the fluid system was verified, and the system met or exceeded all requirements.

9.4.1 Performance Requirements

The system was able to consistently deliver the required mass flow rates of hydrogen and air into the combustor across various test configurations. These results were validated using upstream and downstream pressure transducer data, matched against modeled performance curves generated by the MATLAB-based flow calculator.

9.4.2 Tolerance and Sensitivity

Orifice sizes and regulator setpoints were tuned iteratively based on system feedback. The system demonstrated tolerance to small variations in upstream pressure, with negligible impact on flow-rate thanks to the established choked flow regime. Temperature sensors showed limited sensitivity drift between runs, remaining within a consistent range.

9.4.3 Reliability and Safety

No failures in actuation, flow delivery, or instrumentation were observed throughout the hot fire and cold flow test campaigns. The use of pneumatic run valves and check valves effectively prevented reverse flow. All fittings and connections remained leak-free under pressure, and the flexible hosing successfully decoupled engine movement from the rigid fluid system.

9.4.4 Failure Modes

Potential failure modes considered included valve sticking, transducer dropout, or orifice erosion. No such failures occurred during the testing period. Relief valves, redundant venting mechanisms, and proper wiring routing reduced the likelihood of overpressurization or data loss.

Note: Full test procedures, equipment specifications, and DAQ calibration settings used to validate the fluid system are provided in Appendix C.

10 Significant Accomplishments and Open Issues

Partially due to the mixing problems encountered during the first iteration of the combustor, the torch ignition system did not perform as expected. The thought process behind this approach was to induce a deflagration to detonation transition in the annulus, removing the need for a long tube used in the pre-det ignition approach. However, very well mixed propellants are necessary for the energy release necessary to transition to a detonation. Forcing extremely efficient mixing via reducing the gap between injectors or considering adding special geometry would significantly help to create a homogeneous mixture to begin with. At that point, the use of a torch ignition system could prove viable and extremely promising in terms of a combustor ready for integration with a flight vehicle. The torch worked effectively in a vacuum, enduring the extreme conditions inside of it with minimal damage, and providing it with a more ideal and predictable propellant mixture would drastically increase its chances of performing in the context of initiating a detonation. A possible upgrade to consider would be switching to a different spark plug integration method. Currently, the electrode is directly in the gas impingement area, which aids with ease of ignition. This also exposes the spark plug to extreme conditions outside of its design operation range, which led to ceramic insulation damage in one of the tests while trying to extract more performance out of the torch. Some spark plugs are made following the NPT standard, so scaling up the torch cross and implementing one of these spark plugs could greatly reduce the chances of failure even in off-nominal performance scenarios.

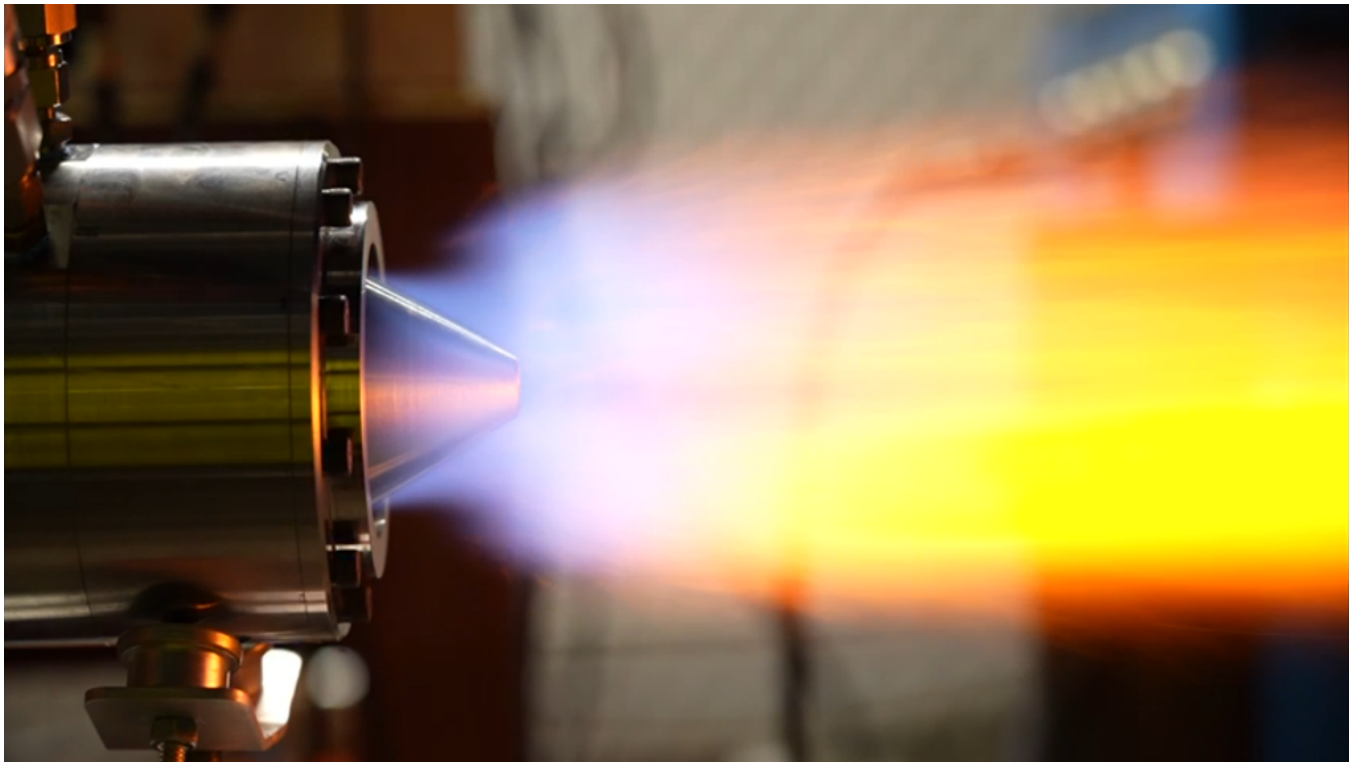

The SABR team achieved several major milestones in the development and integration of the fluid system as well. One of the most significant accomplishments was the successful implementation of a choked-flow system architecture that isolated the upstream supply from downstream transients. This enabled a reliable and repeatable way to control mass flow rates and equivalence ratios, supporting one of the core technical goals of identifying a range of operating conditions for sustained detonation.

Additionally, the fluid system was designed and constructed with a high level of reusability and adaptability in mind. The integration of COTS components and standardized fittings, as well as ease of access to every section of the lines ensures the system can be quickly and easily reconfigured or serviced. This design foresight will directly benefit future teams by simplifying maintenance, component replacement, and expansion of the system for different engine configurations.

The team also successfully developed and validated custom MATLAB tools to support orifice sizing and predict flow behavior under a variety of supply conditions. These tools were instrumental in establishing initial test conditions and remain valuable for future iterations of the SABR test platform. The flow calculator's outputs were verified through

cold flow testing, where measured pressures and temperatures upstream of the orifices confirmed the presence of sonic flow conditions. This validation closed the loop between modeling and experimental data, demonstrating that the methodology used for system sizing was sound.

While the system met all key design requirements and test objectives related to cold flow operation, not all planned hot fire tests were completed within the project timeline. This was largely due to extended integration time and interdependencies with other subsystems such as ignition and data acquisition. However, these delays underscored the importance of designing the system with modularity and resilience, enabling future teams to complete hot fire testing without needing to rework the fluid system.

The team also produced comprehensive assembly documentation, testing procedures, and maintenance guides to support long-term test stand operations. These contributions directly align with the broader project objective of establishing a reusable modular platform for future senior design groups. By documenting system behavior and configuration strategies, the team created a foundation that lowers the barrier for future work on RDEs and expands the usefulness of the SABR test infrastructure.

Remaining open issues include the lack of hot fire data needed to verify flow behavior during actual detonation events. While choked flow conditions were confirmed in cold flow testing, it remains to be seen how combustion dynamics and backpressure transients may influence system behavior during engine operation. These are areas for future works to investigate, and they represent natural extensions of this year's work.

11 Conclusions and Recommendations

Initial testing with the chosen torch igniter method yielded unreliable results, with only one deflagration mode achieved at the time of testing. This led to the decision to pivot to the backup pre-detonator tube in order to validate the rest of the system's operation and ensure the best chances of achieving stable detonation. Future testing with different set pressures into the torch, as well as different conditions in the RDE itself will be necessary to further mature the technology in this application. Additionally, possible rearranging of the torch structure could be implemented to shield the spark plug elements from the full heat release of the combustion process, as some damage was seen after an attempt to extract more performance out of the torch.

All in all, the DAQ and Electronics system worked phenomenally. The control system developed is straightforward and easy to operate, all acquired data is instantly stored in a measurement file to prevent data loss, and DAQ test conditions are easily repeatable. However, there is still room for improvement. In an ideal world, a NI c-DAQ chassis would be deployed in place of the plethora of data acquisition devices used in this project. This would make wiring significantly simpler and reduce overall system complexity. Additionally, the loop execution rate of the LabVIEW script can be bolstered to 1ms, from 30ms, by syncing each sample read with one iteration of the loop, as outlined in Section 8. With these improvements the system would be perfect and even without them, the system has displayed impeccable performance and reliability.

The development of the SABR fluid system represents a significant step toward enabling stable, repeatable, and safe testing of a small-scale air-breathing rotating detonation engine. Through a modular and robust design, the team achieved the construction of a fully functional fluid delivery system capable of precise flow control using simple, cost-effective components. The design adhered to key fluid system requirements, including decoupling dynamic combustion effects through choked flow, incorporating fast-acting actuation, and integrating appropriate safety mechanisms. Cold flow testing confirmed the system's ability to deliver predictable mass flow rates of air and hydrogen while maintaining measurement accuracy and operational safety.

Based on lessons learned during this project, several recommendations are offered to improve system performance and reliability for future iterations. First, hot fire testing should be prioritized early in the schedule, with additional

buffer time allocated for system integration and testing procedures. This would help close remaining knowledge gaps related to flow stability and combustion-coupled transients. Second, additional flow sensors, such as downstream pressure transducers or differential sensors across the orifices, could enhance system diagnostics and allow for better real-time performance monitoring. These additions would provide insight into detonation-induced pressure fluctuations and potential deviations from choked flow behavior during operation. Future teams could also further explore the use of sonic nozzles which would allow for more confident flow choking and less pressure losses in the system.

In conclusion, the SABR fluid system met its stated objectives by delivering a safe, modular, and high-precision architecture that supports the needs of an experimental RDE.

12 Appendix A - Customer Requirements

12.1 SABR System Requirements

Tag	ID	Name	Description	Requirement Type	Verification Method
SABR	1	Thrust	SABR shall produce measurable thrust.	Functional	Test
SABR	2	Detonation	SABR should demonstrate the capability of detonation.	Functional	Test
SABR	3	Oxidizer	SABR should operate using compressed atmospheric air.	Functional	Test
SABR	4	System Scale	SABR shall scale its components and performance metrics to a small scale compared to current operational systems.	Performance	Analysis
SABR	5	Reusability	SABR should not sustain extensive damage for the duration of the engine burn.	Sustainability	Demonstration
SABR	6	System Interface	SABR shall interface with the equipment provided by PERL.	Interface	Inspection
SABR	7	Operational Verification	SABR shall be static fire tested at a variation of equivalence ratio.	Verification	Demonstration
SABR	8	System Cost	SABR should not exceed a cost of $5,000.	Cost	Inspection

Table 6: SABR Requirements

12.2 RDE Requirements

Tag	ID	Name	Description	Requirement Type	Verification Method
SABR-RDE	1	Ignition	SABR-RDE shall employ a means for ignition.	Functional	Inspection
SABR-RDE	2	Injection	SABR-RDE shall inject propellants at a specified mass flow rate.	Functional	Analysis
SABR-RDE	3	Flow Stabilization	SABR-RDE shall stabilize flow conditions received from SABR-FS.	Functional	Analysis
SABR-RDE	4	Thrust Structure	SABR-RDE shall withstand thrust generated.	Functional	Demonstration
SABR-RDE	5	Startup Time	SABR-RDE should transition the combustion mode to detonation within milliseconds of ignition.	Performance	Test
SABR-RDE	6	Material Selection	SABR-RDE shall be manufactured out of materials that withstand operating conditions.	Performance	Analysis
SABR-RDE	7	Mass Flow	SABR-RDE should inject propellants at a combined mass flow around 250 g/s.	Performance	Analysis
SABR-RDE	8	Thrust	SABR-RDE should produce measurable thrust in the range of 75 - 250 N.	Performance	Test
SABR-RDE	9	Propellants	SABR-RDE should perform reliably with atmospheric air and gaseous hydrogen.	Performance	Test
SABR-RDE	10	Operational Time	SABR-RDE should combust propellants for at least 0.25 seconds.	Performance	Test
SABR-RDE	11	Propellant Interface	SABR-RDE shall receive propellants delivered from SABR-FS.	Interface	Demonstration
SABR-RDE	12	Structural Interface	SABR-RDE shall transfer thrust to the test stand's structure.	Interface	Analysis
SABR-RDE	13	Data Acquisition Interface	SABR-RDE shall include necessary sensor ports for integration with data acquisition.	Interface	Demonstration
SABR-RDE	14	Interface Verification	SABR-RDE shall undergo interface verification of its components and subassemblies.	Verification	Inspection
SABR-RDE	15	Functional Verification	SABR-RDE shall undergo functional verification of its components and subassemblies.	Verification	Demonstration
SABR-RDE	16	Performance Verification	SABR-RDE shall undergo performance verification of its components and subassemblies.	Verification	Test
SABR-RDE	17	Manufacturability Verification	SABR-RDE shall undergo manufacturability verification of its components and subassemblies.	Verification	Analysis/Test
SABR-RDE	18	Manufacturability	SABR-RDE shall be designed to maximize the manufacturing capabilities available to the team.	Other	Demonstration
SABR-RDE	19	Sustainability	SABR-RDE shall be sustainable in a manner that is convenient to service and build upon.	Other	Analysis

Table 7: SABR-RDE Requirements

12.3 Test Stand Requirements

Tag	ID	Name	Description	Requirement Type	Verification Method
SABR-TS	1	Structural Limits	SABR-TS shall withstand all applied force and vibrational forces in a static loading case.	Functional	Analysis
SABR-TS	2	Sustainability	SABR-TS shall be sustainable in manner that is convenient to service and build upon.	Functional	Analysis
SABR-TS	3	Engine Support	SABR-TS shall provide mounting and support for the engine.	Functional	Demonstration
SABR-TS	4	Fluid System Support	SABR-TS shall provide mounting and support for the fluid system.	Functional	Demonstration
SABR-TS	5	Electronics Support	SABR-TS shall provide mounting and support for the electronics.	Functional	Demonstration
SABR-TS	6	Transportable	SABR-TS shall be easily transportable.	Functional	Demonstration
SABR-TS	7	Loads	SABR-TS shall be able to withstand all loads.	Functional	Demonstration
SABR-TS	8	Loads on Fluids System	SABR-TS shall be able to reduce structural loads on the fluids system.	Functional	Analysis
SABR-TS	9	Form Factor	SABR-TS should fit within a standard-size SUV trunk volume.	Performance	Inspection
SABR-TS	10	Manufacturability	SABR-TS structural components shall consist of widely available metal extrusions.	Performance	Inspection
SABR-TS	11	Weight	SABR-TS shall be able to support a weight of 250 N.	Performance	Analysis
SABR-TS	12	Thrust Loads	SABR-TS shall maintain a minimum safety factor of 5 at all times.	Performance	Analysis
SABR-TS	13	Combustor Interface	SABR-TS shall physically interface with the combustor via the thrust plate.	Interface	Inspection
SABR-TS	14	Feed System Interface	SABR-TS shall supply structural support and relevant physical interfaces to feed system outlets.	Interface	Inspection
SABR-TS	15	Lab Interface	SABR-TS shall be physically secured within the allocated lab space at PERL.	Interface	Inspection

Table 8: SABR-TS Requirements

12.4 Fluid System

Tag	ID	Name	Description	Requirement Type	Verification Method
SABR-FS	1	Propellant Flow Rate Control	SABR-FS shall control flow rates for each propellant.	Functional	Test
SABR-FS	2	SABR-RDE Propellant Supply	SABR-FS shall supply SABR-RDE with propellants.	Functional	Demonstration
SABR-FS	3	Air Supply	SABR-FS shall deliver air mass flow to the combustor between 200–300 g/s.	Performance	Analysis
SABR-FS	4	Fuel Supply	SABR-FS shall deliver fuel mass flow to the combustor between 1–20 g/s.	Performance	Analysis
SABR-FS	5	Structural Stability	SABR-FS shall be able to withstand nominal operating conditions.	Performance	Demonstration
SABR-FS	6	SABR-RDE Propellant Mixture	SABR-FS shall provide SABR-RDE with a mixture of gaseous hydrogen and air in the equivalence ratio range of 0.5 to 2.0.	Performance	Test
SABR-FS	7	SABR-RDE Interface	SABR-FS shall integrate with SABR-RDE.	Interface	Inspection
SABR-FS	8	SABR-TS Interface	SABR-FS shall integrate with SABR-TS.	Interface	Inspection
SABR-FS	9	PERL Interface	SABR-FS shall integrate with the PERL air and hydrogen plumbing systems.	Interface	Inspection
SABR-FS	10	Pressure Verification	SABR-FS shall verify its ability to hold pressure without leaks.	Verification	Demonstration
SABR-FS	11	Cold Flow Verification	SABR-FS shall verify its expected pressure loss and mass flow targets at nominal flow conditions.	Verification	Test
SABR-FS	12	Integration Verification	SABR-FS shall undergo integration verification of its components and subassemblies.	Verification	Inspection
SABR-FS	13	Safing Procedure	SABR-FS shall shutdown or fail in a safe condition.	Other	Demonstration

Table 9: SABR-FS Requirements

12.5 Data Acquistiion and Control System

Tag	ID	Name	Description	Requirement Type	Verification Method
SABR-DAQ	1	Imaging Diagnostics	SABR-DAQ should collect imaging diagnostics at a point downstream of the exhaust to validate the presence of detonations.	Functional	Demonstration
SABR-DAQ	2	Pressure Diagnostics	SABR-DAQ shall collect pressure diagnostics at various points throughout the system.	Functional	Demonstration
SABR-DAQ	3	Temperature Diagnostics	SABR-DAQ shall collect temperature diagnostics at various points throughout the system.	Functional	Demonstration
SABR-DAQ	4	Load Cell Diagnostics	SABR-TS should measure applied loads from SABR-RDE.	Functional	Demonstration
SABR-DAQ	5	Thrust Measurements	SABR-DAQ shall be able to measure applied loads exceeding the maximum expected thrust of SABR-RDE.	Performance	Analysis
SABR-DAQ	6	DAQ Interface	SABR-DAQ shall provide the necessary electrical power and data transmission capabilities to all sensors within the system domain.	Interface	Inspection
SABR-DAQ	7	Control System Complexity	SABR-DAQ shall be easily operable and free from unnecessary complexities.	Other	Demonstration

Table 10: SABR-DAQ Requirements

13 Appendix B - System Evaluation Plan

13.1 Order of Operations

#	Procedure	Goal
1	VALVE ACTUATION TEST (DEPRESSURIZED)	Ensure all valves are linked to corresponding LabVIEW controls, all valves are operational, and all sensors are reading nominally.
2	SYSTEM PRESSURIZATION	Verify the fluid system is operating nominally under design pressures.
3	COLD FLOW TEST	Verify control timing is accurate and system pressures and mass flow rates are within expected ranges.
4	IGNITION TEST	Confirm igniter parameters are correct and will successfully ignite the engine.
5	HOT FIRE	Verify successful full-scale operation of the RDE with its supporting systems.

Table 11: Order of Operations for Testing

13.2 Essential Personnel

#	Operator	Function
1	PERL GRADUATE/LAB MANAGER	Oversee all testing operations. Responsible for the safety of all operators. **MUST BE PRESENT DURING FULL DURATION OF PRESSURIZATION EVENTS.**
2	DAQ/CONTROL OPERATOR	Oversee all aspects of the control script during testing. Responsible for inputting test parameters, ensuring control system function, reading system data, and giving final checks for testing events.
3	FLUID SYSTEM OPERATOR	Oversee all aspects of the fluid system during testing. Responsible for system pressurization and depressurization, pressure relief, and safe operation during high-pressure operations.
4	SUPPORTING PERSONNEL	Responsible for all other testing aspects. Assists in fluid system operation and pressurization events. Opens cylinders, sets air regulator pressure, and actuates PERL air pneumatic valve. Helps ensure testing operations are carried out in their *entirety*, and serves as an additional safety *member*.

Table 12: Essential Testing Personnel Roles

13.3 Safety/Personal Protective Equipment

Safety/Personal Protective Equipment		
Equipment	**Name**	**Function**
1	Ear Protection	Prevents hearing damage.
2	Eye Protection	Prevents eye damage.
3	Fire Extinguisher	Used for stopping the spread of fire.
4	First Aid Kit	For use on open wounds or other bodily injury.
5	Eye Wash Station	For use washing eyes out in event of FOD or chemical injury.

Table 13: Safety and PPE Equipment Required for Operation

13.4 Valve Actuation Test

Valve Actuation Test (Depressurized)	
Step	**Instruction**
1	Plug in SABR control laptop to both USB DAQ's (NI-USB 6001, NI-USB 6210) and to power. Plug in the 3 DAQ power supplies (5VDC, 12VDC, 24VDC).
2	***Note: NEVER attempt to run valves without 5V PSU plugged in. The DAQ's power is boosted through the 5V supply in order to provide relays with enough switching current. Failure to do so will result in PERMANENT DAMAGE to the DAQ.***
3	Disconnect the spark plug cap from spark plug.
4	Launch the SABRctrl LabVIEW script.
5	Set physical channels as specified in IO list in LabVIEW under the "Configuration" tab.
6	Fill out "Test Name" on the "Live" Tab.
7	Start the LabVIEW script.
8	Click the "Execute Valve Test" button to start the valve test.
9	Check for valve actuation. This should be done audibly, visually, and by touching the solenoid housing. Each solenoid valve will make a clicking noise and a strong vibration when actuated, and the igniter valves will have an LED indicator that lights up.
10	If successful, the background of the Valve Test Panel will turn green, if unsuccessful, it will turn red.
11	If the panel turns red, actuate each valve individually using the "Manual Testing" Panel to identify the faulty valve. Ensure valve is connected properly then re-run a valve test.
12	Click the "End Program" button after finished with valve testing.

Table 14: Valve Actuation Test Procedure (Depressurized)

13.5 System Pressurization

Table 15: System Pressurization Procedure

System Pressurization
IMPORTANT INFORMATION: MAXIMUM ALLOWABLE WORKING PRESSURES (MAWPs): ALL AIR LINES: **1000 PSIG** H2 LINES **DOWNSTREAM** OF PRESSURE REGULATOR: **1000 PSIG** H2 LINES **UPSTREAM** OF PRESSURE REGULATOR: **3000 PSIG** MAXIMUM EXPECTED OPERATING PRESSURES: AIR LINES: **950 PSIG** H2 LINES: **950 PSIG** All lines have hand valves that allow for pressure relief anywhere within the system. **MAIN OPERATORS NEED TO BE AWARE** of each isolation and vent valve and understand how to quickly relieve pressure in each location if needed. PRVs are located in each of the main lines. These valves have set cracking pressures that will begin relieving pressure when over pressurization events occur. **INSPECT PRVs PRIOR TO OPERATION.** Make sure that the locknuts are secure and ensure that the cracking pressure is at the desired set points for each line. The H2 main source isolation hand valve has an aftermarket handle called the "Mandle." **ENSURE THAT THE HANDLE IS FULLY TIGHTENED AND WON'T COME LOOSE DURING OPERATION.**
Prior to system pressurization: - Inspect all open sealing surfaces, vent valves, and other components to ensure they are clear of debris and operational. - Make sure valve checkouts were run prior to pressurizing the system. - Ensure all bottles and valves are closed before operation.

Continued on next page

System Pressurization (continued)

- **Ensure the H2 regulator is fully backed out** and will prevent flow.

- Ensure that all pressure gauges and pressure sensors are reading **0 psig**.

Before pressurizing the system, the operator must connect all line interfaces with the lab facilities.

These will include the ¼" lines going to the H2 cylinder, the 1" lines from the compressed air pallet, the low pressure compressed air hoses for pneumatically actuated valves, and the oxygen interface on the 6" RDE test table if the pre-detonation tube is being used.

After the lines have been connected to the system, start by pressurizing the air lines:

Ensure that the PERL dome loaded regulator is receiving control pressure (diaphragm is being loaded).

This is done by opening the "back" valves on the air pallets. After pressurizing the control side of the dome loaded regulators, the air pallet "front" valves can be opened to introduce a load pressure to the dome loaded regulators.

The hand regulator is used to control the dome's loaded pressure setpoint.

ENSURE THAT THE SET PRESSURE IS NOT ABOVE THE MAWP OF THE SABR AIR LINES!!!!

The system will not see the set pressures until the main 1" pneumatic valve on the PERL facility wall is manually actuated. If the pressure is set too high, relieve control pressure through the self-venting hand regulator.

Start with low pressures to ensure correct operation.

Slowly increase pressures up to nominal operating pressures, continuously checking for signs of gas leaks, failing seals, or valves in the wrong state.

Check the air line main gauge as well as the air pressure transducer to confirm pressures.

Occasionally, a bubbling liquid indicator should be applied to all sealing locations to detect small leaks in the system.

If desired, run a flow test of just the air line by opening the main and igniter air valves. This can be used to check valve actuation under pressure and ensure that plenum pressures are reading nominally.

Continued on next page

System Pressurization (continued)
The operator can now begin pressurizing the H2 line. While one operator opens the H2 bottle, another operator should be stationed at the H2 regulator to monitor bottle pressures. **IF A LEAK IS DETECTED**, the main H2 source isolation hand valve should be immediately closed, the bottle should be immediately closed, and the H2 venting needle valve just upstream of the regulator should be opened to relieve any trapped pressure. After confirming depressurization, all sealing surfaces should be inspected and adjusted accordingly. During re-pressurization, air can be used instead of H2 to check for failing seal locations.
Open the main H2 source isolation hand valve. The upstream regulator gauge will now read H2 bottle pressures. Pressure should be slowly introduced to the system by tightening the H2 regulator. If any leaks are audibly detected, the regulator should be backed out and the H2 relief valve should be opened immediately to prevent over pressurizing the main line. **THE DATA ACQUISITION OPERATOR** should read the H2 main line pressures as this process occurs to ensure that the regulator gauge is reading correctly. After pressurizing both lines, check pressure transducer data and the pressure gauges again to ensure that the correct pressures are being read. The system is now fully pressurized and ready for cold flow testing.

13.6 Cold Flow Test

Step	Procedure
1	Plug in SABR control laptop to both USB DAQ's (NI-USB 6001, NI-USB 6210) and to power
2	Plug in the 3 DAQ power supplies (5VDC, 12VDC, 24VDC). Note: NEVER attempt to run valves without 5V PSU plugged in. The DAQ's power is boosted through the 5V supply in order to provide relays with enough switching current. Failure to do so will result in PERMANENT DAMAGE to the DAQ.
3	Disconnect the spark plug cap from spark plug
4	Launch the SABRctrl LabVIEW script
5	Set physical channels as specified in IO list in LabVIEW under the "Configuration" tab.
6	Fill out "Test Name" on the "Live" Tab
7	Start the LabVIEW script
8	At this point, the System Pressurization Procedure should be successfully completed.
9	Confirm that the system is under nominal pressures for the desired testing conditions.
10	Confirm that operators are in their designated positions and are fully aware of their responsibilities during test events.
11	Ensure that a member of the operating team is located at the PERL air pneumatic valve.
12	Enable "Cold Flow", the "FIRE" button should turn into a blue button labeled "Cold Flow"
13	Set timing parameters for each valve
14	Verify pressure readings are within expected values
15	Ensure personnel in surrounding area are notified of a high-pressure test, have proper hearing protection, and are clear from the line of fire
16	Signal to the PERL air pneumatic valve operator to manually open the run valve.
17	Click the "Arm System" button
18	Notify surrounding personnel of impending high-pressure test
19	Click the "Cold Flow" button

13.7 Ignition Test

Step	Procedure
1	Plug in SABR control laptop to both USB DAQ's (NI-USB 6001, NI-USB 6210) and to power
2	Plug in the 3 DAQ power supplies (5VDC, 12VDC, 24VDC)
3	Disconnect the spark plug cap from spark plug
4	Launch the SABRctrl LabVIEW script
5	Set physical channels as specified in IO list in LabVIEW under the "Configuration" tab
6	Fill out "Test Name" on the "Live" Tab
7	Start the LabVIEW script
8	At this point, the System Pressurization Procedure should be successfully completed.
9	Set timing parameters for each valve
10	Verify pressure readings are within expected values
11	Ensure personnel in surrounding area are notified of a high-pressure test, have proper hearing protection, and are clear from the line of fire
12	Click the "Arm System" button
13	Notify surrounding personnel of impending high-pressure test
14	Click the "FIRE" button
15	Click the "End Program" button after finished with Igniter test

13.8 Hot Fire

Step	Procedure
1	Plug in SABR control laptop to both USB DAQ's (NI-USB 6001, NI-USB 6210) and to power
2	Plug in the 3 DAQ power supplies (5VDC, 12VDC, 24VDC)
3	Disconnect the spark plug cap from spark plug
4	Launch the SABRctrl LabVIEW script
5	Set physical channels as specified in IO list in LabVIEW under the "Configuration" tab
6	Fill out "Test Name" on the "Live" Tab
7	Start the LabVIEW script
8	At this point, the System Pressurization Procedure should be successfully completed.
9	Set timing parameters for each valve
10	Verify pressure readings are within expected values
11	Ensure personnel in surrounding area are notified of a high-pressure test, have proper hearing protection, and are clear from the line of fire
12	Click the "Arm System" button
13	Notify surrounding personnel of impending high-pressure test
14	Click the "FIRE" button
15	Click the "End Program" button after finished with test

14 Appendix C - User Manual

14.1 Safety Briefing

Safety Briefing
Prior to the operation of the SABR system, the following safety briefing must be given.
The safety of all personnel is the top priority during the operation of this system. If any off-nominal events occur, the first course of action is to ensure **safety** of all personnel subject to any danger. Review all current emergency standards of PERL and the action plans for any perceived hazard. The safety of the facility is always secondary to the safety of personnel; however, if there is no imminent danger to personnel, actions should be taken to preserve the facility as much as possible without imposing danger. To mitigate events where safety is compromised, the following should always be followed: • All personnel should wear the PPE outlined in the Safety/Personal Protective Equipment Table of the Appendix B: System Evaluation Plan. • Any significant events, including but not limited to connecting instruments to power, pressurizing the system, and running commands on the control panel, should be clearly verbally communicated to all personnel. • All plumbing components, when not connected, should have FOD covers and be checked for FOD before assembly. • Personnel should be at a safe viewing distance for all tests. • Operators should sound the facility horn to notify bystanders of an upcoming test corresponding to the pattern defined in the PERL safety standards. • All valves from source pressures should be opened slowly to ensure longevity of equipment. • Bleed valves should be opened slowly.

14.2 Essential Personnel

Essential Personnel		
Operator	**Role**	**Function**
1	PERL GRADUATE/LAB MANAGER	Oversee all testing operations. Responsible for the safety of all operators. **MUST BE PRESENT DURING FULL DURATION OF PRESSURIZATION EVENTS.**
2	DAQ/CONTROL OPERATOR	Oversee all aspects of the control script during testing. Responsible for inputting test parameters, ensuring control system function, reading system data, and giving final checks for testing events.
3	FLUID SYSTEM OPERATOR	Oversee all aspects of the fluid system during testing. Responsible for system pressurization and depressurization, pressure relief, and safe operation during high-pressure operations.
4	SUPPORTING PERSONNEL	Responsible for all other testing aspects. Assists in fluid system operation and pressurization events. Opens cylinders, sets air regulator pressure, and actuates PERL air pneumatic valve. Helps ensure testing operations are carried out in their entirety, and serves as an additional safety member.

14.3 Facility Operations

Facility Operations	
Step	**Procedure**
1	Conduct safety briefing.
2	Notify bystanders of ensuing tests.
3	Conduct Valve Actuation Test (Depressurized) as listed in its respective table in Appendix B: System Evaluation Plan.
4	Conduct System Pressurization as listed in its respective table in Appendix B: System Evaluation Plan.
5	Conduct Cold Flow Test as listed in its respective table in Appendix B: System Evaluation Plan.
6	Conduct Ignition Test as listed in its respective table in Appendix B: System Evaluation Plan.
7	Conduct Cold Flow Test as listed in its respective table in Appendix B: System Evaluation Plan with only air flow to cool hardware.
8	Conduct Hot Fire Test as listed in its respective table in Appendix B: System Evaluation Plan.
9	Ensure system safety prior to approaching the system.
10	Safe system by removing spark plug wire connection.
11	Conduct basic analysis of system operation from sensor plots on the control panel to inform operators of system performance.

15 Appendix D - Cost Analysis and Manufacturability Analysis

15.1 Manufacturing Cost Estimate and Make-Buy Analysis

The estimated total **manufacturing cost** of the RDE system based on the bill of materials is approximately **$8,000**, distributed as follows:

- **Combustion and Injector System Components:** $2,900

  Includes machined injector plates, flanges, and annular sections made of stainless steel and Inconel. These parts typically require high-tolerance CNC machining and post-process inspection.

- **Cooling System Hardware:** $600

  Involves copper tubing, compression fittings, and brazing consumables.

- **Instrumentation and Data Acquisition:** $2,200

  Includes pressure transducers, thermocouples, CTAP ports, and DAQ modules.

- **Structural Supports and Mounting:** $800

  Includes aluminum and steel mounting brackets, fasteners, and adjustable rails.

- **Valving and Feed System:** $1,000

  Pneumatic solenoid valves, stainless steel tubing, Swagelok fittings, and regulators.

- **Miscellaneous Supplies:** $500

  Includes sealants, o-rings, gaskets, abrasives, and PPE.

Make-Buy Analysis of Critical System Elements

Component	Make/Buy	Rationale
Injector Plate (SS 316/718)	Make	Requires custom flow pattern and tight tolerance; not commercially available.
Annular Combustion Chamber	Make	Geometry is unique; precision curvature and wall thickness essential.
Pressure Transducers	Buy	Calibrated and certified sensors are more cost-effective and reliable.
Pneumatic Solenoid Valves	Buy	Off-the-shelf components cheaper and standardized (e.g., SMC or Parker).
Cooling System (tubing layout)	Make	Custom geometry adapted to injector and nozzle layout for heat mitigation.
Mounting Brackets	Make	Designed for specific flight configuration or particular test stand geometry and integration.
DAQ System (e.g., NI modules)	Buy	Commercial systems are robust, tested, and integrate easily with LabVIEW.

Table 16: Make-Buy Analysis of Critical RDE Components

Manufacturability Considerations

As the system is not intended for mass production, the current configuration emphasizes:

- **Custom fit** over manufacturing ease.
- **Modularity** for rapid component replacement (e.g., injector faceplates).
- **Refurbishability** of injector and combustion sections through cleaning or light machining.

For future scaling to mass production, key manufacturability issues include:

- **Complex geometry:** Annular chambers and injector interfaces require precise welding and forming; scalable solutions may include casting or metal additive manufacturing.
- **Material cost:** Inconel usage is cost-prohibitive; alternatives or coatings should be investigated.
- **Tight tolerances:** Injector orifice precision may necessitate high-throughput micro-drilling or EDM processing.

16 Appendix E - Expense Report

Item Name	Description	QTY	Pkg Size	Unit Price	Total Price	Vendor
1’ -6AN to -6AN Braided Stainless Steel Hose Assembly	For fluid system air manifold to RDE inlet	3.0	1.0	12.95	38.85	eBay
1’ Tube Stub 1/2 Braided Stainless Steel Hose Assembly	For fluid system hydrogen outlet to RDE inlet	1.0	1.0	25.60	25.60	eBay
High-Pressure 304 Stainless Steel Pipe Fitting (Spark Plug)	Hunter E-Bay Find	1.0	1.0	15.99	15.99	eBay
Ignition Coil	Standard Motor Products UC15T Ignition Coil for 12V Vehicles Without Electronic Ignition System	1.0	1.0	24.49	24.49	Amazon
TVS Diode	TVS Diode	10.0	1.0	0.65	6.53	Digikey
Coil Capacitors	1uF 250V Radial Ceramic Caps	10.0	1.0	0.98	9.80	Digikey
Tuning/Bleed Resistor	4.7 Ohm 0.6W Resistor	10.0	1.0	0.09	0.87	Digikey
Spark Relay	SPDT 30A 12v	2.0	1.0	2.15	4.30	Digikey
Resonant Caps	22uF 50V	1.0	5.0	5.99	5.99	Amazon
Cross Tap for Spark Plug	M14 by 1.25	1.0	1.0	9.13	9.13	Amazon
Cutting Disk	Dewalt cutting disk	1.0	1.0	9.72	9.72	
Flapper Disk	FLapper disk for sanding	1.0	10.0	18.97	18.97	
Nitrile Glove (100 Ct)	Nitrile Glove (100 Ct)	1.0	1.0	9.98	9.98	
Shop Towel	Shop towel	1.0	1.0	17.50	17.50	
Isopropyl	Iso	1.0	1.0	5.00	5.00	

Item Name	Description	QTY	Pkg Size	Unit Price	Total Price	Vendor
Test Stand Resurfacing Equipment (includes acetone and other chemicals)		1.0	1.0	100.00	100.00	
Test Stand Paint	Sprays for primer and paint	1.0	1.0	25.00	25.00	
Straight Adapter for 1/4 Tube OD x 1/4 NPT Female”	Transducer Female Fitting	1.0	1.0	20.26	20.26	McMaster
Straight Adapter for 1/4 Tube OD x 1/4 NPT Male”	Torch Transducer Male	1.0	1.0	13.05	13.05	McMaster
1/4 Stub x 1/4 Male NPT Adapter Stainless Steel — Tube Fittings”	Connector for air igniter line isolation hand valve	1.0	1.0	5.86	5.86	Titan Fittings
1/2 316 Hex Nipple - 316 Stainless”	Cross connection fittings for air line	1.0	1.0	6.96	6.96	Titan Fittings
1/4 Tube x 1/4 Male NPT Connector Stainless Steel — Tube Fittings”	For new isolation valve for H2 igniter line	1.0	1.0	12.74	12.74	Titan Fittings
1/4 Tube x 1/4 Female NPT Connector Stainless Steel — Tube Fittings”	For o-keefe connections main H2 line	2.0	1.0	15.70	31.40	Titan Fittings

Item Name	Description	QTY	Pkg Size	Unit Price	Total Price	Vendor
1/2 x 1/4 Reducing Hex Nipple - 316 Stainless SN: S8346RH004003”	For new Air Vent Valve Connection	1.0	1.0	7.83	7.83	Titan Fittings
1/2 x 1/4 Forged Threaded Hex Bushing 3000 316 Stainless SN: S4036HB004002”	PT Connections	2.0	1.0	4.96	9.92	Titan Fittings
-4 MNPT to -4 COMPRESSION	Main line vent hand valve	1.0	1.0	12.74	12.74	Titan Fittings
Isopropyl Alchohol		1.0	1.0	37.50	37.50	Amazon
SDTC Tech 2-Pack Pipe Plug Fittings 1/2 NPT Male Thread 304 Stainless Steel Internal Hex Socket Countersunk Adapter	Plugs for igniter testing	1.0	1.0	7.50	7.50	Amazon
1/2 Forged Threaded Female Threaded Cross 3000 304 Stainless	Cross Connector	3.0	1.0	29.49	88.47	Titan Fittings
Type K SS Sheathed Thermocouples		2.0	1.0	61.00	122.00	Evolution Snsors
Snoop		1.0	1.0	16.00	16.00	Amazon
Blue Monster Tape		2.0	1.0	5.85	11.70	Amazon
-16 BORED THROUGH COMPRESSION to -4 MNPT	For thermocouple sheat connections	2.0	1.0	15.00	30.00	Harold G

Item Name	Description	QTY	Pkg Size	Unit Price	Total Price	Vendor
-4 JIC to -4 FNPT	Ignitier Hose Fittings Downstream (JIC to FNPT on Okeefe)	2.0	1.0	12.07	24.14	Titan Fittings
-8 MNPT to -4 COM-PRESSION	Main -8 to -4 Vent Line Adapters	1.0	1.0	16.75	16.75	Titan Fittings
-12 FNPT to -8 COM-PRESSION	Air ROU Nipple connections	2.0	1.0	33.09	66.18	Titan Fittings
-12 FNPT to -8 MNPT	Air ROU Nipple connections	2.0	1.0	33.73	67.46	Titan Fittings
-16 FNPT to -8 FNPT	Air Hose PERL Interface Fitting	1.0	1.0	27.66	27.66	Titan Fittings
-4 Stub to -4 FNPT	For PT Connections off the crosses (not twisting wires)	2.0	1.0	8.60	17.20	Titan Fittings
-8MNPT to -4 COM-PRESSION	For PT Connections off the crosses (not twisting wires)	2.0	1.0	16.75	33.50	Titan Fittings
-4 JIC37 to -4 COM-PRESSION	H2 Hose PERL Interface Fittings	1.0	1.0	13.11	13.11	Titan Fittings
1/4 Ferrules Front	For valves with missing ferrules	6.0	1.0	1.76	10.56	Titan Fittings
Ferrules Back	For valves with missing ferrules	6.0	1.0	1.88	11.28	Titan Fittings
Nuts	For valves with missing ferrules	6.0	1.0	4.24	25.44	Titan Fittings
WIC Valve 1/4 High Pressure Solenoid 304 SS	Igniter Valves	2.0	1.0	108.90	217.80	WIC
12 304 SS Nipple	Straight length for upstream of Air ROU	1.0	1.0	19.86	19.86	Titan Fittings
SHIPPING COSTS	Only for the two mcmaster and three titan orders	1.0	1.0	75.71	75.71	
6 304 SS Nipple	Straight length for downstream of Air ROU	1.0	1.0	11.39	11.39	Titan Fittings

Item Name	Description	QTY	Pkg Size	Unit Price	Total Price	Vendor
*-4 COMPRESSION CROSS	Igniter Line Vent Split	1.0			-	
*-4 COMPRESSION TEE	Igniter Line Vent Split	1.0			-	
*-4 COMPRESSION TEE with INLINE -4 MNPT	H2 Igniter Line	1.0			-	
*-8 MNPT to -8 COMPRESSION	Used throughout the main lines.	30.0			-	
*-8 FNPT to -8 COMPRESSION	For H2 Orifice Connections InLine	2.0			-	
Smooth-Bore Seamless 304 Stainless Steel Tubing (6ft each)	1/4 Line	2.0			-	
Smooth-Bore Seamless 304 Stainless Steel Tubing (6ft each)	1/2 Line	3.0			-	
316 SS Check Valve (Spring Loaded Piston)	Air and H2 Main Check Valves	2.0			-	
1/2 Pneumatic Ball Valve	Air and H2 Main Valves	2.0			-	
Pneumatic Pilot Solenoids		2.0			-	
K-Type Probe Thermocouple		2.0	1.0	53.70	107.40	McMaster

Item Name	Description	QTY	Pkg Size	Unit Price	Total Price	Vendor
S-Type Load Cell - 100kg		3.0	1.0	45.00	135.00	Phidgets
SparkFun Load Cell Amplifier		3.0	1.0	10.95	32.85	SparkFun
5VDC Power Supply Unit (4ch Relay Module)		1.0	1.0	16.75	16.75	Amazon
24VDC Power Supply Unit (Solenoid + PT)	AC/DC DIN RAIL SUPPLY 24V XW	1.0	1.0	28.13	28.13	Amazon
Control Box	QILIPSU UL94-V0 Outdoor WiFi Enclosure 13.8x9.9x5.9	1.0	1.0	49.41	49.41	Amazon
12V PSU	for solenoid valves and spark plug	1.0	1.0	11.99	11.99	Amazon
3v Relays	spark plug relay	1.0	1.0	9.99	9.99	Amazon
Pressure Transducers (KXR)		2.0			-	
Through Hole Terminal Block	Load cell amp wire to board terminal block (TERM BLOCK 5POS 45DEG 2.5MM PCB)	10.0	1.0	0.65	6.51	Digikey
Pressure Transducers (PERL)		6.0			-	
4-Channel Solid State Relay (PERL)	SRD-05VDC-SL-C	1.0			-	
8-Channel Solid State Relay (PERL)		1.0			-	
Ball Transfer Mount		1.0	1.0	12.39	-	Send Cut Send
Calibration Platform		1.0	1.0	-	-	Send Cut Send

Item Name	Description	QTY	Pkg Size	Unit Price	Total Price	Vendor
Engine Interface Plate		1.0	1.0	69.80	-	Send Cut Send
Frame Interface Plate		1.0	1.0	72.86	-	Send Cut Send
Frame Lift Handle		1.0	2.0	9.99	9.99	Amazon
Optical Table		1.0	1.0	-	-	Free
Pulley Arm		2.0	1.0	11.41	-	Send Cut Send
Pulley Wheel		2.0	1.0	6.44	12.88	McMaster
Quick Link		4.0	1.0	3.17	12.68	Home Depot
					3547.39	

17 Appendix F - List of Manuals and Other Documents

DAQ and Control System Documentation

- Arduino UNO R3 User Manual [36]
- NI Field Wiring and Noise Considerations for Analog Signals [37]
- NI USB-6001 User Manual [38]
- NI USB-6210 User Manual [39]
- OMEGA Pressure Transducer Wiring [40]
- SparkFUN HX711 Data Sheet [41]
- SparkFUN HX711 User Manual [42]

Fluid System Documentation

- Topworx Chemical Compatibility Guide [43]
- WIC Pneumatic Ball Valve Documentation [44]
- Airtac 4V200 Pneumatic Solenoid Valve [45]
- Harris Regulator Catalog [46]
- Hydrogen Piping Standard B31.12-2023 [47]
- MacWeld ROU Quotation 104788 [54]
- NPT Compression Fitting Technical Guide [49]
- PRV Installation Guide [50]
- Sales Receipt - Evolution Sensors and Controls [51]

- Type K Thermocouple Specifications [52]

18 Appendix G - Design Competencies

Project Title: Small-Scale Air-Breathing RDE (SABR)

Term: Fall 2024-Spring 2025

18.1 ABET Design Competence Matrices

18.1.1 Aeronautical and/or Astronautical Topics Utilized

Topic	Criticality to Project	Section - Page(s)	Comments
Aerodynamics	Only a passing reference		Limited discussion with only passing relevance in understanding RDE exhaust flow and nozzle design.
Aerospace Materials	Critical/Main Contributor		Critical to ensuring components withstand high temperatures and pressures, with extensive trade studies and material selection discussions.
Flight Mechanics	Only a passing reference		Minimal mention; focused more on RDE propulsion design and testing rather than flight dynamics.
Propulsion	Critical/Main Contributor		Central to the project, with detailed analysis of RDE design, operation, and trade studies on combustion, ignition, and injector performance.
Stability & Control	Necessary but not a primary contributor		Necessary for ensuring system reliability but not extensively covered beyond maintaining detonation stability and controlling fluid dynamics.
Structures	Critical/Main Contributor		Essential in test stand and engine design, with in-depth trade studies on structural configurations and load distribution.
Attitude Determination & Control	Only a passing reference		Only tangentially mentioned, as the project is focused on propulsion rather than vehicle navigation.
Rocket Propulsion	Critical/Main Contributor		Key focus area, with significant content on detonation mechanics, thrust generation, and optimization of RDE components.
Space Structures	Critical/Main Contributor		Discussed in the context of structural analysis for test stand and engine components, with emphasis on lightweight, high-strength designs.
Telecommunications	Necessary but not a primary contributor		Only briefly mentioned concerning data acquisition and control for testing purposes.

Table 18: Aeronautical and Astronautical Topics Utilized

18.1.2 Mechanical Topics Utilized

Topic	Criticality to Project	Section and Page(s)	Comments
Thermal-Fluid Energy Systems	Critical/Main Contributor		Central to understanding the engine's thermal and fluid behavior, with extensive discussion on injector and cooling system design.
Machines and Mechanical Systems	Critical/Main Contributor		Focus on designing robust test stands and integrating mechanical systems like actuators and load cells.
Controls and Mechatronics	Critical/Main Contributor		Highlighted in data acquisition and control systems, ensuring precise operation and measurement of experimental setups.
Materials Selection	Critical/Main Contributor		Critical to the project's success, with extensive trade studies on combustor materials and detailed selection criteria.
Modeling and Measurement Systems	Critical/Main Contributor		Integral for design validation and testing, with emphasis on data acquisition accuracy and computational modeling.
Manufacturing	Critical/Main Contributor		Essential to ensure feasibility and reproducibility, with discussions on manufacturability, costs, and timelines for various components.

Table 19: Mechanical Topics Utilized

18.2 Topic Criticality Matrices

18.2.1 Aeronautical

AERONAUTICAL	Critical/ Main contributor	Strong contributor	Necessary but not a primary contributor	Necessary but only a minor contributor	Only a passing reference	Not Included in this Design Project
Aerodynamics					X	
Aerospace Materials	X					
Flight Mechanics						X
Propulsion	X					
Stability & Control				X		
Structures	X					

Table 20: Aeronautical Contribution Assessment

18.2.2 Astronautical

ASTRONAUTICAL	Critical/ Main contributor	Strong contributor	Necessary but not a primary contributor	Necessary but only a minor contributor	Only a passing reference	Not Included in this Design Project
Aerospace Materials	X					
Attitude Determination & Control					X	
Orbital Mechanics						X
Rocket Propulsion	X					
Space Environment						X
Space Structures	X					
Telecommunications		X				

Table 21: Astronautical Contribution Assessment

18.2.3 Mechanical Engineering Design Areas

ME DESIGN AREAS	Critical/ Main contributor	Strong contributor	Necessary but not a primary contributor	Necessary but only a minor contributor	Only a passing reference	Not Included in this Design Project
Thermal-Fluid Energy Systems	X					
Machines and Mechanical Systems	X					
Controls and Mechatronics	X					
Materials Selection	X					
Modeling and Measurement Systems	X					
Manufacturing	X					

Table 22: Mechanical Engineering Design Contribution Assessment

19 Appendix H - Engineering Drawings

19.1 Aerospike Plug

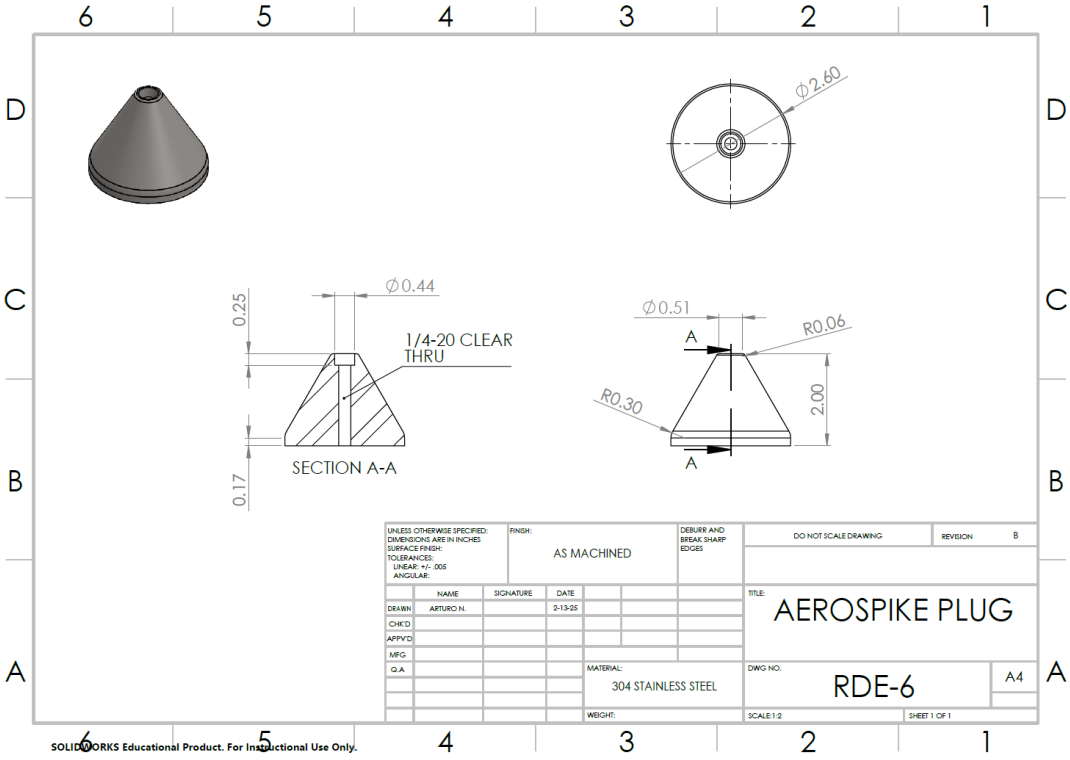

Figure 64: Detailed drawing of the aerospike plug used for flow expansion in the internal expansion nozzle of the RDE.

19.2 Cowl

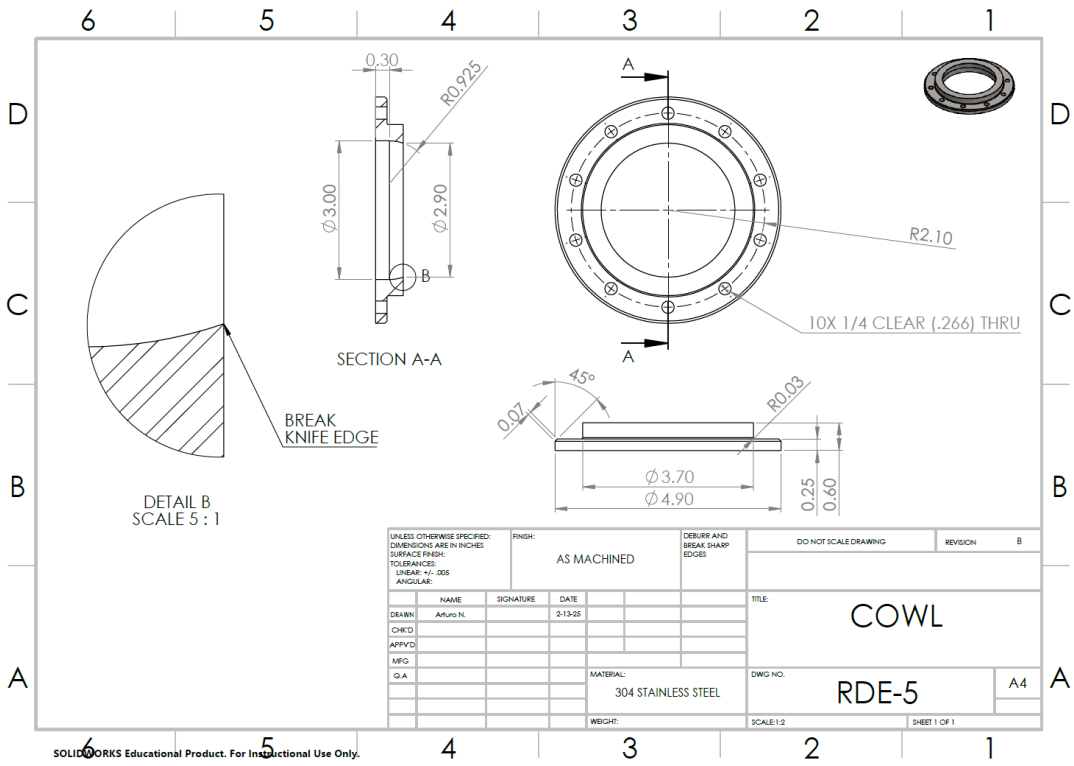

Figure 65: Engineering drawing of the RDE outer cowl which serves as a structural shell and provides aerodynamic enclosure.

19.3 Injector Plate

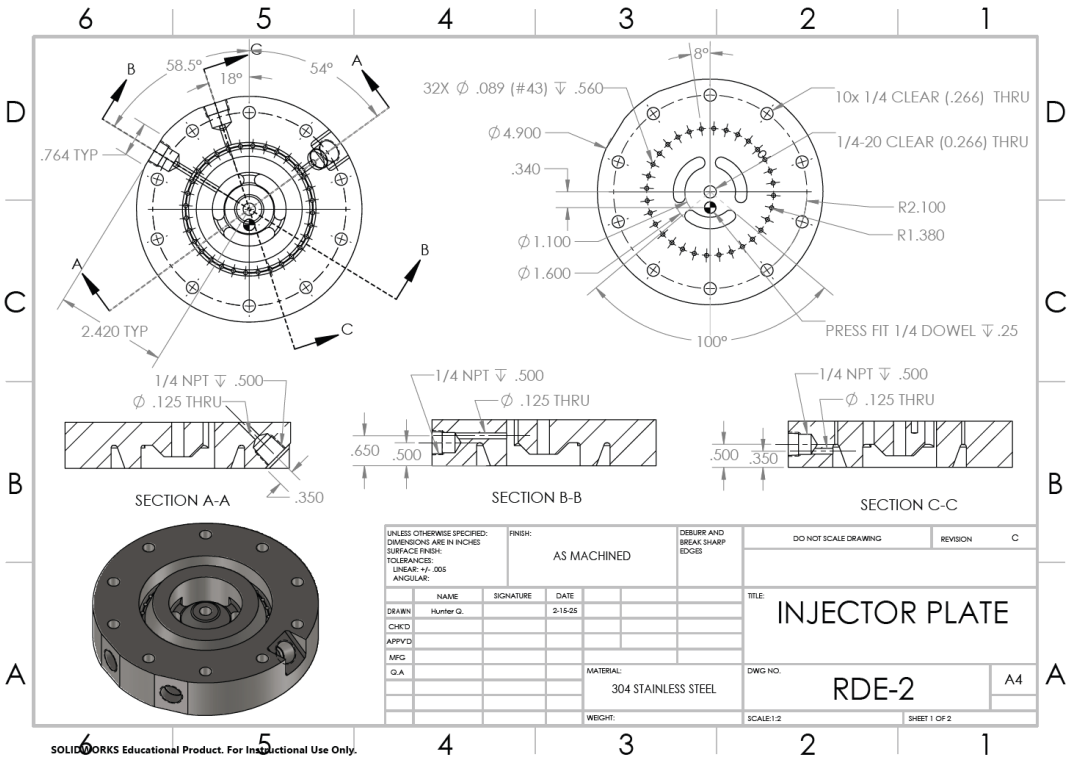

Figure 66: Injector plate showing the orifice configuration for hydrogen and air injection into the detonation annulus.

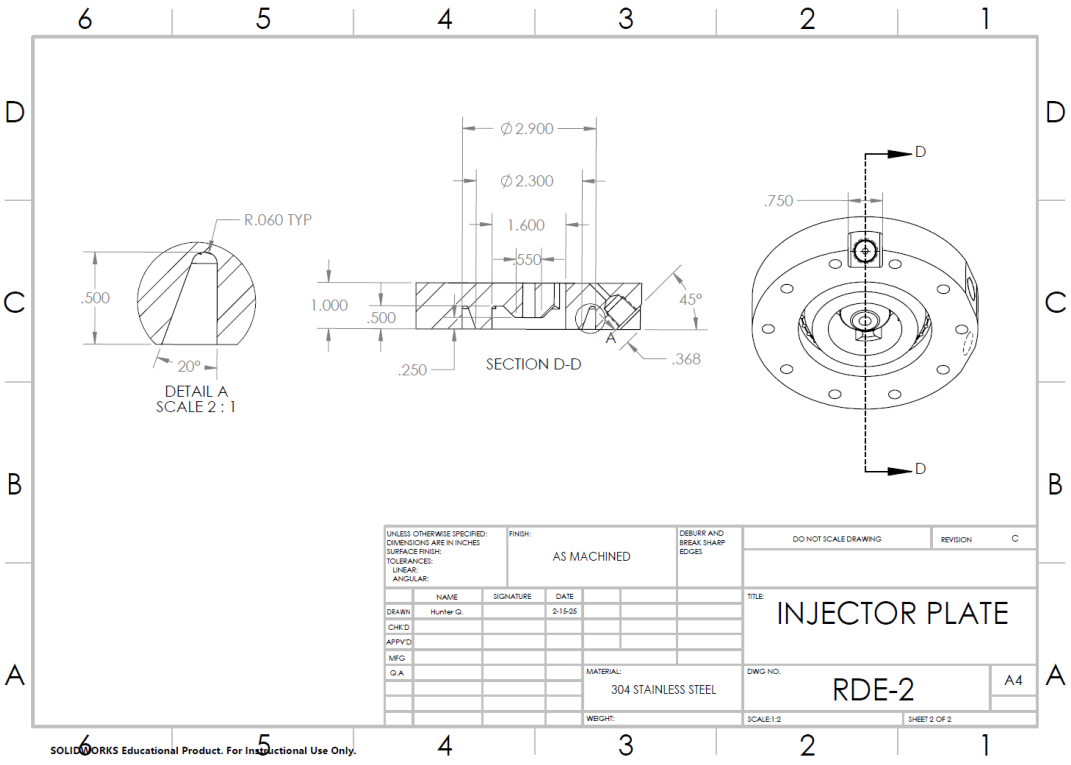

Figure 67: Alternate injector plate layout detailing internal flow paths and mounting features.

19.4 Inner Body

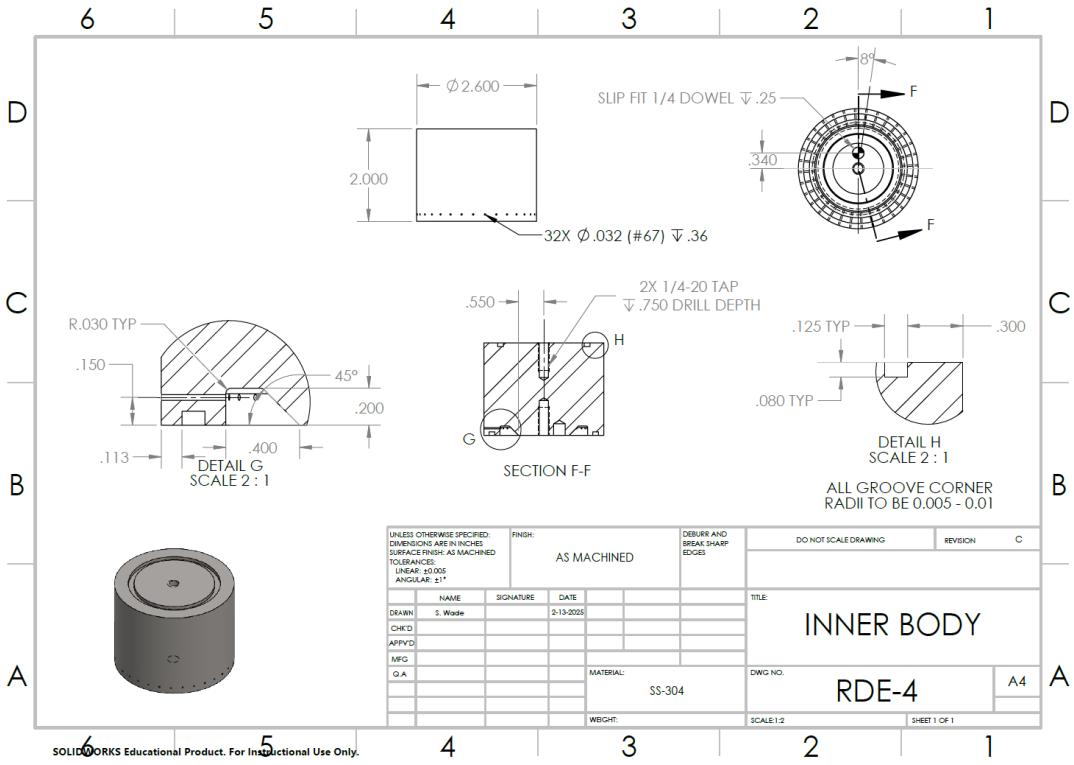

Figure 68: Drawing of the inner body of the RDE, which forms one side of the detonation annulus and supports internal components.

19.5 Outer Body

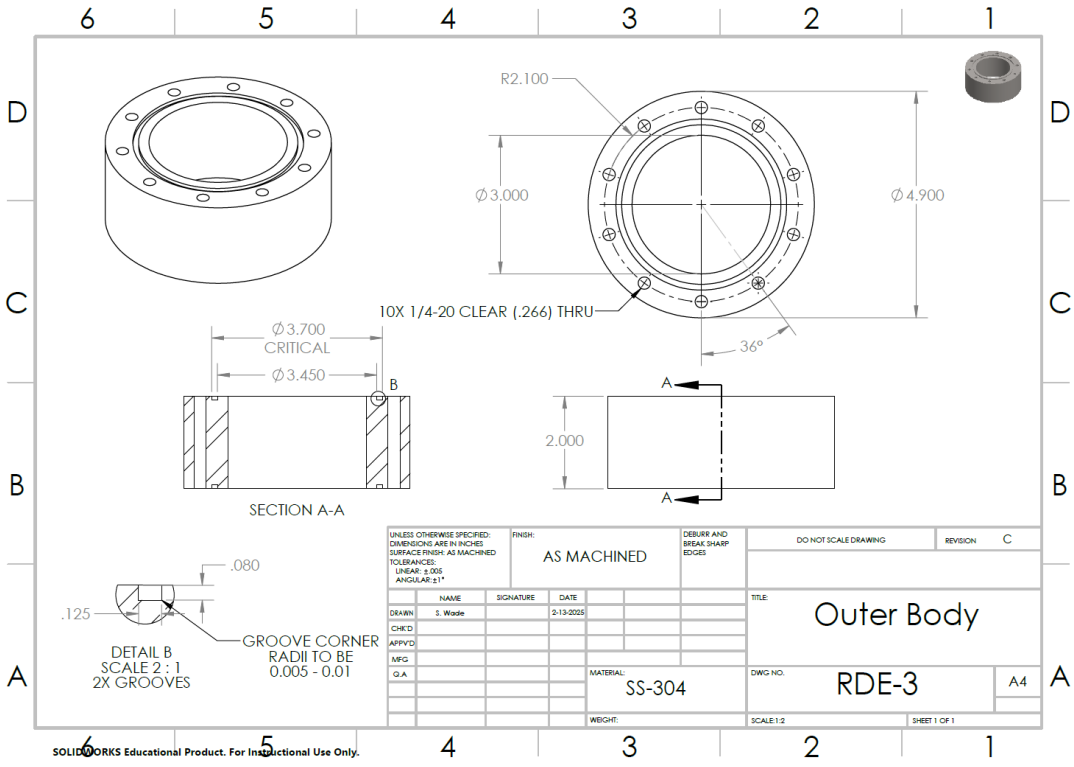

Figure 69: Outer body drawing which houses the detonation channel and interfaces with the structural support system.

19.6 Port Plate

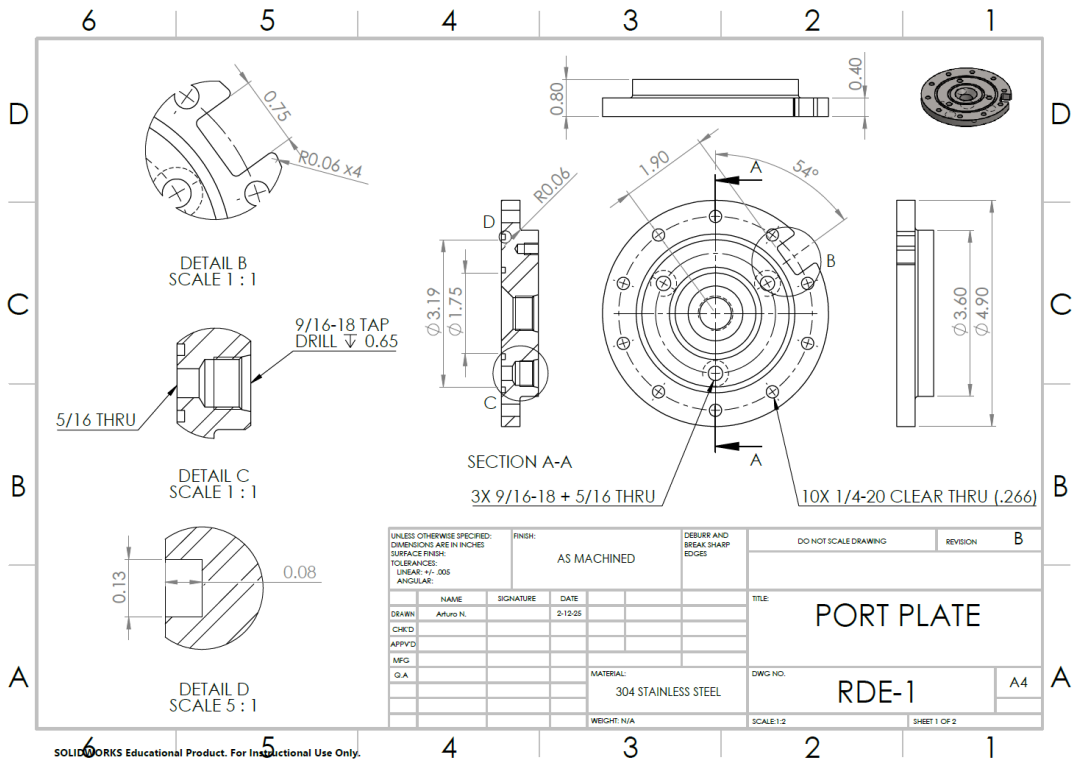

Figure 70: Port plate illustrating fluid inlet locations and mounting features for the plenum assemblies.

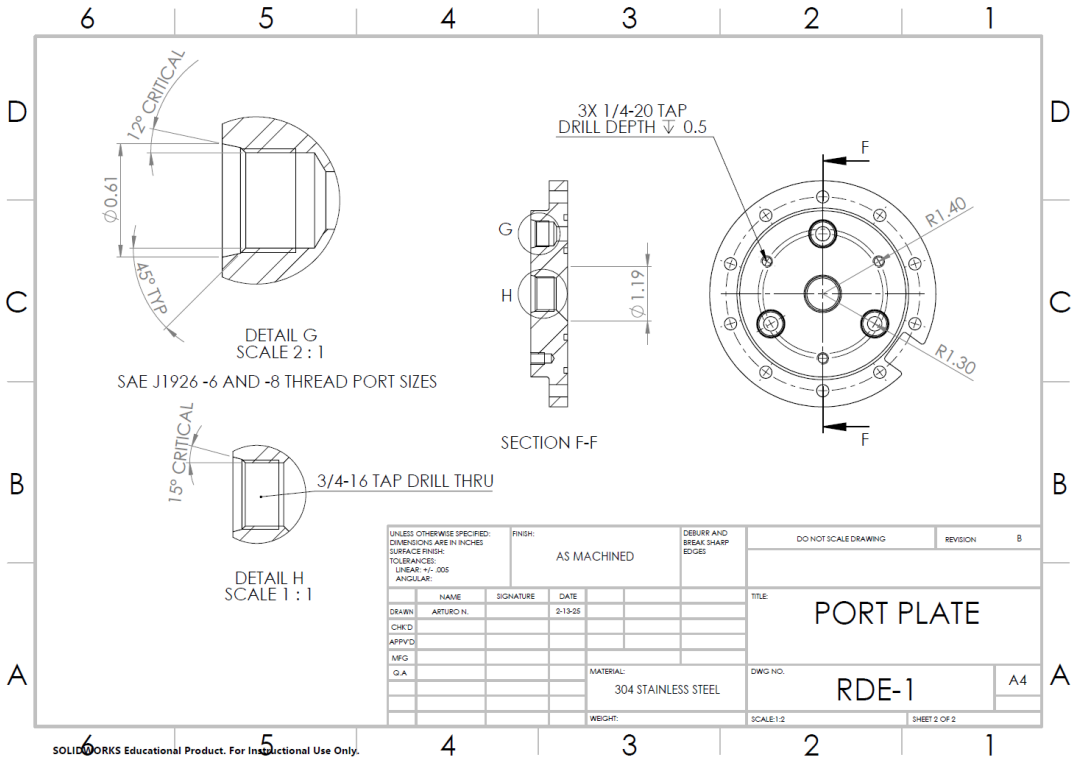

Figure 71: Secondary view of the port plate with detailed cutouts for instrumentation and seal interfaces.

19.7 Test Stand Assembly Drawing

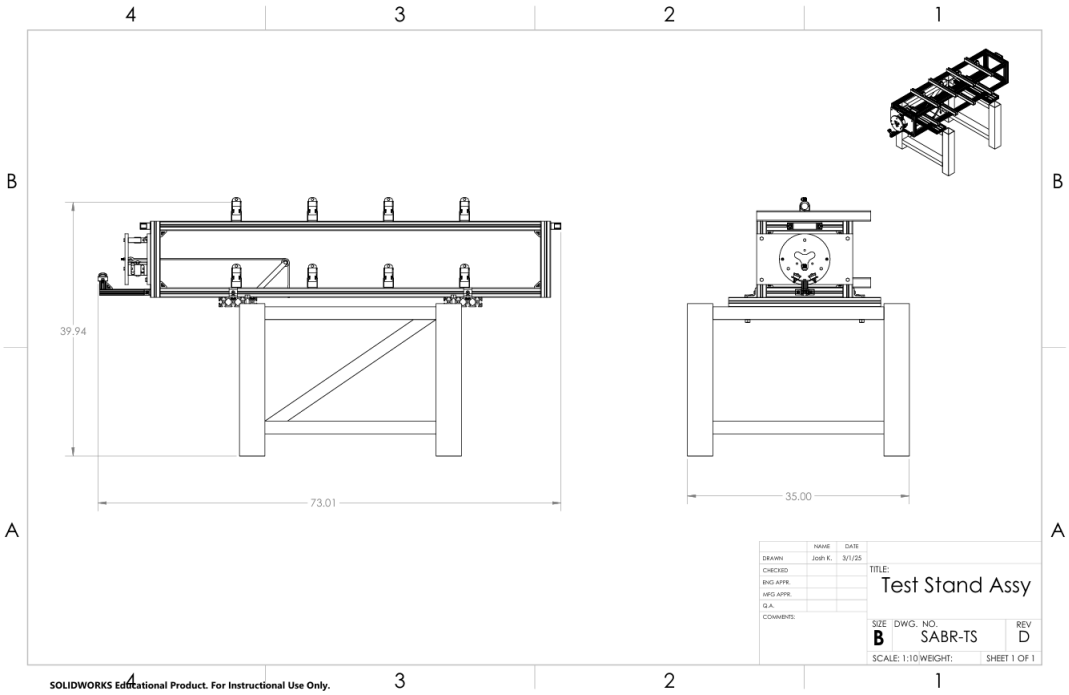

Figure 72: Test stand assembly drawing featuring calibration method, load cells, and ball transfer mount.

References

[1] cosmos, "The World's First Space Flight for the Rotating Detonation Engine, and a Glimpse at a New Sample Return Capsule," *ISAS / JAXA*, May 19, 2022. https://cosmos.isas.jaxa.jp/the-worlds-first-space-flight-for-the-rotating-detonation-engine-and-a-glimpse-at-a-new-sample-return-capsule/

[2] International Air Transport Association, *Fuel Fact Sheet*, 2023. https://www.iata.org/en/publications/economic-reports/airline-costs-and-fuel/

[3] Bigler, B.R., "Injector Mixing Effects in Rotating Detonation Rocket Engines," Aug. 2019. https://www.doi.org/10.2514/6.2019-3869

[4] National Instruments, "Fundamentals," 2023. [Online]. Available: https://www.ni.com/docs/en-US/bundle/ni-scope/page/fundamentals.htm

[5] Yokoo, R., Goto, K., Kim, J., Kawasaki, A., Matsuoka, K., Kasahara, J., Matsuo, A., and Funaki, I., "Propulsion performance of cylindrical rotating detonation engine," *AIAA Journal*, vol. 58, Nov. 2019, pp. 5107–5116.

[6] Shaw, I. J., et al., "A Theoretical Review of Rotating Detonation Engines," in *Direct Numerical Simulations - An Introduction and Applications*, IntechOpen, 2019. doi: 10.5772/intechopen.90470.

[7] Fiorino, N. T., Snow, N. J., Schauer, F. R., Polanka, M. D., Schumaker, A. S., and Sell, B. C., "Improving detonability in a small-scale rotating detonation engine using partial premixing," *Journal of Propulsion and Power*, Oct. 2022, pp. 1–10.

[8] Dechert, J. R., "Development of a Small Scale Rotating Detonation Engine," 2020. Theses and Dissertations. 3212. https://scholar.afit.edu/etd/3212

[9] Fiorino, N. T., "Improving the Stability and Operability of a Small-Scale Rotating Detonation Engine," 2021. Theses and Dissertations. 5067. https://scholar.afit.edu/etd/5067

[10] Russo, R. M., "Operational Characteristics of a Rotating Detonation Engine Using Hydrogen and Air," 2011. Theses and Dissertations. 1352.

[11] Connolly-Boutin, S., Joseph, V., Ng, H. D., and Kiyanda, C. B., "Small-size rotating detonation engine: scaling and minimum mass flow rate," *Shock Waves*, vol. 31, no. 7, 2021, pp. 665–674. doi:10.1007/s00193-021-00991-2.

[12] Bykovskii, F. A., Zhdan, S. A., and Vedernikov, E. F., "Continuous spin detonations," *Journal of Propulsion and Power*, vol. 22, Nov. 2006, pp. 1204–1216.

[13] Law, H., Baxter, T., Ryan, C. N., and Deiterding, R., "Design and testing of a small-scale laboratory rotating detonation engine running on ethylene-oxygen," *AIAA Propulsion and Energy 2021 Forum*, Jul. 2021.

[14] NASA, "Mass flow choking," [Online]. Available: https://www.grc.nasa.gov/www/k-12/airplane/mflchk.html

[15] NASA, "Mass flow rate equations," [Online]. Available: https://www.grc.nasa.gov/www/k-12/VirtualAero/BottleRocket/airplane/mchkdrv.html

[16] Lightfoot, M., Danczyk, S. A., Watts, J., and Schumaker, S. A., "Accuracy and Best Practices for Small-Scale Rocket Engine Testing." https://apps.dtic.mil/sti/citations/ADA555453

[17] Asia Industrial Gases Association, "Standard Procedures for Hydrogen Supply Systems," AIGA, 126/24, 2024. https://www.asiaiga.org/uploaded_docs/en_AIGA_126_24_Guide_for_H2_Supply_Systems.pdf

[18] Asia Industrial Gases Association, "Cleaning of Equipment for Oxygen Service," AIGA, 012/19, 2019. https://www.asiaiga.org/uploaded_docs/en_AIGA_012_19_Cleaning_of_Equipment_for_Oxygen_Service.pdf

[19] NASA, "Safety standard for oxygen and oxygen systems: Guidelines for oxygen system design, materials selection, operations, storage, and transportation." https://ntrs.nasa.gov/citations/19960021046

[20] Crane Co., NY, *Flow of Fluids through Valves, Fittings and Pipes*, Metric Edition-SI Units, Technical Paper No. 410M, 1982.

[21] ASME, "Measurement Of Fluid Flow In Pipes Using Orifice, Nozzle & Venturi," MFC-3M-2004, 2004.

[22] NASA, "John C. Stennis Space Center tubing systems for facility systems, special test equipment, and aerospace hardware," SSTD-8070-0126-PIPE, 2019. https://standards.nasa.gov/standard/SSC/SSTD-8070-0126-PIPE

[23] Heister, S., et al., "Rotating Detonation Combustion for Advanced Liquid Propellant Space Engines," *Aerospace Propulsion*, Oct. 2022. https://doi.org/10.3390/aerospace9100581

[24] Breitung, W., et al., "Flame Acceleration and Deflagration-to-Detonation Transition in Nuclear Safety," *Nuclear Energy Agency*, Aug. 2000. https://www.nrc.gov/docs/ML0313/ML031340619.pdf

[25] Robey, R., "Handbook of Shock – Transition to Detonation," *ScienceDirect*, 2001. https://www.sciencedirect.com/topics/engineering/transition-to-detonation

[26] Jones, K. M., "Analysis of Dual-Bell Nozzle Altitude Compensating Performance," NASA Technical Report, NASA/TM-2000-209765, Mar. 2000. https://ntrs.nasa.gov/api/citations/20000025558/downloads/20000025558.pdf

[27] Anderson, J. D., "Section 1.2: Governing Equations of Fluid Dynamics," Utah State University, MAE 6530 Course Material. http://mae-nas.eng.usu.edu/MAE_6530_Web/New_Course/Section1/section1.2.pdf

[28] Callaghan, A., "Get to Know O-Rings: Types and Applications," APG Knowledge Center, 2022. https://knowledge.callapg.com/blog/get-to-know-o-rings-types-and-applications

[29] Marco Rubber & Plastics, "O-Ring Material Test Data Explanation," 2022. https://www.marcorubber.com/oring-material-test-data-explanation.htm

[30] Global O-Ring and Seal, "PTFE (Teflon) O-Rings," 2022. https://www.globaloring.com/ptfe-teflon-o-rings/

[31] Parker Hannifin, "Metal Seals Standard Cross Sections," Composite Sealing Systems Division, 2019. https://www.parker.com/content/dam/Parker-com/Literature/Composite-Sealing-Systems-Division/Parker-CSS-Brochure-5170---Metal-Seals-Overview.pdf

[32] NH O-Ring, "PTFE O-Rings — Materials Simply Explained," 2022. https://nh-oring.de/en/ptfe-o-rings-materials-simply-explained/

[33] Silmid, "RTV Silicones — Sealants Knowledge Centre," 2022. https://www.silmid.com/knowledge-centre/sealants-content/rtv-silicones/

[34] The Engineering ToolBox, "Young's Modulus, Tensile Strength and Yield Strength Values for some Materials," 2003. https://www.engineeringtoolbox.com/young-modulus-d_417.html

[35] Hamilton Law, Tom Baxter, Charlie N. Ryan, and Ralf Deiterding, "Design and Testing of a Small-Scale Laboratory Rotating Detonation Engine Running on Ethylene-Oxygen," *AIAA Propulsion and Energy 2021 Forum*, AIAA 2021-3658, August 2021. https://doi.org/10.2514/6.2021-3658

[36] Arduino, "UNO R3 User Manual," 2020. https://docs.arduino.cc/hardware/uno-rev3

[37] National Instruments, "Field Wiring and Noise Considerations for Analog Signals," 2019. https://www.ni.com/pdf/manuals/371932c.pdf

[38] National Instruments, "NI USB-6001 User Manual," 2020. https://www.ni.com/pdf/manuals/374669a.pdf

[39] National Instruments, "NI USB-6210 User Manual," 2020. https://www.ni.com/pdf/manuals/371931f.pdf

[40] OMEGA Engineering, "Pressure Transducer Wiring Guide," 2021. https://www.omega.com/

[41] SparkFun, "HX711 Load Cell Amplifier Datasheet," 2019. https://cdn.sparkfun.com/datasheets/Sensors/Force/hx711_english.pdf

[42] SparkFun, "HX711 User Manual," 2019. https://learn.sparkfun.com/tutorials/load-cell-amplifier-hx711-breakout-hookup-guide

[43] Topworx, "Chemical Compatibility Guide," 2023. https://www.topworx.com

[44] WIC Valve, "1/2" Pneumatic Air Actuated Ball Valve Double Acting," 2022. https://www.wicvalve.com

[45] Airtac, "4V200 Pneumatic Solenoid Valve Manual," 2023. https://www.airtac.com

[46] Harris, "Regulator Product Catalog," 2023. https://www.harrisproductsgroup.com

[47] ASME, "Hydrogen Piping Standard B31.12-2023," 2023. https://www.asme.org

[48] MacWeld, "ROU Quotation 104788," 2024. https://www.macweld.com

[49] Swagelok, "NPT Compression Fitting Technical Guide," Rev7, 2023. https://www.swagelok.com

[50] WIKA, "PRV Installation Guide," 2022. https://www.wika.com

[51] Evolution Sensors and Controls, "Sales Receipt 15122," 2025. https://www.evolutionsensors.com

[52] Evolution Sensors and Controls, "Type K Thermocouple Probe Specifications," 2025. https://www.evolutionsensors.com

[53] O'Keefe Controls Co., "Precision Orifices for Flow Control," 2024. https://www.okeefecontrols.com/

[54] Mac-Weld Machining Ltd., "Restriction Orifice Unions (ROU)," 2024. https://www.mac-weld.com/restriction-orifice-unions/

[55] Fox Valve Development Corp., "Sonic Choke Nozzles," 2024. https://www.foxvalve.com/venturi-flow-controls/sonic-choke